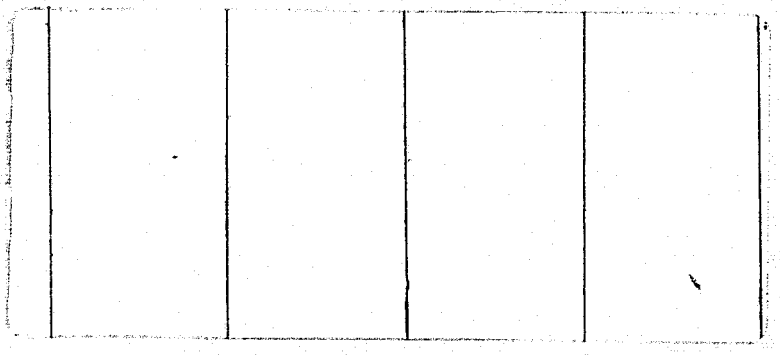

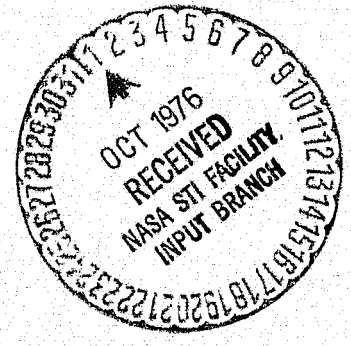

HOWARD UNIVERSITY
SCHOOL OF ENGINEERING
DEPARTMENT OF MECHANICAL ENGINEERING
WASHINGTON, D.C. 20059

FINAL REPORT

NASA GRANT: NSG-1181

THE DYNAMICS OF SPIN STABILIZED SPACECRAFT WITH MOVABLE APPENDAGES (PART II)

by

Peter M. Bainum
Professor of Aerospace Engineering
Principal Investigator

and

R. Sellappan
Graduate Research Assistant

May 1976

ABSTRACT

This report considers the dynamics of spin stabilized spacecraft with movable appendages and is an extension of the research reported in Part I (May 1974 - May 1975) where two basic types of appendages were treated: (1) a hinged type of fixed length whose orientation with respect to the main part can vary and (2) a telescoping type of varying length which could represent extensible antennas or a tether connected to the main part of the spacecraft.

In this report, the dynamics and stability of a spin stabilized spacecraft with a hinged appendage system are treated analytically and numerically. The hinged system consists of a central hub with masses attached to (assumed) massless booms of fixed length whose orientation relative to the main part can change. The general three dimensional deployment dynamics of such a hinged system is considered here without any restriction on the location of the hinge points. The equations of motion for the hinged system, with viscous damping at both hinge points, are linearized about the nominal equilibrium position where the booms are orthogonal to the nominal spin axis for the case of two dimensional and three dimensional motion. Analytic stability criteria are obtained from the necessary condition on the sign of all the coefficients in the system characteristic equation. For stability it is found that (hinge) damping must be present and that for limiting cases, where the spin axis is an axis of symmetry, certain inequalities relating the hinge point offset coordinates to the moment of inertia ratio and end masses must be satisfied.

The hinge damping is always required for the nominal deployment of hinge members. Numerical results indicate that the rate damping is required to remove the transverse angular velocities effectively since the hinge dampers alone do not provide satisfactory nutation time constants for the system parameters selected.

Next, the control of a spin-stabilized spacecraft with movable telescoping appendages is considered with an application of the linear regulator problem. It is assumed that the spacecraft consists of a rigid central hub and one or two movable telescoping booms (with end masses) which are in general linearly offset from the hub principal axes. The equations of rotational motion are developed and linearized about either of two desired final states: (1) a flat spin about only one of the hub principal axes or (2) a zero inertial angular velocity state. A control law for the boom end mass position is sought such that a quadratic cost functional involving the weighted components of angular velocity plus the control is minimized when the final time is unspecified. For such a system the computation of the control involves the solution of the matrix Riccati algebraic equation. For three axis control more than one offset boom (orthogonal to each other) is required. When only two-axis control is required and a single boom is offset in only one direction, an analytic solution of the matrix Riccati equation is achieved; when this system is used for reducing the nutation angle of a spinning spacecraft the time constant obtained is one order of magnitude smaller than previously achieved using non-optimal control logic. For the general case of three axis control results are obtained numerically.

The problem of optimal control with a minimum time criterion has been examined analytically for the special case of a single offset boom where it is assumed that the initial conditions are such that the system can be driven to the equilibrium (rest) state with only a single switching maneuver in the bang-bang optimal sequence. For this system it is possible to obtain an analytical solution for the switching and final times in terms of the initial conditions and magnitude of the maximum value of the control force.

TABLE OF CONTENTS

TABLE OF CONTENTS

NOMENCLATURE

a_*	=	offset of the vertical hinge point(s) from the '2' axis
a	=	offset of the control boom with end mass m_1 from the 2,3 (y,z) plane
A	=	linearized system state matrix
b	=	offset of the control boom with end mass m_1 from the 3,1 (z,x) plane
B	=	linearized system control matrix
c	=	offset of the control boom with end mass m_2 from the 3,1 (z,x) plane
C*	=	maximum value of the control U
c_α	=	hinge damping (viscous) coefficient about the hinge points
d	=	offset of the control boom with end mass m_2 from the 1,2 (x,y) plane
I_1, I_2, I_3	=	principal moments of inertia of the main part of the spacecraft
J	=	cost functional for optimal control
K	=	symmetric positive definite gain matrix
ℓ	=	constant length of hinged appendages
ℓ_m	=	maximum value of each control boom length
M	=	mass of main part of the spacecraft
m	=	end mass
m_1, m_2	=	control boom end masses
Q	=	positive definite symmetric state weighting matrix
r_0	=	offset of the hinge point(s) from the '3' axis
$\bar{r}_i$	=	position vector of the $i^{\underline{th}}$ mass with respect to the center of the coordinate system (center of mass of the main hub)

R	=	positive definite symmetric control weighting matrix
t	=	time
t_f	=	time of stopping of all operations with the principal axes booms in the recovery sequence of the spacecraft
T	=	kinetic energy
T_{3_f}	=	switching time in the recovery sequence to achieve final spin about the '3' axis
U	=	control vector
$\bar{V}_i$	=	inertial velocity of the $i^{\underline{th}}$ mass of the (hinged) system
$\bar{V}_{M/cm}$	=	velocity of the main part of the spacecraft with respect to the system center of mass
$\bar{V}_{M/o}$	=	velocity of the main part of the spacecraft with respect to the center of the coordinate system (o)
$\bar{V}_{m_i/o}=\dot{\bar{r}}_i$	=	velocity of the $i^{\underline{th}}$ mass in the system with respect to the center of the coordinate system
$\bar{V}_{o/cm}$	=	velocity of point 'o' with respect to the system center of mass
x	=	coordinate of the control boom end mass m_2 along the '1' axis (control variable)
X	=	state vector of the system
z	=	coordinate of the control boom end mass m_1 along the '3' axis (control variable)
α_1,α_2	=	coordinates describing the orientation of the hinged appendages relative to the spacecraft hub
ω_i	=	angular velocities about the 1,2,3 axes respectively (i=1,2,3)
$\omega_{T_{max}}$	=	maximum expected value of transverse rate
Ω	=	nominal main body spin rate

α	=	ω_1/Ω , nondimensionalized form of ω_1
β	=	ω_2/Ω, nondimensionalized form of ω_2
γ	=	ω_3/Ω-1, variation of the nondimensionalized form of ω_3 from the nominal value
ρ	=	boom density
τ	=	Ωt, dimensionless time
τ_s	=	switching time
τ_f	=	final time
ζ	=	z/ℓ_m, dimensionless form of z
ξ	=	x/ℓ_m, dimensionless form of x
θ	=	nutation angle
F	=	Rayleigh dissipation function
.	=	indicates differentiation with respect to t
'	=	indicates differentiation with respect to τ
(0)	=	indicates initial conditions
1,2,3	=	principal axes of main spacecraft

LIST OF ILLUSTRATIONS

LIST OF ILLUSTRATIONS

I. INTRODUCTION

This report will describe a continuation of the research already accomplished during the first year (May 1974-May 1975) on the dynamics of spin stabilized spacecraft with movable appendages.[1] Part I concentrated on the analysis of the motion of a spinning spacecraft during the deployment of two types of movable appendages - the telescoping rod type of varying length during deployment, and fixed length appendages whose orientation with respect to the main hub can vary. In addition the use of these appendages to detumble a spacecraft with a random spin to achieve final states of (1) close to zero inertial angular rate and (2) a final spin rate about one of the principal axis was also considered.[1] In this report (Part II), the following topics are treated: the dynamics and an extensive stability analysis of a spacecraft with hinged appendages; an examination of linear optimal control theory as applied to the deployment maneuver of a telescoping boom system by selecting different integrand functions in the cost functional; and the time optimal control of a nutating spacecraft using a single offset telescoping boom system.

The first phase of the current study will examine the general three dimensional motion of a spacecraft with hinged appendages. The hinged system consists of a central hub with masses attached to (assumed) massless booms of fixed length whose orientation relative to the main part can change.

The booms are attached at a given radius from the spin axis and when the booms are released they swing outward from the spin axis under the influence of centrifugal forces.

The dynamics of this type of fixed length appendage system during the deployment maneuver has been previously studied only for the case where the transverse components of the angular velocity vector are assumed to be zero throughout deployment and where the hinge points are located on the hub's principal transverse axes.[2] The motion and stability of such a system will be studied, analytically for special cases, and numerically for the general case. It is assumed that there is no restriction on the location of the hinge points.

The second phase of the study will consider the control of a spin-stabilized spacecraft with movable telescoping appendages with an application of the linear regulator problem. It is assumed that the spacecraft consists of a rigid central hub and one or two movable telescoping booms (with end masses) which are in general linearly offset from the hub principal axes. An advantage of such a telescoping system as used in the control of a tumbling spacecraft is its potential reuse. The booms can be retracted at the end of each control sequence (for very fine pointing requirements the small residual angular velocity components could be removed by temporarily activating on-board damping devices).

Methods of recovering a tumbling spacecraft using three sets of telescoping booms deployed along the hub principal axes were examined in a recent paper.[3] From an application of Lyapunov's second method (using a modified form of the rotational kinetic energy as a Lyapunov function) sequences of boom extension maneuvers can be determined so that the spacecraft will approach either of two desired final states: close to a zero inertial angular velocity state, or a final spin rate about only one of the principal axes.[3] Although these sequences of boom maneuvers will result in recovery of a tumbling system they will not, generally, satisfy any criteria of optimal control theory.

In a related problem, Edwards and Kaplan[4,5] have examined the problem of detumbling a spacecraft using a single internal mass which is constrained to move along a linear track within the vehicle. A control law was selected such that the net average time rate of change of excess rotational kinetic energy will be negative. It was concluded that system performance could be improved by making the control mass as large as possible and allowing for larger amplitude motions along the track.[4,5] The amplitude of any internal device would be limited by the size of the spacecraft; on the other hand, externally controlled appendages will be subject to external perturbations(such as solar pressure) and if sufficient length is extended, the flexibility of such a structure must be considered.

Recently Amieux and Liegeois[6] have applied linear optimal control theory to the two-axis control of a spinning spacecraft system using a motor controlled internal single-degree-of-freedom pendulum.

It was assumed that the spin rate remains much greater than the magnitude of the transverse angular velocity vector during the decay of the nutation angle.

In the present study both two and three axis optimal control of a spin-stabilized spacecraft using movable telescoping appendages will be considered. The control will be implemented by varying the position of boom end masses which are considered large in comparison with the boom mass itself.

The difficulty in determining a control sequence of extension rates for different pairs of telescoping booms which would yield a time-optimal recovery of a tumbling spacecraft has already been reported.[7,1] The problem has been that when the equations are written in standard state form - e.g. for a case of two sets of booms parallel to the spin axis - (where symmetry about this axis is maintained during extension), the control function (two different extension rates) is non-linearly coupled with the state variables.[7,1] Here the problem of time optimal control will be examined analytically for the special case of a single telescoping offset boom under a particular range of initial conditions.

II. MOTION AND STABILITY OF THE HINGED SYSTEM

1. Derivation of Kinetic Energy

The hinged system to be studied is shown schematically in Fig. 2.1(a). The co-ordinate system representation is shown in Fig. 2.1(b). The system consists of a central hub with masses attached to massless booms of constant length ℓ, which in turn are attached to the main spacecraft at radius r_0. The end masses are released at $t = t_0$ and thereafter swing out from the spin axis. The angles between the booms and the spin axis are denoted by α_1 and α_2 as shown in Fig. 2.1(b) and are assumed to be zero initially. A special case of this type was considered in Ref. 2 (where it was assumed that the transverse angular velocities during deployment remained at zero), but here we consider the general three dimensional deployment dynamics.

The development of the kinetic energy of this type of hinged system from first principles is considered below:

The total kinetic energy of the system, in terms of rotational and translational energies, can be written as,

$$T = T_r + T_t + \text{const. due to (circular) orbital motion} \qquad (2.1)$$

where

$$T_r = \frac{1}{2}\left(I_1\omega_1^2 + I_2\omega_2^2 + I_3\omega_3^2\right) \qquad (2.2)$$

$$T_t = \frac{1}{2} M V_{M/cm}^2 + \sum_{i=1}^{n} m_i V_{m_i/cm}^2 \qquad (2.3)$$

(M = mass of main body)

From the definition of the center of mass of the system:

$$\bar{r}_{cm/o} = \frac{m \sum_{i=1}^{n} \bar{r}_{i/o}}{M + \sum_{i=1}^{n} m_i} \tag{2.4}$$

where point 'o' is the center of the coordinate system (and also the center of mass of the main hub) and the masses are assumed to be equal ($m_i = m$). The velocity of the various components relative to the system center of mass may be expressed:

$$\bar{V}_{m_i/cm} = \bar{V}_{m_i/o} + \bar{V}_{o/cm} \tag{2.5}$$

$$\bar{V}_{M/cm} = \bar{V}_{M/o} + \bar{V}_{o/cm} \tag{2.6}$$

The components appearing in Eqs. (2.5) and (2.6) can be further represented as:

$$\bar{V}_{m_i/o} = \dot{\bar{r}}_i \tag{2.7}$$

$$\bar{V}_{o/M} = 0 \tag{2.8}$$

$$\bar{V}_{o/cm} = -\bar{V}_{cm/o} = -\dot{\bar{r}}_{cm/o} = -\frac{m \sum \dot{\bar{r}}_i}{M + \Sigma m_i} \tag{2.9}$$

After substitution of Eqs. (2.7), (2.8) and (2.9) into Eq. (2.3), the translational energy may be expressed as

$$T_t = \frac{M}{2} |\bar{V}_{o/cm}|^2 + \frac{1}{2} \Sigma m_i |\bar{V}_{m_i/o}|^2 + \frac{1}{2} \Sigma m_i |\bar{V}_{o/cm}|^2 + \Sigma m_i (\bar{V}_{m_i/o}) \cdot (\bar{V}_{o/cm}) \tag{2.10}$$

After some algebraic manipulations, we obtain,

$$T_t = \frac{m}{2} \Sigma(\bar{V}_i \cdot \bar{V}_i) - \frac{m^2}{2\bar{M}} (\Sigma \bar{V}_i \cdot \Sigma \bar{V}_i) \tag{2.11}$$

where

$$\bar{V}_i = \dot{\bar{r}}_i\Big|_{rot} + \bar{\omega} \times \bar{r}_i$$

$$\bar{M} = M + \Sigma m_i$$

Thus, the total kinetic energy of the system is given by:

$$T = \frac{1}{2} (I_1\omega_1^2 + I_2\omega_2^2 + I_3\omega_3^2) + \frac{m}{2} \sum_{i=1}^{n} (\bar{V}_i \cdot \bar{V}_i)$$

$$- \frac{m^2}{2\bar{M}} \left(\sum_{i=1}^{n} \bar{V}_i \cdot \sum_{i=1}^{n} \bar{V}_i \right) + \text{const.} \tag{2.12}$$

As an example, we consider the case from Ref. 2 where $m = m/2$, $\alpha_1 = \alpha_2 = \alpha$, $I_3 = I$ and $\omega_3 = \dot{\theta}$. The kinetic energy is then obtained as (neglecting orbital motion)

$$T = \frac{1}{2} I \dot{\theta}^2 + \frac{m}{2} [\ell^2 \dot{\alpha}^2 + \dot{\theta}^2 (r_o + \ell \sin \alpha)^2]$$

$$- \frac{m^2}{2} \frac{\ell^2}{(M + m)} \sin^2\alpha \, \dot{\alpha}^2 \tag{2.13}$$

which corresponds identically with Eq. (18) of Ref. 2, which was presented without development.

Next, a more general case of the hinged deployment system considered is shown in Fig. 2.2. Here there is no restriction on the location of the hinge points. The co-ordinates of the two masses are given by

$$x_1 = 0 \qquad x_2 = 0$$
$$y_1 = r_0 + \ell \sin \alpha_1 \qquad y_2 = -(r_0 + \ell \sin \alpha_2)$$
$$z_1 = a_* - \ell \cos \alpha_1 \qquad z_2 = a_* - \ell \cos \alpha_2 \qquad (2.14)$$

Here 'a_*' is the offset of the hinge point from the '2' axis. Upon substituting Eqs. (2.14) into Eq. (2.12), and after algebraic simplifications, the resulting equation for kinetic energy is:

$$\begin{aligned}
T = {} & \frac{1}{2}\left[I_1\omega_1^2 + I_2\omega_2^2 + I_3\omega_3^2\right] \\
& + \frac{m}{2}\left[\{2(r_0^2+a_*^2+\ell^2)+2\ell\ \{r_0(\sin\alpha_1+\sin\alpha_2)-a_*(\cos\alpha_1+\cos\alpha_2)\}\right]\omega_1^2 \\
& + \{2a_*^2-2a_*\ell(\cos\alpha_1+\cos\alpha_2)+\ell^2(\cos^2\alpha_1+\cos^2\alpha_2)\}\ \omega_2^2 \\
& + \{2r_0^2+2r_0\ell(\sin\alpha_1+\sin\alpha_2)+\ell^2(\sin^2\alpha_1+\sin^2\alpha_2)\}\ \omega_3^2 \\
& - \{2\ell\ \{a_*(\sin\alpha_1-\sin\alpha_2)-r_0(\cos\alpha_1-\cos\alpha_2)\} \\
& - 2\ell^2(\sin\alpha_1\cos\alpha_1-\sin\alpha_2\cos\alpha_2)\}\ \omega_2\omega_3 \\
& + \{2\ell^2(\dot\alpha_1 - \dot\alpha_2) + 2\ell\ \{\dot\alpha_1\ (r_0\sin\alpha_1 - a_*\cos\alpha_1) \\
& - \dot\alpha_2(r_0\sin\alpha_2 - a_*\cos\alpha_2)\}\}\ \omega_1 + \ell^2(\dot\alpha_1^2 + \dot\alpha_2^2)\Big] \\
& - \frac{m^2}{2(M+2m)}\left[\{2(2a_*^2 + \ell^2) + 2\ell^2\cos(\alpha_1+\alpha_2)-4a_*\ell(\cos\alpha_1+\cos\alpha_2)\}\omega_1^2\right. \\
& + \{2a_* - \ell(\cos\alpha_1+\cos\alpha_2)\}^2\ \omega_2^2 + \ell^2(\sin\alpha_1-\sin\alpha_2)^2\ \omega_3^2 \\
& - 2\ell(\sin\alpha_1-\sin\alpha_2)\ \{2a_*-\ell(\cos\alpha_1 + \cos\alpha_2)\}\ \omega_2\omega_3 \\
& + 2\ell\{\ell(\dot\alpha_1-\dot\alpha_2) + \ell\cos(\alpha_1+\alpha_2)(\dot\alpha_1-\dot\alpha_2) \\
& \left. - 2a_*(\cos\alpha_1\dot\alpha_1 - \cos\alpha_2\ \dot\alpha_2)\}\ \omega_1 + \ell^2\{\dot\alpha_1^2+\dot\alpha_2^2-2\dot\alpha_1\dot\alpha_2\cos(\alpha_1+\alpha_2)\}\right] + \text{const.} \qquad (2.15)
\end{aligned}$$

2. Development of Equations of Motion

The equations of motion in the five variables: ω_1, ω_2, ω_3, α_1 and α_2 are developed using the Quasi-Lagrangian formulation[8] for ω_i, i = 1,2,3, and the general Lagrangian formulation for the variables α_1, α_2. The equations of motion for this system, neglecting external torques, can be represented as:

$$\frac{d}{dt}\frac{\partial T}{\partial \omega_1} - \omega_3 \frac{\partial T}{\partial \omega_2} + \omega_2 \frac{\partial T}{\partial \omega_3} = 0 \qquad (2.16)$$

$$\frac{d}{dt}\frac{\partial T}{\partial \omega_2} - \omega_1 \frac{\partial T}{\partial \omega_3} + \omega_3 \frac{\partial T}{\partial \omega_1} = 0 \qquad (2.17)$$

$$\frac{d}{dt}\frac{\partial T}{\partial \omega_3} - \omega_2 \frac{\partial T}{\partial \omega_1} + \omega_1 \frac{\partial T}{\partial \omega_2} = 0 \qquad (2.18)$$

$$\frac{d}{dt}\frac{\partial T}{\partial \dot{\alpha}_1} - \frac{\partial T}{\partial \alpha_1} + \frac{\partial F}{\partial \dot{\alpha}_1} = 0 \qquad (2.19)$$

$$\frac{d}{dt}\frac{\partial T}{\partial \dot{\alpha}_2} - \frac{\partial T}{\partial \alpha_2} + \frac{\partial F}{\partial \dot{\alpha}_2} = 0 \qquad (2.20)$$

where

T = Total kinetic energy of the system

F = Rayleigh dissipation function

The dissipation function which accounts for linear viscous damping, assumed to be present about the hinge points, is given by:

$$F = \frac{1}{2} c_\alpha \ell^2 (\dot{\alpha}_1^2 + \dot{\alpha}_2^2) \qquad (2.21)$$

where

c_α = the hinge damping coefficient

With the the approximation: $m^2/\bar{M} \ll m$ or $(m/\bar{M} \ll 1)$, the equations of motion are obtained as follows:

$$I_1\dot{\omega}_1-(I_2-I_3)\omega_2\omega_3+m[2(r_0^2+a_*^2+\ell^2)+2\ell\{r_0(s\alpha_1+s\alpha_2)-a_*(c\alpha_1+c\alpha_2)\}]\dot{\omega}_1$$

$$-m\{2a_*^2-2a_*\ell(c\alpha_1+c\alpha_2)+\ell^2(c2\alpha_1+c2\alpha_2)-2r_0^2-2r_0\ell(s\alpha_1+s\alpha_2)\}\omega_2\omega_3$$

$$+2m\ell\ \{\ r_0(c\alpha_1\dot{\alpha}_1+c\alpha_2\dot{\alpha}_2)+a_*(s\alpha_1\dot{\alpha}_1+s\alpha_2\dot{\alpha}_2)\}\ \omega_1$$

$$+m\ell\ \{a_*\ (s\alpha_1-s\alpha_2)-r_0(c\alpha_1-c\alpha_2)-\frac{\ell}{2}\ (s2\alpha_1-s2\alpha_2)\}(\omega_3^2-\omega_2^2)$$

$$+m\{\ell\{\ddot{\alpha}_1-\ddot{\alpha}_2)+(\dot{\alpha}_1)^2(r_0c\alpha_1+a_*s\alpha_1)+\ddot{\alpha}_1(r_0s\alpha_1-a_*c\alpha_1)$$

$$-(\dot{\alpha}_2)^2(r_0c\alpha_2+a_*s\alpha_2)-\ddot{\alpha}_2(r_0s\alpha_2-a_*c\alpha_2)\}=0 \qquad (2.22)$$

$$I_2\dot{\omega}_2-(I_3-I_1)\omega_3\omega_1+m\{2a_*^2-2a_*\ell(c\alpha_1+c\alpha_2)+\ell^2(c^2\alpha_1+c^2\alpha_2)\}\dot{\omega}_2$$

$$-m\ell\{a_*(s\alpha_1-s\alpha_2)-r_0(c\alpha_1-c\alpha_2)-\frac{\ell}{2}\ (s2\alpha_1-s2\alpha_2)\}\ \dot{\omega}_3$$

$$+m\ell\{a_*(s\alpha_1-s\alpha_2)-r_0(c\alpha_1-c\alpha_2)-\frac{\ell}{2}\ (s2\alpha_1-s2\alpha_2)\}\ \omega_1\omega_2$$

$$-m\{\ell^2(s^2\alpha_1+s^2\alpha_2)-2(a_*^2+\ell^2)+2\ell a_*(c\alpha_1+c\alpha_2)\}\omega_3\omega_1$$

$$+m\{2a_*\ell(s\alpha_1\dot{\alpha}_1+s\alpha_2\dot{\alpha}_2)-\ell^2(s2\alpha_1\dot{\alpha}_1+s2\alpha_2\dot{\alpha}_2)\}\ \omega_2$$

$$+m\ell\{\ell(\dot{\alpha}_1-\dot{\alpha}_2)-2a_*(c\alpha_1\dot{\alpha}_1-c\alpha_2\dot{\alpha}_2)+\ell(c2\alpha_1\dot{\alpha}_1-c2\alpha_2\dot{\alpha}_2)\}\ \omega_3=0 \qquad (2.23)$$

$$I_3\omega_3-(I_1-I_2)\omega_1\omega_2+m\{2r_0^2+2r_0\ell(s\alpha_1+s\alpha_2)+\ell^2(s^2\alpha_1+s^2\alpha_2)\}\ \dot{\omega}_3$$

$$-m\ell\{a_*(s\alpha_1-s\alpha_2)-r_0(c\alpha_1-c\alpha_2)-\frac{\ell}{2}(s2\alpha_1-s2\alpha_2)\}\ \dot{\omega}_2$$

$$-m\{2(r_0^2+\ell^2)+2\ell r_0(s\alpha_1+s\alpha_2)-\ell^2(c^2\alpha_1+c^2\alpha_2)\}\ \omega_1\omega_2$$

$$-m\ell\{a_*(s\alpha_1-s\alpha_2)-r_0(c\alpha_1-c\alpha_2)-\frac{\ell}{2}(s2\alpha_1-s2\alpha_2)\}\ \omega_3\omega_1$$

$$-m\ell\{2r_0(s\alpha_1\dot{\alpha}_1-s\alpha_2\dot{\alpha}_2)-\ell\ (c2\alpha_1\dot{\alpha}_1-c2\alpha_2\dot{\alpha}_2)+\ell\ (\dot{\alpha}_1-\dot{\alpha}_2)\}\ \omega_2$$

$$+m\{2r_0\ell(c\alpha_1\dot{\alpha}_1+c\alpha_2\dot{\alpha}_2)+\ell^2(s2\alpha_1\dot{\alpha}_1+s2\alpha_2\dot{\alpha}_2)\}\ \omega_3=0 \qquad (2.24)$$

$$\ell\ddot{\alpha}_1 + (\ell+r_0 s\alpha_1 - a_* c\alpha_1)\dot{\omega}_1 - (r_0 c\alpha_1 + \frac{\ell}{2} s2\alpha_1)\omega_3^2 - (a_* s\alpha_1 - \frac{\ell}{2} s2\alpha_1)\omega_2^2$$

$$-(r_0 c\alpha_1 + a_* s\alpha_1)\omega_1^2 + (a_* c\alpha_1 + r_0 s\alpha_1 - \ell c2\alpha_1)\omega_3\omega_2 + \frac{c\alpha}{m}\ell\dot{\alpha}_1 = 0 \qquad (2.25)$$

$$\ell\ddot{\alpha}_2 - (\ell + r_0 s\alpha_2 - a_* c\alpha_2)\dot{\omega}_1 - (r_0 c\alpha_2 + \frac{\ell}{2} s2\alpha_2)\omega_3^2 - (a_* s\alpha_2 - \frac{\ell}{2} s2\alpha_2)\omega_2^2$$

$$-(r_0 c\alpha_2 + a_* s\alpha_2)\omega_1^2 - (a_* c\alpha_2 + r_0 s\alpha_2 - \ell c2\alpha_2)\omega_3\omega_2 + \frac{c\alpha}{m}\ell\dot{\alpha}_2 = 0 \qquad (2.26)$$

where

$s\alpha_i = \sin\alpha_i$ and $c\alpha_i = \cos\alpha_i$

3. Two Dimensional Motion Analysis

a. Small amplitude analysis about equilibrium state

(i) linearization of the equations of motion

The equations of motion for the two dimensional case with no offset are obtained by assuming $\omega_1=\omega_2=a_*=0$. Also the hinge members are assumed to move in-phase ($\alpha_1=\alpha_2=\alpha$) and the viscous damping about the hinge points is assumed to be absent. Eqs. (2.22) - (2.26) then reduce to:

$$\{I_3 + 2m(r_0^2 + 2r_0\ell\sin\alpha + \ell^2\sin^2\alpha)\}\dot{\omega}_3 + 2m\ell\{2r_0\cos\alpha\,\dot{\alpha} + \ell\sin2\alpha\,\dot{\alpha}\}\omega_3 = 0 \qquad (2.27)$$

$$\ell\ddot{\alpha} - (r_0\cos\alpha + \frac{\ell}{2}\sin2\alpha)\,\omega_3^2 = 0 \qquad (2.28)$$

These two dimensional motion equations are linearized about the nominal equilibrium state: $\alpha = \pi/2$ and $\omega_3 = \Omega$ (Ω=nominal spin)

The original coordinates can then be related to the variational coordinates by:

$$\alpha = \frac{\pi}{2} + \varepsilon$$

$$\omega_3 = \Omega + \delta$$

where

$$\varepsilon << 1, \quad \delta << \Omega$$

The linearized equations which result are:

$$\omega_3 = \Omega + \delta(0) \simeq \Omega \tag{2.29}$$

$$\ddot{\varepsilon} + \frac{(r_0+\ell)}{\ell} \Omega^2 \varepsilon = 0 \tag{2.30}$$

When hinge damping is present, Eq. (2.30) has the following form

$$\ddot{\varepsilon} + \frac{c_\alpha}{m} \dot{\varepsilon} + \frac{(r_0+\ell)}{\ell} \Omega^2 \varepsilon = 0 \tag{2.31}$$

(ii) stability criteria

Eq. (2.31) can be written as

$$\varepsilon + d_\alpha \dot{\varepsilon} + \lambda^2 \varepsilon = 0 \tag{2.32}$$

where

$$d_\alpha = c_\alpha/m \text{ and } \lambda = \sqrt{1+r_0/\ell}\,\Omega$$

For stability of this second order system the following conditions must be satisfied:

(1) $d_\alpha > 0$ - Positive damping is required

(2) $d_\alpha < 2\lambda \rightarrow c_\alpha < 2m\Omega \sqrt{1+r_0/\ell}$ - which implies a lower bound on the magnitude of the damping coefficient.

(iii) closed form solutions

The solution of Eq. (2.30) is given by

$$\varepsilon = \varepsilon_o \cos(\lambda t+\Psi) \tag{2.33}$$

where ε_o is the initial displacement from $\alpha = \pi/2$ and Ψ is the initial phase angle. The corresponding solution of Eq. (2.31), assuming that the stability condition $d_\alpha < 2\lambda$ is satisfied, is given by

$$\varepsilon = A\, e^{-d_\alpha/2} \cos(\lambda t+\Psi) \tag{2.34}$$

Where A and Ψ are found from the initial conditions. Eq. (2.33) describes the oscillatory nature of the hinge members about the equilibrium state while Eq. (2.34) indicates the damping of this oscillation.

(iv) numerical results

The nonlinear equations of motion describing the deployment of the hinged system are programmed for numerical integration using the Nova 840 computer. The details of the subroutines used[9], the listing of the program and the computer time required are given in the section COMPUTER PROGRAMS (at the end of this report). For numerical integration Eqs. (2.22) - (2.26) are used with the following system parameters (Fig. 2.2)[2]:

$I_1 = I_2 = 8.5$ slug-ft^2; $I_3 = 10.5$ slug-ft^2

$r_o = 1$ ft; $\ell = 4$ ft; $a_* = 0$

$m = 0.125$ slug; $\omega_3 = \Omega = 4.82$ rad/sec

Figs. 2.3(a) and (b) simulate the dynamic response of the two dimensional motion of the hinged system to an initial perturbation in the hinge angle of 0.1 radians with hinge damping absent and then, present, respectively. For the damped case a hinge damping coefficient of c_α=0.1 lb/ft/sec is selected. These figures verify the closed form analytical results obtained in Eqs. (2.33) and (2.34) using the small angle analysis about the equilibrium state ($\alpha_1 = \alpha_2 = \alpha = 90^0$, $\omega_3=\Omega = 4.82$ rad/sec).

b. Large amplitude analysis

(i) closed form solutions

Eqs. (2.27) and (2.28) are used to simulate the large amplitude two dimensional motion when there is no damping about the hinge points. (Throughout the two dimensional analysis, the hinged members are assumed to move in phase and there is no vertical offset of the hinge points.) From Eq. (2.27), the closed form solution relating the spin rate to the hinge angle, with the initial conditions $\omega_3(0) = \Omega$, $\alpha=0$, is

$$\omega_3(t) = \frac{\Omega(I_3+2m\, r_0^2)}{I_3+2m(r_0+\ell\, \sin\alpha)^2} \qquad (2.35)$$

Here it is observed that $\omega_3(t)$ attains a maximum value when $\alpha=0, \pi$, etc., and a minimum when $\alpha=\pi/2, 3\pi/2$, etc. Eq. (2.35) may be substituted into Eq. (2.28). This can then be integrated once with respect to time under the following assumed initial conditions: $\alpha(0) = \dot{\alpha}(0) = 0$. The resulting expression gives the phase plane relationship of $\dot{\alpha}$ with α as,

$$\dot{\alpha} = \frac{\Omega}{\ell}\sqrt{\frac{(2r_0+\ell\sin\alpha)\,\ell\sin\alpha(I_3+2mr_0^2)}{I_3 + 2m(r_0+\ell\sin\alpha)^2}} \qquad (2.36)$$

(ii) numerical results

The deployment of the system from the position where the hinged members are initially parallel to the spin axis (α=0) is simulated in Fig. 2.4(a) without damping, and in Fig. 2.4(b) with hinge damping. The 'x' represents the maximum time simulated by Lang and Honeycutt.[2] It is seen that without damping the hinged members exhibit a flapping-type motion as momentum is exchanged between the hinge and spin motions. The hinge motions are not exactly sinusoidal as shown. Fig. 2.4(a) verifies the closed form analytic solution obtained relating spin rate with hinge angle. This figure also indicates the maximum and minimum spin rate obtained during the flapping motion which verifies the closed form solution obtained with the large angle analysis. Fig. 2.4(b) shows that, with the hinge damping coefficient selected, the system can be fully deployed in about 10 seconds.

Thus for the case of the two dimensional analysis, closed form analytical solutions are obtained for small amplitude oscillations about the equilibrium state. Also, from the large amplitude analysis, a closed form analytical solution relating the spin rate to the hinge angle and the hinge angle rate to the hinge angle are obtained.

4. Three Dimensional Motion Analysis

a. Small amplitude analysis about equilibrium state

(i) linearization of equations of motion

The three dimensional equations of motion, Eqs. (2.22) - (2.26), are linearized about the nominal equilibrium state: $\omega_1 = \omega_2 = 0$, $\alpha_1 = \alpha_2 = \pi/2$, $\omega_3 = \Omega$. The original coordinates are related to the variational coordinates by:

$$\alpha_1 = \pi/2 + \varepsilon_1$$

$$\alpha_2 = \pi/2 + \varepsilon_2$$

$$\omega_3 = \Omega + \delta$$

Based on the assumptions that ω_1/Ω, ω_2/Ω, δ/Ω, ε_i and $\dot{\varepsilon}_i/\Omega$ are small compared to 1, the equations of motion can be approximated by a linear set in which $\omega_3 = \Omega + \delta(o) \simeq \Omega$ is a constant. With $\tau = \Omega t$ as the independent variable, $\alpha = \omega_1/\Omega$ and $\beta = \omega_2/\Omega$ as dependent variables, and

$$h = \frac{2m}{I} a_*^2 \,, \quad g = \frac{2m}{I} (r_0+\ell)^2, \quad k = \frac{m\ell}{I} (r_0+\ell)$$

$$2\rho = c_\alpha/m\Omega, \quad f = 1 + (r_0/\ell), \quad n = (I_3/I) - 1$$

(Here the relationship $g = 2kf$ is to be noted) as nondimensional constants, the linear equations become:

$$(1+g+h)\,\alpha' + (n+g-h)\,\beta + k(\varepsilon_1''+\varepsilon_1) - k(\varepsilon_2''+\varepsilon_2) = 0 \qquad (2.37)$$

$$(1+h)\,\beta' - (n-h)\,\alpha = 0 \qquad (2.38)$$

$$\varepsilon_1'' + 2\rho\,\varepsilon_1' + f\,\varepsilon_1 + f\,\alpha' + f\,\beta = 0 \qquad (2.39)$$

$$\varepsilon_2'' + 2\rho\,\varepsilon_2' + f\,\varepsilon_2 - f\,\alpha' - f\,\beta = 0 \qquad (2.40)$$

where primes denote derivatives with respect to τ.

(ii) stability criteria

The necessary and sufficient conditions for stability of the system are obtained by applying the Routh-Hurwitz criterion similar to the procedure of Ref. 10. The stability conditions for the system are obtained by setting the characteristic determinant, corresponding to Eqs. (2.37) - (2.40), given by

$$\begin{vmatrix} (1+g+h)s & (n+g-h) & k(s^2+1) & -k(s^2+1) \\ -(n-h) & (1+h)s & 0 & 0 \\ fs & f & s^2+2\rho s+f & 0 \\ -fs & -f & 0 & s^2+2\rho s+f \end{vmatrix}$$

equal to zero. Here 's' denotes the characteristic exponent.

The characteristic determinant is expanded to obtain the factored sixth order algebraic equation

$$(s^2+2\rho s+f)[\{(1+g+h)(1+h)s^2+(n+g-h)(n-h)\}(s^2+2\rho s+f) - g(s^2+1)\{(1+h)s^2+(n-h)\}] = 0 \qquad (2.41)$$

It is seen that the system characteristic equation separates into two factors - a second order factor describing a mode where both hinged members move in phase as a unit, and a second factor represented by a more complex fourth order polynomial. (Such a separation of the system characteristic equation was also observed by Auelmann and Lane[11] in studing the stability of a spinning spacecraft with a ball-in-tube nutation damping system.) From the quadratic factor the stability condition is found to be: $c_\alpha < 2m\Omega\sqrt{1+r_0/\ell}$. This condition was also obtained earlier in the analysis of the two dimensional hinged system.

As the stability, also, depends on the fourth order factor in Eq. (2.41), we will consider different configurations of the system in the following special cases. Case 1(a): I_3 maximum moment of inertia (n>0) with no offset of hinge points (h=0).

The fourth order factor in Eq. (2.41) with h=0 reduces to

$$p_o s^4 + p_1 s^3 + p_2 s^2 + p_3 s + p_4 = 0 \qquad (2.42)$$

where

$$p_o = 1,\ p_1 = 2\rho(1+g)$$

$$p_2 = (n+g)\ n + (1+g)\ f - g(1+n)$$

$$p_3 = 2\rho(n+g)\ n,\ p_4 = (n+g)\ nf - gn$$

The non-trivial Routh-Hurwitz stability conditions are

$$p_1 p_2 - p_o p_3 > 0 \qquad (2.43)$$

$$(p_1 p_2 - p_o p_3)\ p_3 - p_1^2 p_4 > 0 \qquad (2.44)$$

Expansion of Ineqs.(2.43)and (2.44) results in complex algebraic relationships involving the system parameters. An attempt to algebraically rearrange the terms in Ineqs. (2.43) and (2.44) did not yield simplified results. However, it can be seen from consideration of the signs of each of the coefficients in Eq. (2.42) that $p_1>0$ and $p_3>0$. Since both g and n are positive, therefore, for stability, $\rho>0$, implying the necessity of (positive) hinge damping.

Case 1(b): I_3 maximum moment of inertia (n>0) with offset of hinge points ($h\neq 0$).

The fourth order factor in Eq. (2.41) with $h \neq 0$ can be written as

$$(q_o - q_2)s^4 + 2\rho q_o s^3 + (f q_o + q_1 - q_2 - q_3)s^2 + 2\rho q_1 s + (q_1 f - q_3) = 0 \qquad (2.45)$$

where

$$q_o = (1+g+h)\ (1+h)$$

$$q_1 = (n+g-h)\ (n-h)$$

$$q_2 = g(1+h)$$

$$q_3 = g(n-h)$$

The necessary and sufficient conditions are obtained from the rule of signs of the coefficients in the characteristic equation and also the Routh-Hurwitz criterion and can be expressed as:

$$|a_*| \leq \sqrt{\frac{I_3 - I}{2m}} \qquad (2.46)$$

$$W_1 W_2 - W_o W_3 > 0 \qquad (2.47)$$

$$(W_1 W_2 - W_o W_3)\ W_3 - W_1^2 W_4 > 0 \qquad (2.48)$$

where

$$W_o = q_o - q_2$$

$$W_1 = 2\rho q_o$$

$$W_2 = f q_o + q_1 - q_2 - q_3$$

$$W_3 = 2\rho q_1$$

$$W_4 = q_1 f - q_3$$

In Ineq. (2.46) the magnitude of the hinge offset from the (1,2) hub plane is limited by the differences in the hub moments of inertia and the size of the end masses. Case 2(a): I_3 minimum moment of inertia ($n<0$) with no offset of hinge points ($h=0$).

The necessary condition from the rule of signs of the coefficients is obtained as

$$(r_0+\ell) < \text{minimum of} \begin{cases} \sqrt{(I-I_3)/2m} \\ (I-I_3)/2mr_0 \end{cases} \tag{2.49}$$

Case 2(b): I_3 minimum moment of inertia ($n<0$) with offset of hinge points ($h\neq 0$).

Similar to case 2(a), the necessary condition is obtained as

$$(r_0+\ell) < \text{minimum of} \begin{cases} \sqrt{\frac{(I-I_3)}{2m} + a_*^2} \\ \frac{(I-I_3)}{2mr_0} + \frac{a_*^2}{r_0} \end{cases} \tag{2.50}$$

It is seen that when $a_*=0$, Ineqs. (2.50) reduce to Ineqs. (2.49). The necessary and sufficient conditions for the cases 2(a) and 2(b) are obtained in a similar procedure by making $n<0$ in the corresponding inequalities, Ineqs. (2.43), (2.44), (2.47), and (2.48).

(iii) numerical results

An example of the three dimensional hinged system dynamics is simulated in Figs. 2.5 (undamped) and 2.6 (with hinge damping). Initial perturbations in both hinge angles and one of the transverse angular velocities are assumed.

The oscillatory nature of the system motion about the equilibrium state when there is no hinge damping present is seen in Figs. 2.5(a) and 2.5(b). Although the hinge damping is effective in reducing the amplitudes of the hinge motion (Fig. 2.6(a)),the time constants associated with the nutation angle decay (Fig. 2.6(b)) are extremely long. It is clear that an additional form of nutation damping must be added for effective removal of excessive transverse rates.

The effect of rate damping about the transverse axes to obtain favorable nutation decay time constants is shown in Fig. 2.7. The rate damping torques about the '1' and '2' axes are assumed to be $R_d\omega_1$ and $R_d\omega_2$, respectively. The response of the transverse angular rates for rate damping coefficients of R_d=1.0 lb-ft-sec and 2.0 lb-ft-sec, respectively, are considered. The simulation results (Fig. 2.7) indicate that for effective removal of excessive transverse rates rapidly the magnitude of the rate damping coefficient must be large. The simulation study shows that the rate damping does not have any effect on the hinge angles and spin rate responses which are essentially unchanged from Fig. 2.6 for the parameters considered here.

The deployment dynamics of the system when the vertical hinge points are offset ($a_* \neq 0$) from the '2' axis is considered next. The stability condition for a_* when I_3 is a maximum moment of inertia (n>0) is obtained from Ineq. (2.46). With the system parameters selected, the limit of offset from Ineq. (2.46) is $a_* < \sqrt{8}$ ft.

The time response of the transverse angular rates with $a_* = 1.0$ ft ($< \sqrt{8}$ ft) is compared with the deployment dynamics when there is no vertical offset ($a_*=0$) in Fig. 2.8. Here it is found that the time period of the damped response of the transverse angular rates for the case with a vertical offset is larger than the period of this response when there is no offset. This may be attributed to the redistribution of moments of inertia due to the offset. Also, it is to be noted that the vertical offset ($a_*=1.0$ ft) does not have any effect on the time responses of the hinge angles and spin rate (essentially the same as shown in Fig. 2.6). The magnitude of the rate damping coefficient is assumed to be $R_d=2.0$ lb-ft-sec.

From the small amplitude analysis of the three dimensional motion of the hinged system we conclude the following:

1. Hinge damping is required for the nominal deployment of hinge members.
2. For stability, from the rule of signs, certain inequalities relating the hinge point offset to the ratio of the moments of inertia and end masses must be satisfied.
3. Since the hinge dampers alone do not provide satisfactory nutation time constants other types of dampers which provide direct damping of the transverse angular rates are required, and the magnitude of the rate damping coefficient must be large for rapid removal of the transverse rates.

4. The vertical offset of the hinge points increases the time period of the response of the transverse rates, which may be due to the redistribution of the moments of inertia.

5. The simulation of the deployment dynamics shows that the rate damping and vertical offset do not affect the responses of the hinge angles and the spin rate with the system parameters and the initial conditions selected here.

b. Large amplitude analysis

(i) numerical results

The general three dimensional motion analysis for large amplitude (α_1 and α_2 are physically free to vary between 0 and 180^0 - see Fig. 2.1(a))is considered in this section. The nonlinear equations given earlier (Eqs. (2.22)-(2.26)) are used for numerical simulation. The results are illustrated in Figs. 2.9(a)-(c) for different parameters. From the simulation of the nonlinear system motion, (Figs. 2.9 (a)-(c)), the observations made are:

Case (1): For the values $a_*=0$, $c_\alpha=0$ and $R_d=0$, the hinge members would intersect the hub structure ($|\alpha| > 180^0$) as indicated. (It should also be noted that with these parameters, the motion of the system when linearized about $\alpha_i=\pi/2$, $\omega_i=0$, $i\rightarrow 1,2$, $\omega_3=\Omega$ would be unstable in the sense of Routh-Hurwitz).

Case (2): For the values $a_*=0$, c_α =0.1 lb/ft/sec and R_d=2 lb/ft/sec, the hinge motion lies within the physical boundary as indicated.

This Case(2), shows with the hinge and rate damping coefficients selected, that the system can be fully deployed in about 10 secs (Fig. 2.9(a)). The angular rates about the transverse axes are nearly removed (Fig. 2.9(b)) and the spin rate reaches a steady-state value of 4.1 rad/sec from an initial value of $\omega_3(0) = 4.82$ rad/sec. (Fig. 2.9(c)).

Case (3): For the values: $a_*=1.0$ ft, $c_\alpha=0.1$ and $R_d=2$, the hinge motion would interfere with the main satellite structure, as in Case (1).

Case (4): Since there are no criteria to determine the magnitude of offset of the hinge points for general nonlinear motion, a value of $a_*=0.5$ ft, which is less than 1.0 ft used in Case (3), is selected keeping the same values for c_α and R_d as in Case (3). The response of the system for these parameters is indicated. The behavior here is similar to that shown in Case (2).

The nutation angle θ is defined by the equation

$$\tan\theta = \frac{I\sqrt{\omega_1^2 + \omega_2^2}}{I_3\,\omega_3}$$

The time response of the nutation angle is shown in Fig. 2.9(c). The cases of $a_*=0$ and $a_*=0.5$ ft are considered. The nutation angle reaches a maximum of 18^o during the deployment and declines to a value of less than 1^o within 10 secs.

The large amplitude analysis of the three dimensional motion for the general case of deployment reveals the following:

1. Hinge damping must always be present for the nominal deployment of the hinge members.
2. Rate damping is needed for the effective removal of the transverse angular rates.
3. The selection of the offset of the hinge points can not be done easily as there is no criteria which assures that the hinge motion will remain within physical limits (i.e. $|\alpha| \leq \pi$).

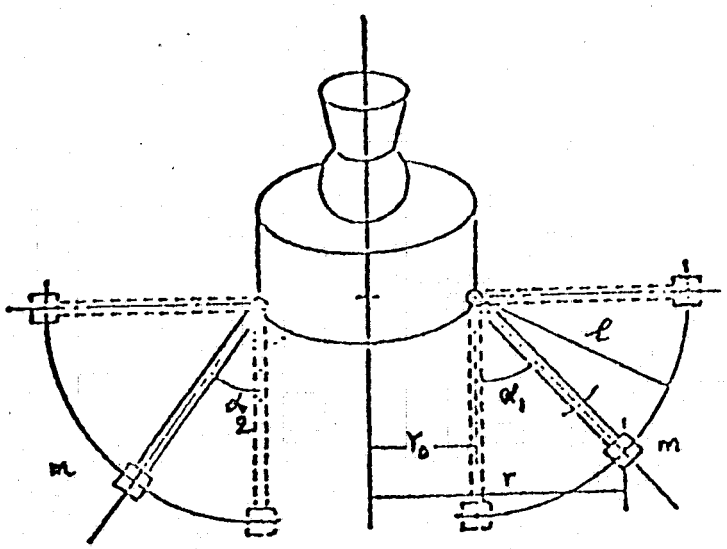

FIG. 2.1(a). HINGED DEPLOYMENT SYSTEM.

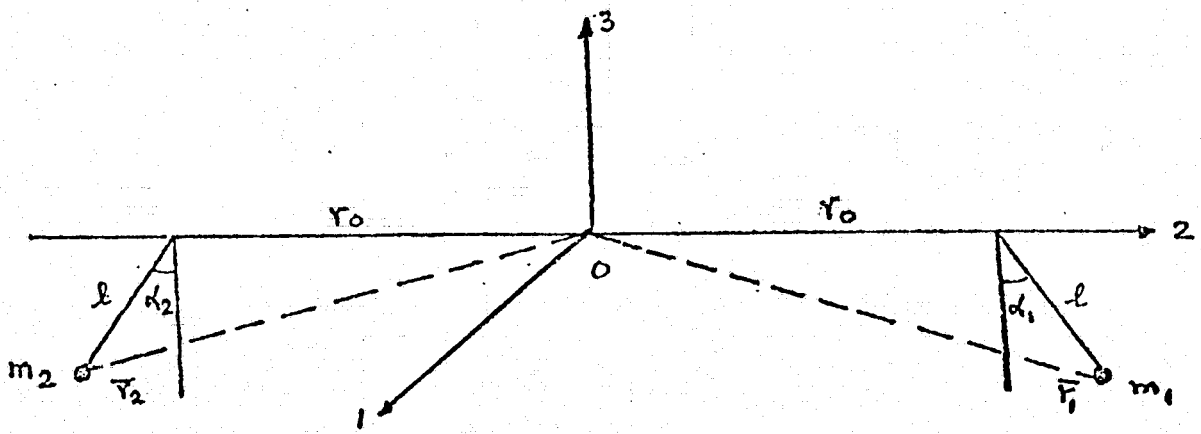

FIG. 2.1(b). COORDINATE SYSTEM FOR FIG. 2.1(a).

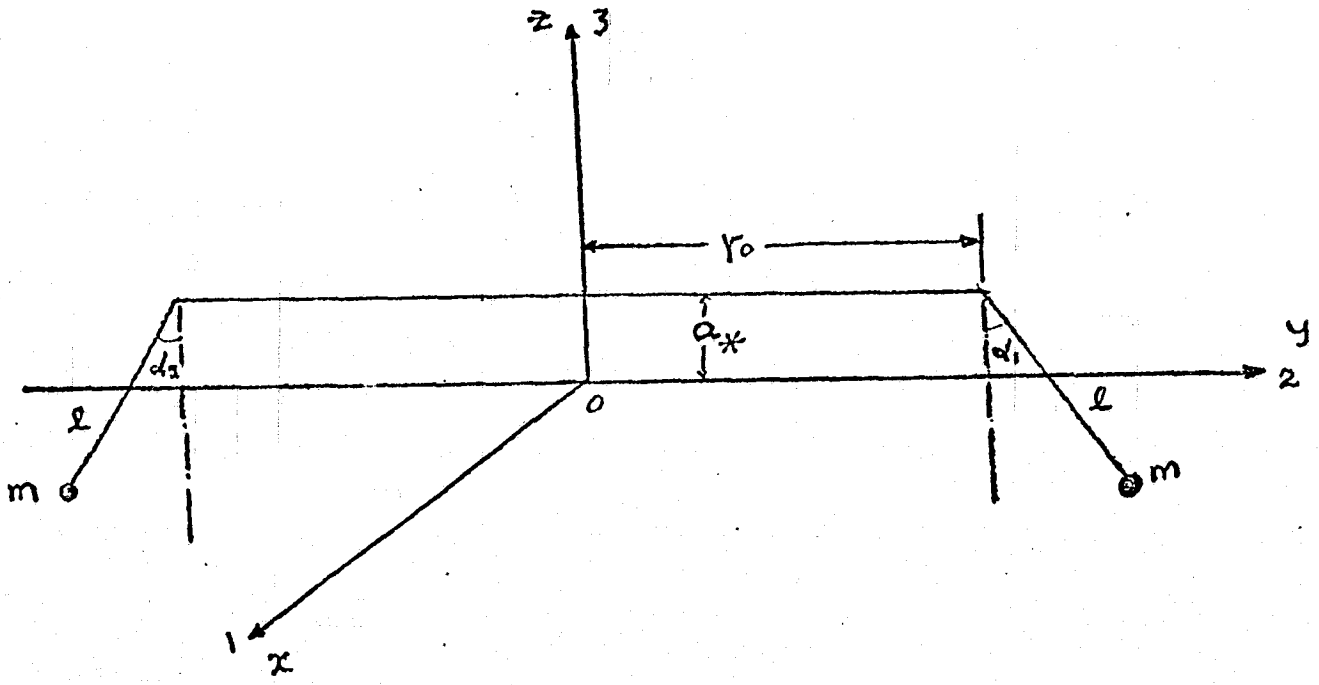

$$x_1 = 0 \qquad x_2 = 0$$

$$y_1 = r_0 + \ell \sin \alpha_1 \qquad y_2 = -(r_0 + \ell \sin \alpha_2)$$

$$z_1 = a_* - \ell \cos \alpha_1 \qquad z_2 = a_* - \ell \cos \alpha_2$$

FIG. 2.2. MORE GENERAL CASE OF HINGED DEPLOYMENT SYSTEM.

TWO DIMENSIONAL MOTION-SMALL AMPLITUDE ANALYSIS

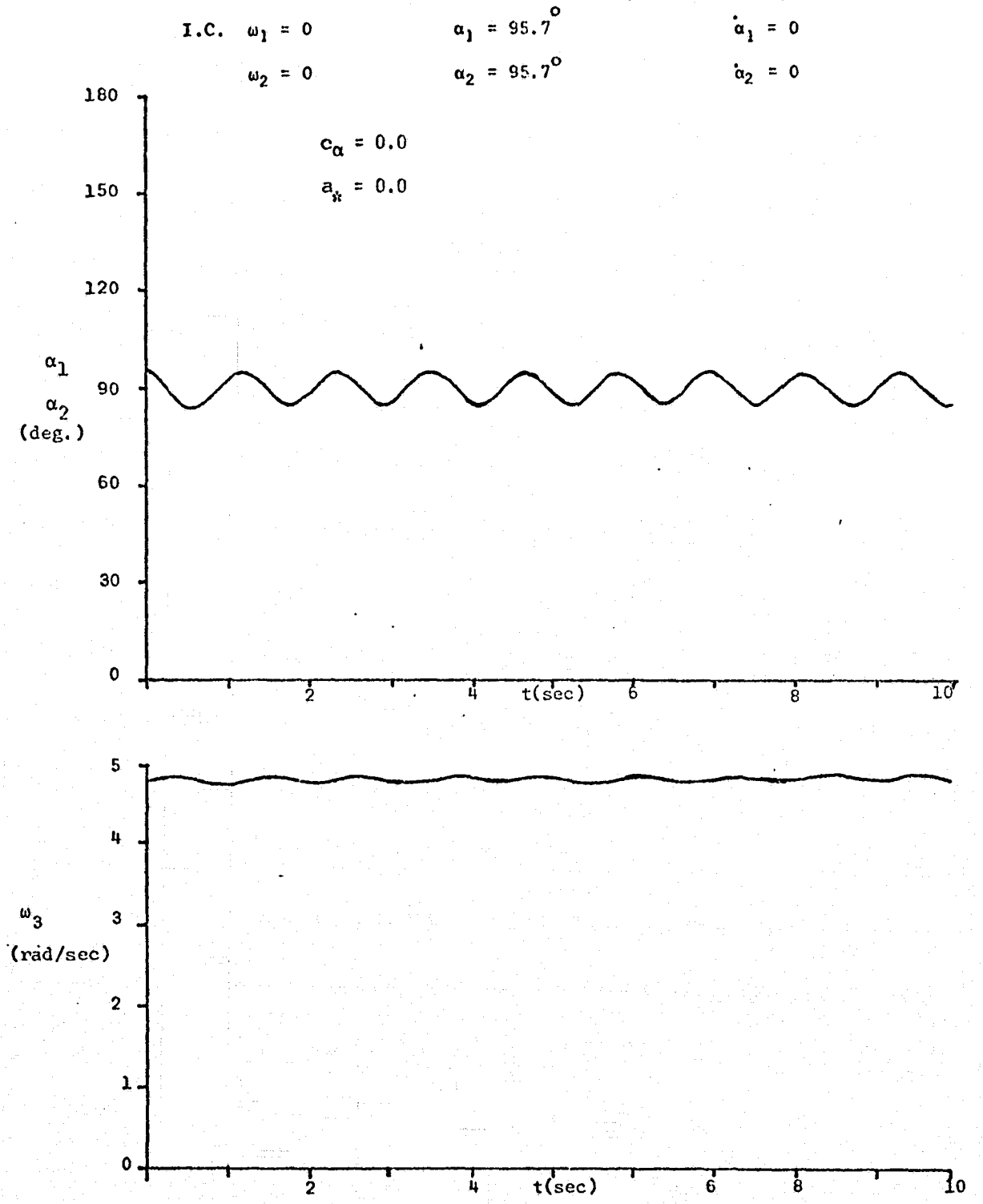

FIG. 2.3(a). DYNAMICS OF THE SYSTEM ABOUT 90° EQUILIBRIUM POSITION (NO HINGE DAMPING).

TWO DIMENSIONAL MOTION-SMALL AMPLITUDE ANALYSIS

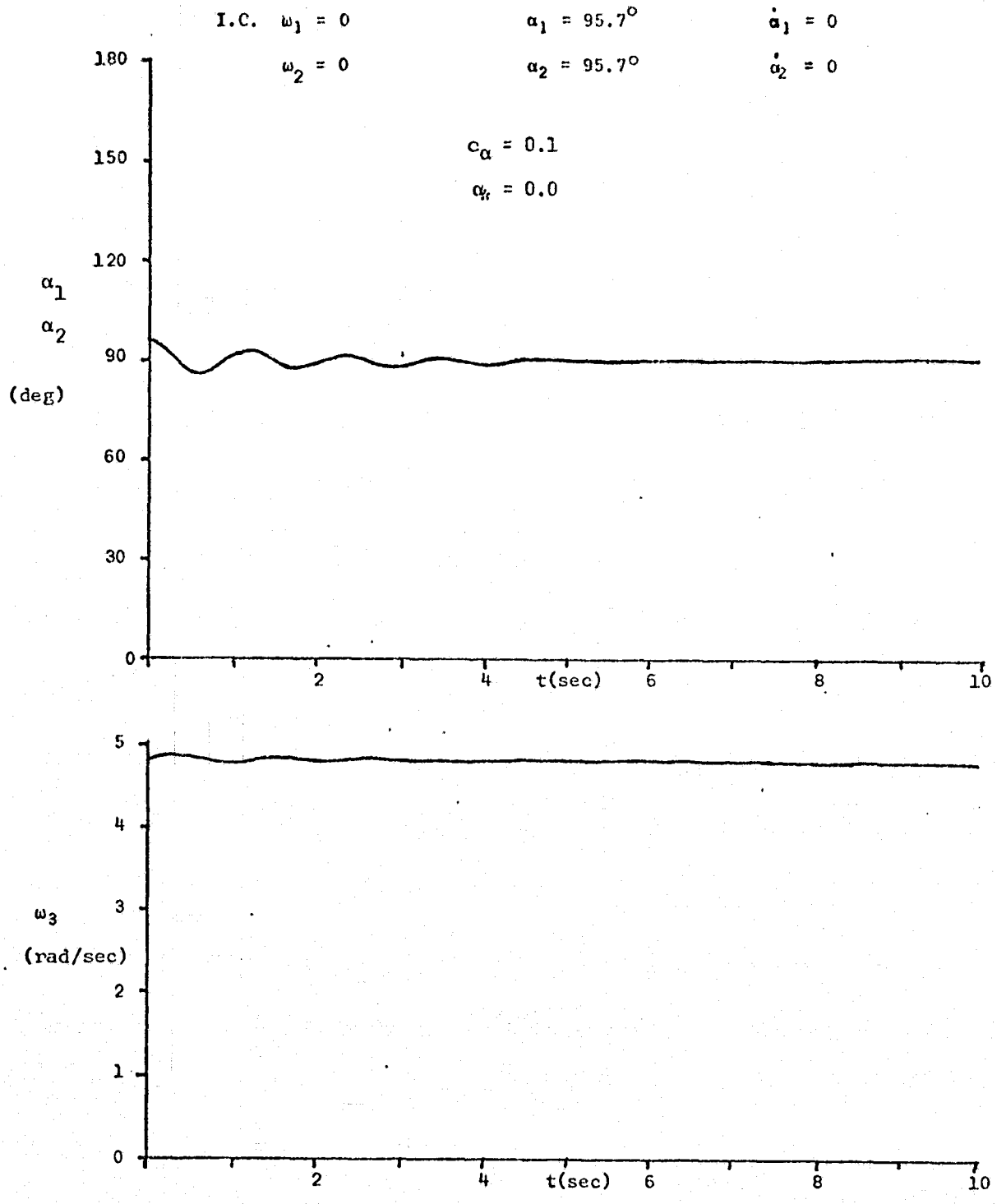

FIG. 2.3(b). DYNAMICS OF THE SYSTEM ABOUT 90° EQUILIBRIUM POSITION WITH HINGE DAMPING.

TWO DIMENSIONAL MOTION-LARGE AMPLITUDE ANALYSIS

I.C. $\omega_1 = 0$ $\alpha_1 = 0$ $\dot{\alpha}_1 = 0$

$\omega_2 = 0$ $\alpha_2 = 0$ $\dot{\alpha}_2 = 0$

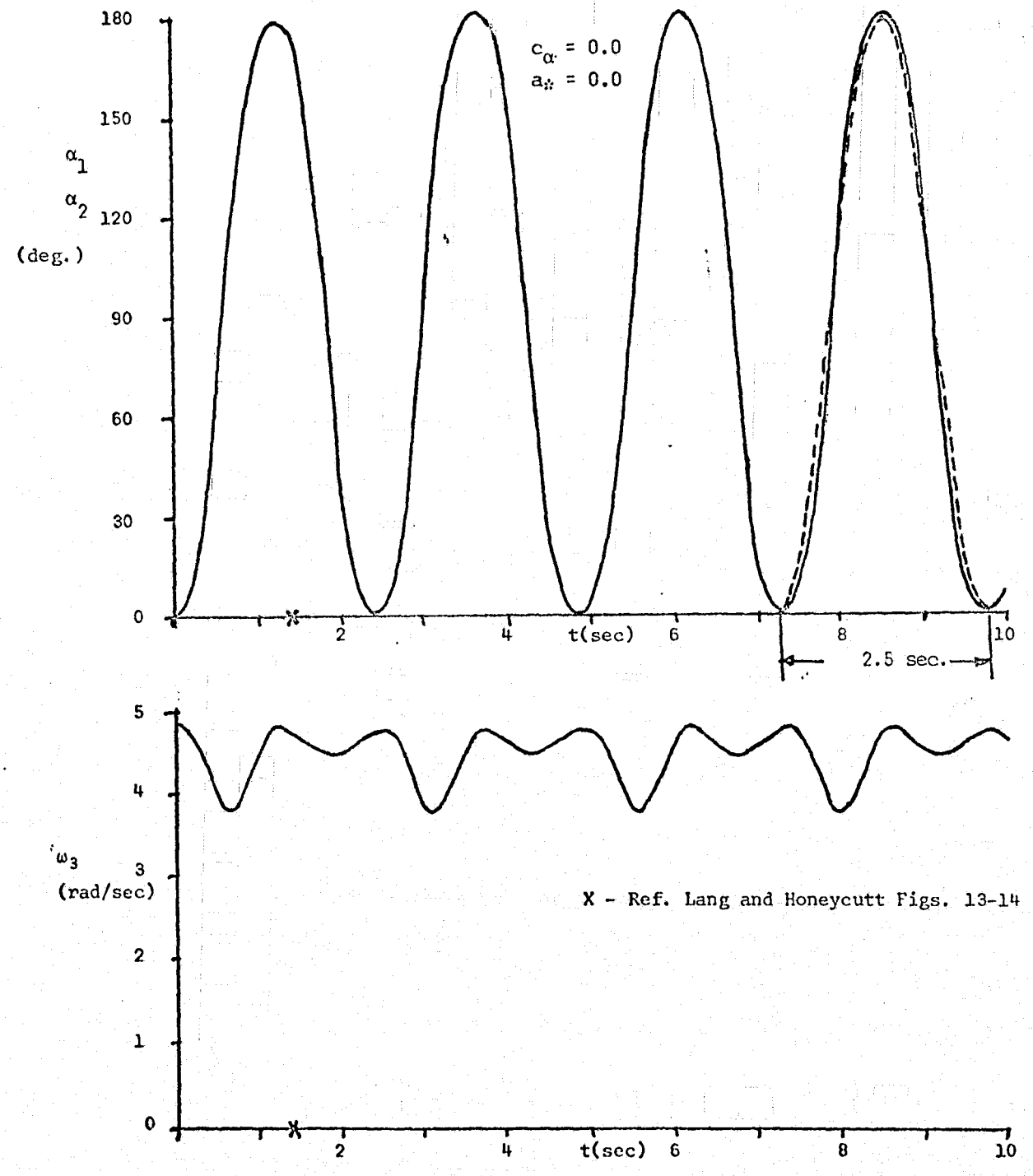

FIG. 2.4(a). DEPLOYMENT DYNAMICS OF THE SYSTEM (ZERO I-CS) - NO HINGE DAMPING

TWO DIMENSIONAL MOTION-LARGE AMPLITUDE ANALYSIS

I.C: $\omega_1 = 0$ $\alpha_1 = 0$ $\dot{\alpha}_1 = 0$

$\omega_2 = 0$ $\alpha_2 = 0$ $\dot{\alpha}_2 = 0$

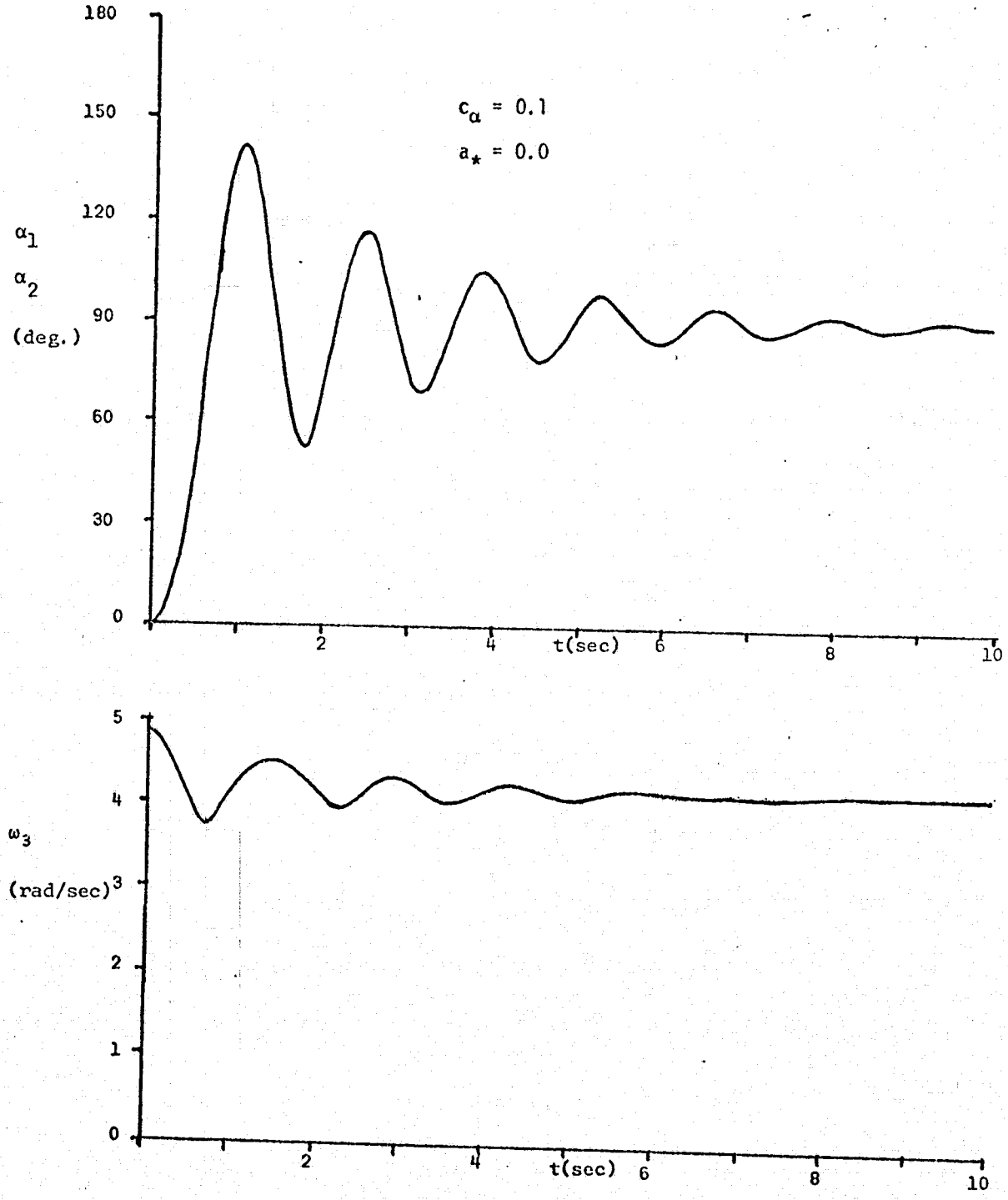

FIG. 2.4(b). DEPLOYMENT DYNAMICS OF THE SYSTEM WITH HINGE DAMPING (ZERO I-CS).

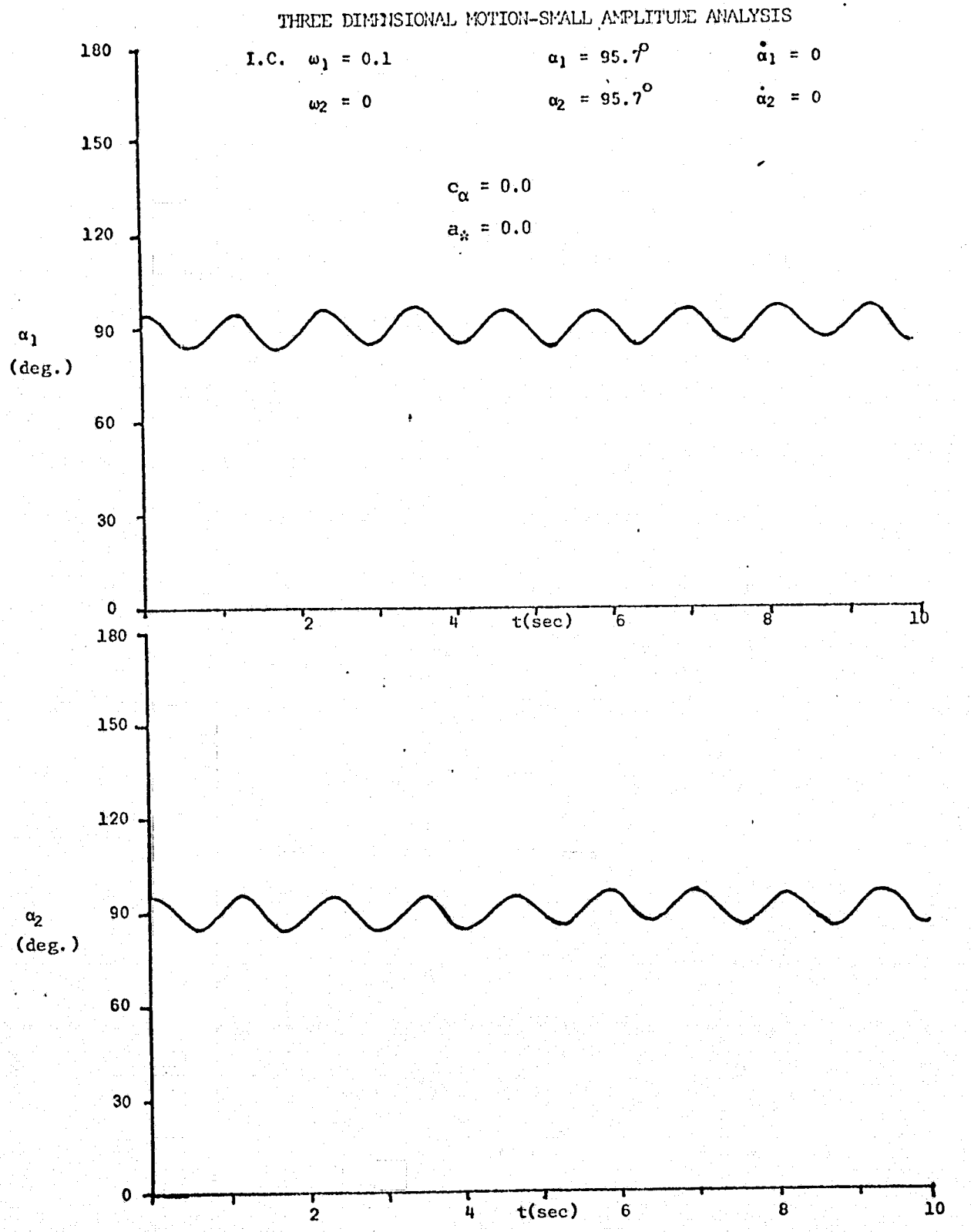

FIG. 2.5(a). TIME RESPONSE OF HINGE ANGLES (ABOUT 90° EQUILIBRIUM STATE) WITH INITIAL TRANSVERSE RATE (NO HINGE DAMPING).

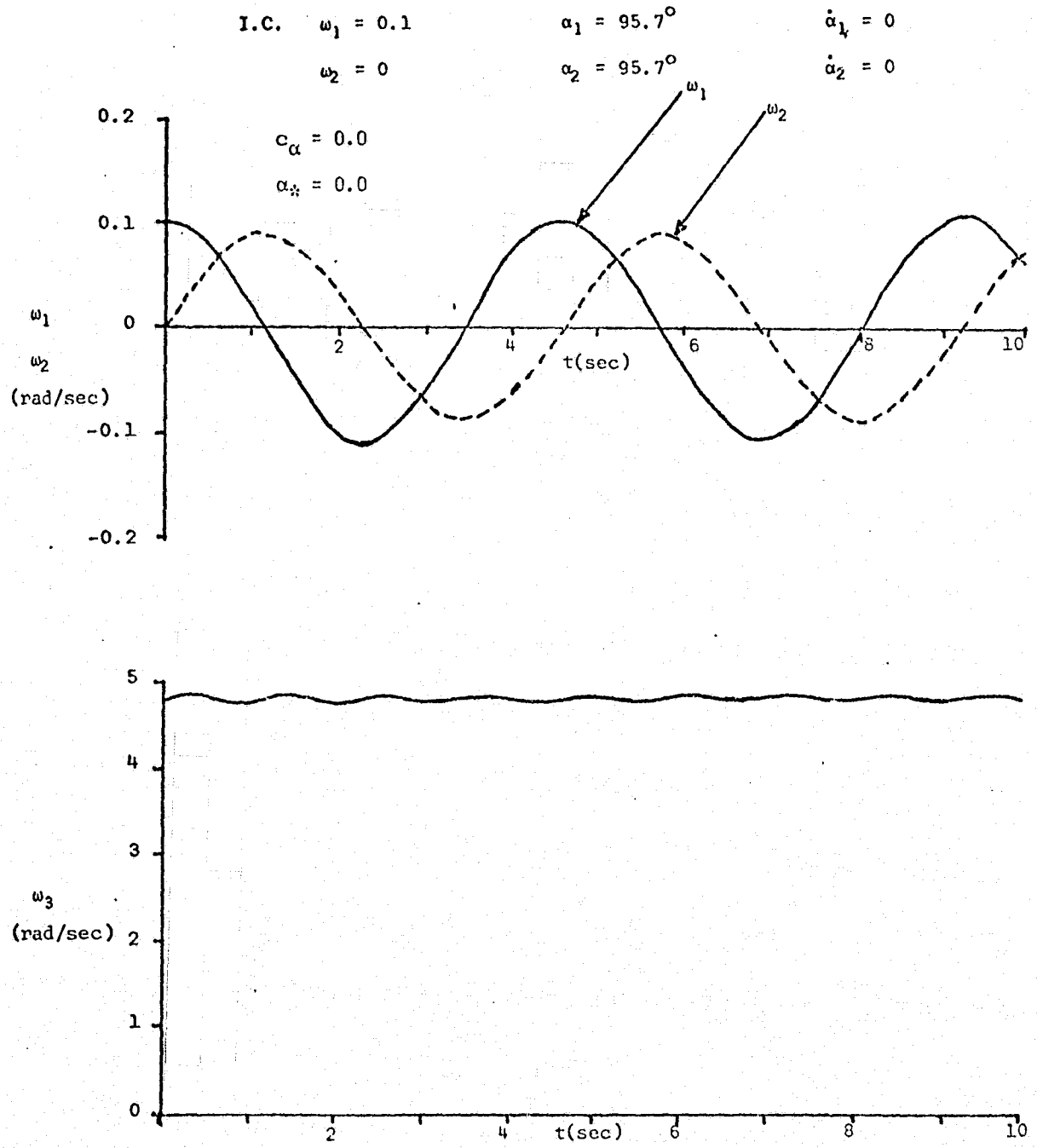

FIG. 2.5(b). TIME RESPONSE OF ANGULAR RATES (ABOUT 90° EQUILIBRIUM STATE) WITH INITIAL TRANSVERSE RATE (NO HINGE DAMPING).

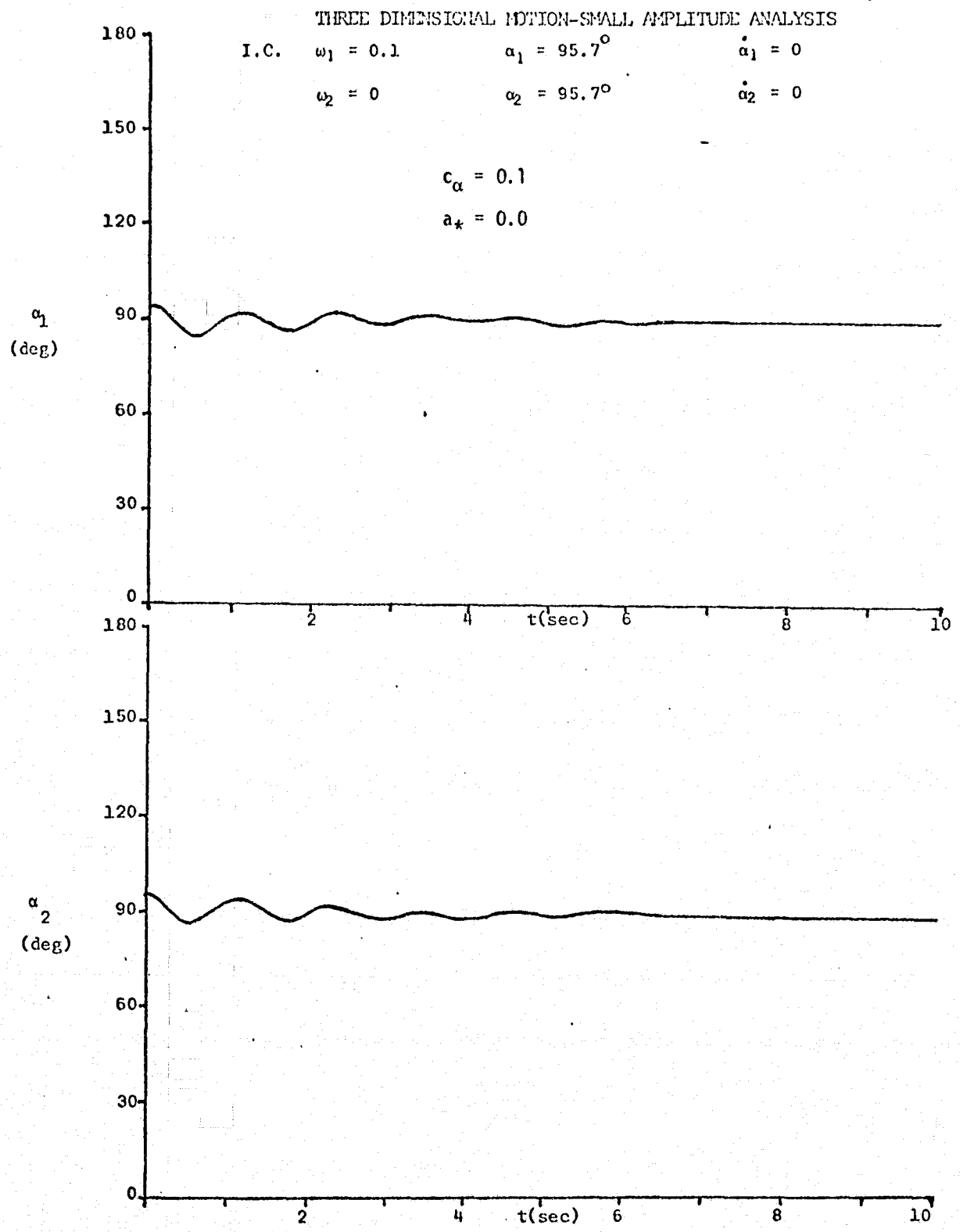

FIG. 2.6(a). TIME RESPONSE OF HINGE ANGLES - SAME AS IN FIG. 2.5(b) - WHEN HINGLE DAMPING IS PRESENT.

THREE DIMENSIONAL MOTION-SMALL AMPLITUDE ANALYSIS

I.C. $\omega_1 = 0.1$ $\alpha_1 = 95.7^\circ$ $\dot{\alpha}_1 = 0$

$\omega_2 = 0$ $\alpha_2 = 95.7^\circ$ $\dot{\alpha}_2 = 0$

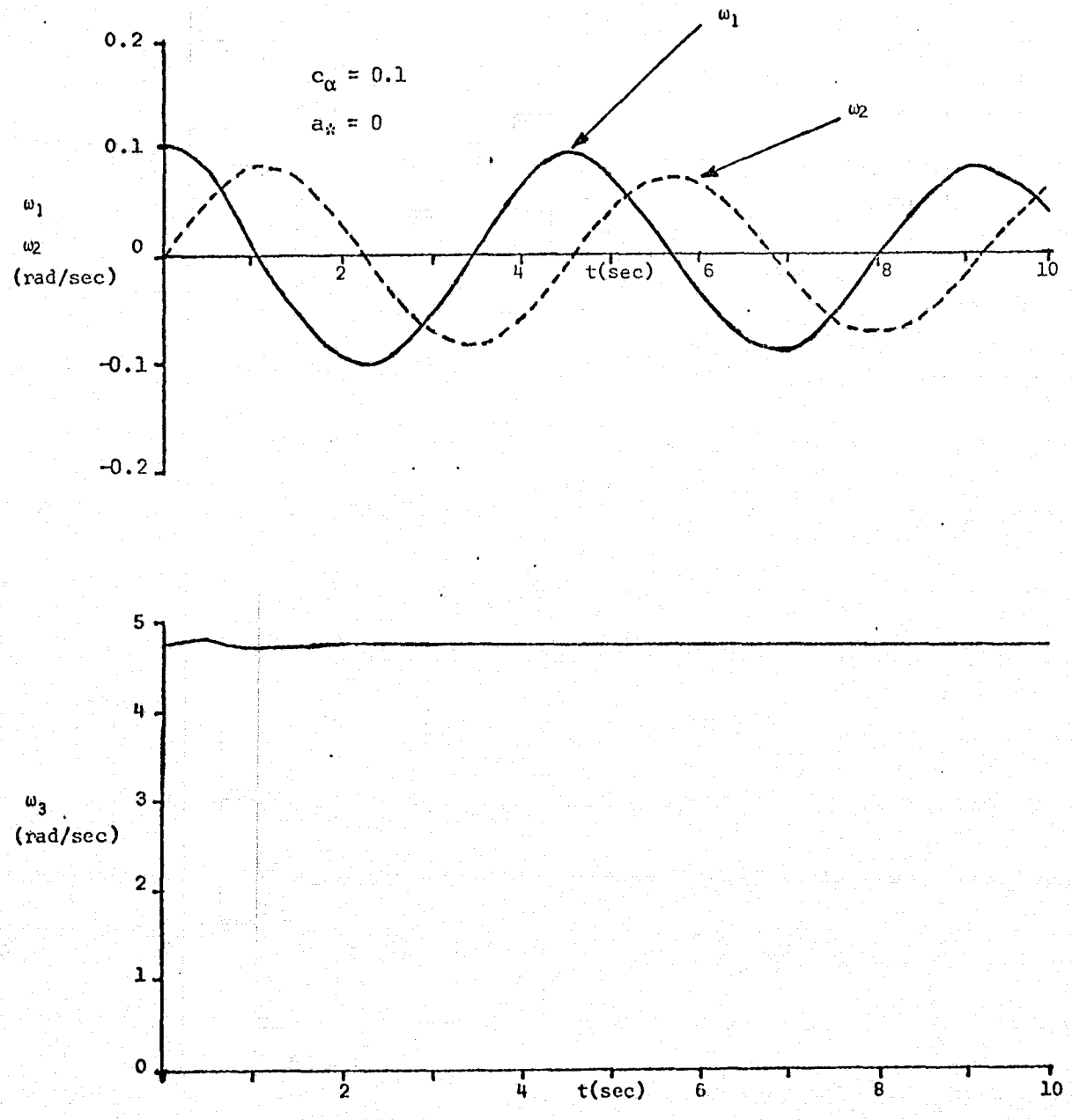

FIG. 2.6(b). TIME RESPONSE OF ANGULAR RATES - SAME AS IN FIG. 2.5(b) WHEN HINGE DAMPING IS PRESENT.

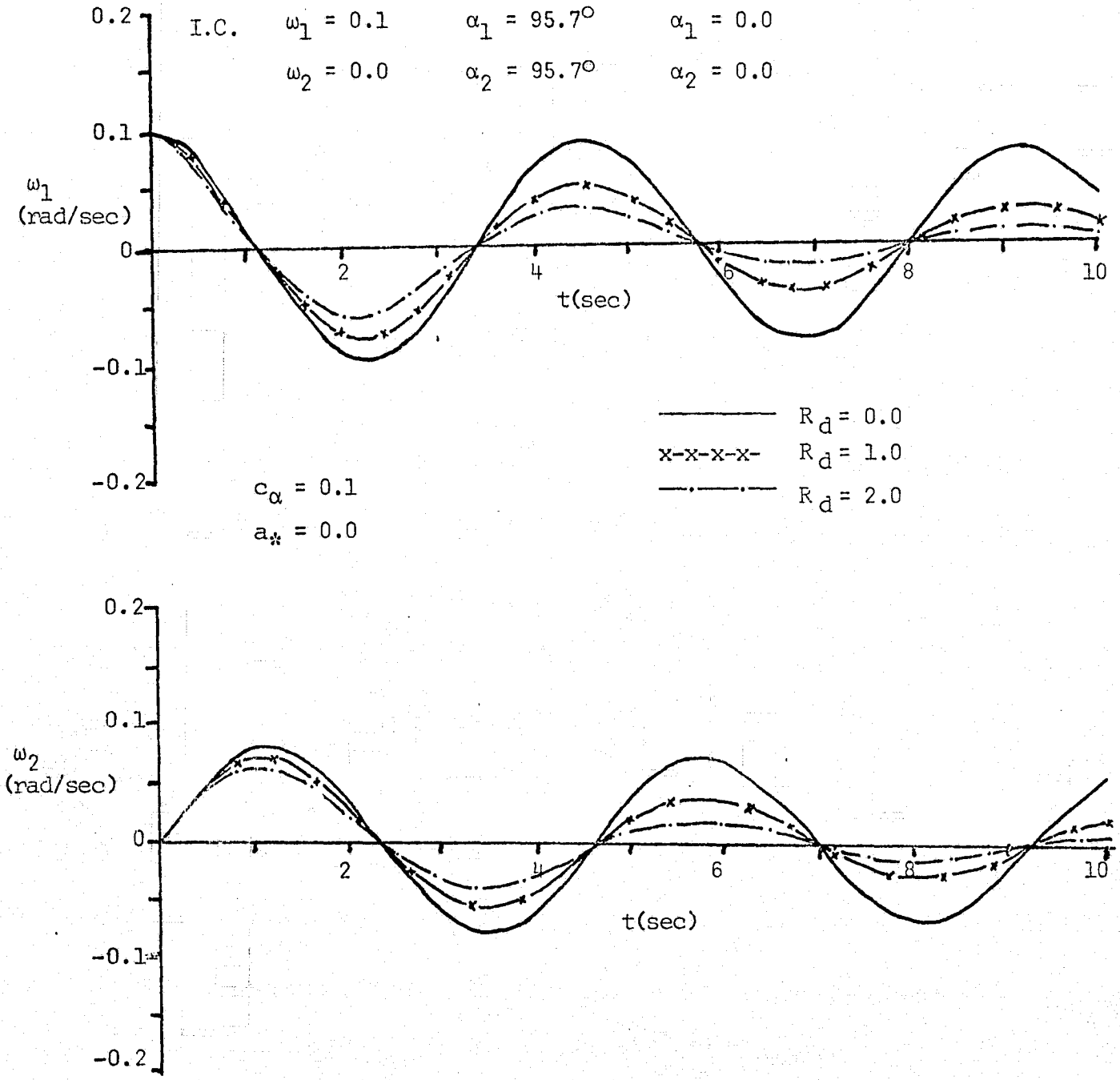

FIG. 2.7. TIME RESPONSE OF THE TRANSVERSE ANGULAR RATES WITH VARIATION OF RATE DAMPING.

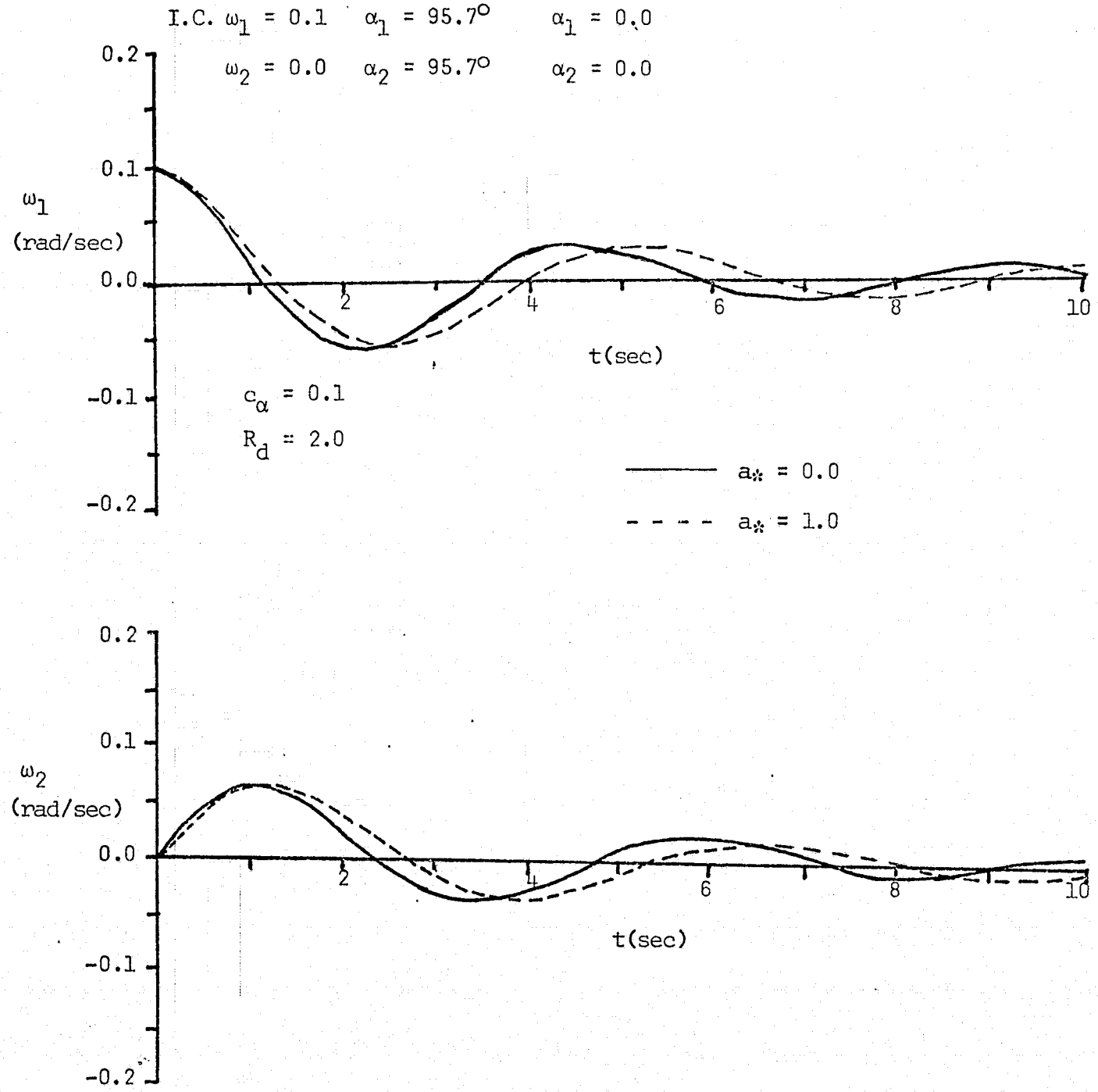

FIG. 2.8. EFFECT OF VERTICAL OFFSET (a_*) ON THE TIME RESPONSE OF THE TRANSVERSE ANGULAR RATES

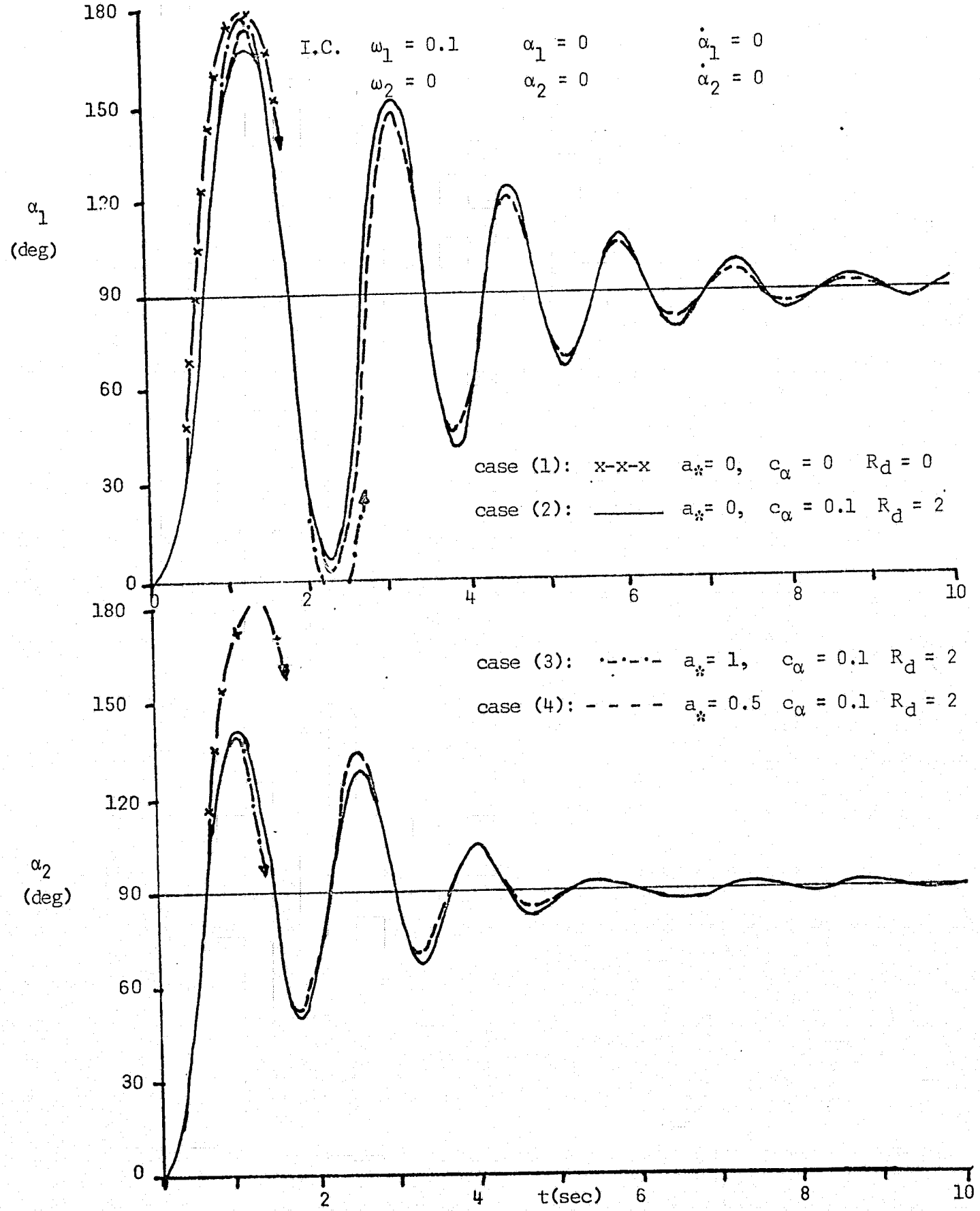

FIG. 2.9(a). DEPLOYMENT DYNAMICS OF THE MORE GENERAL CASE

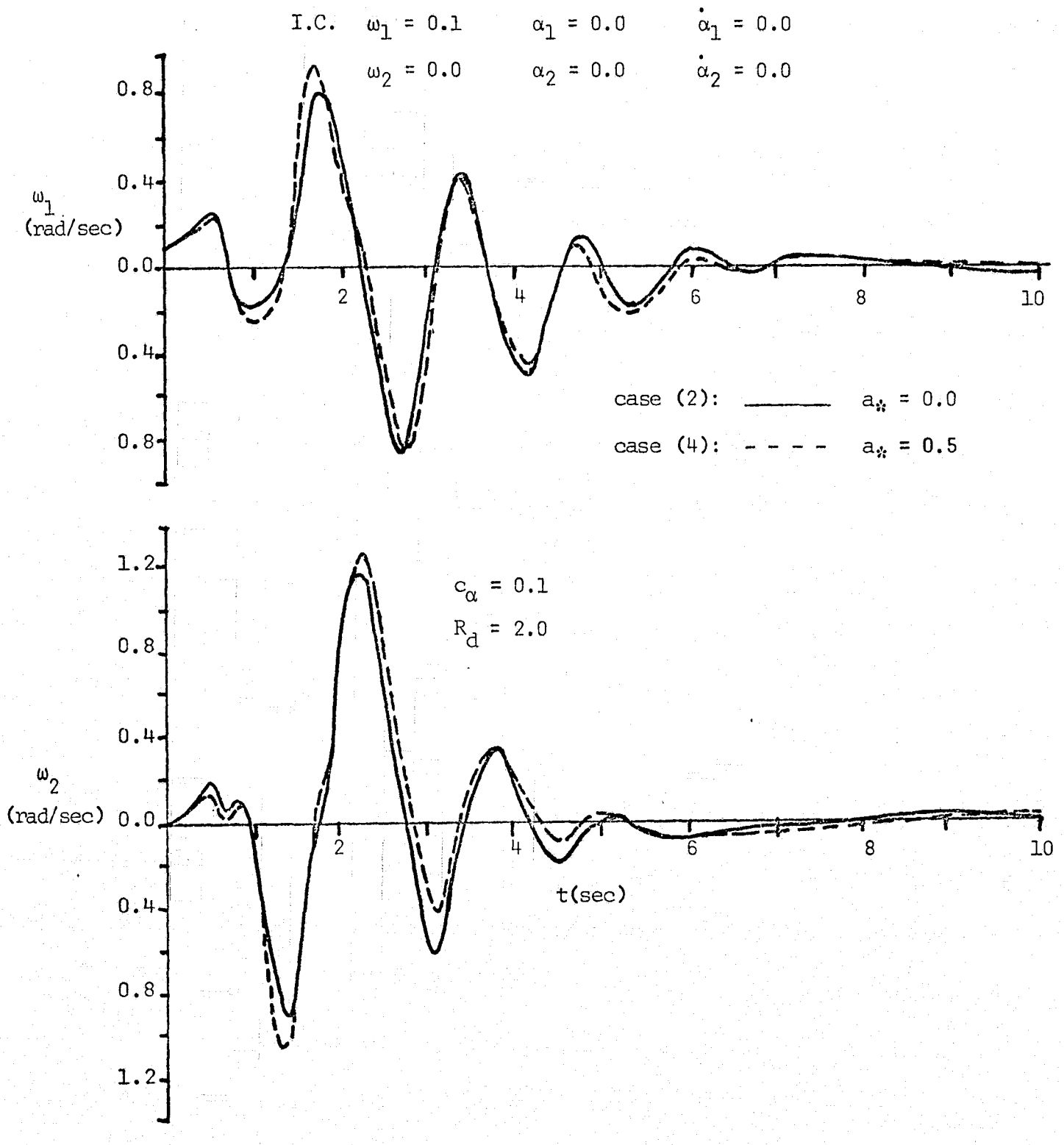

FIG. 2.9(b). DEPLOYMENT DYNAMICS OF THE MORE GENERAL CASE.

THREE DIMENSIONAL MOTION-LARGE AMPLITUDE ANALYSIS

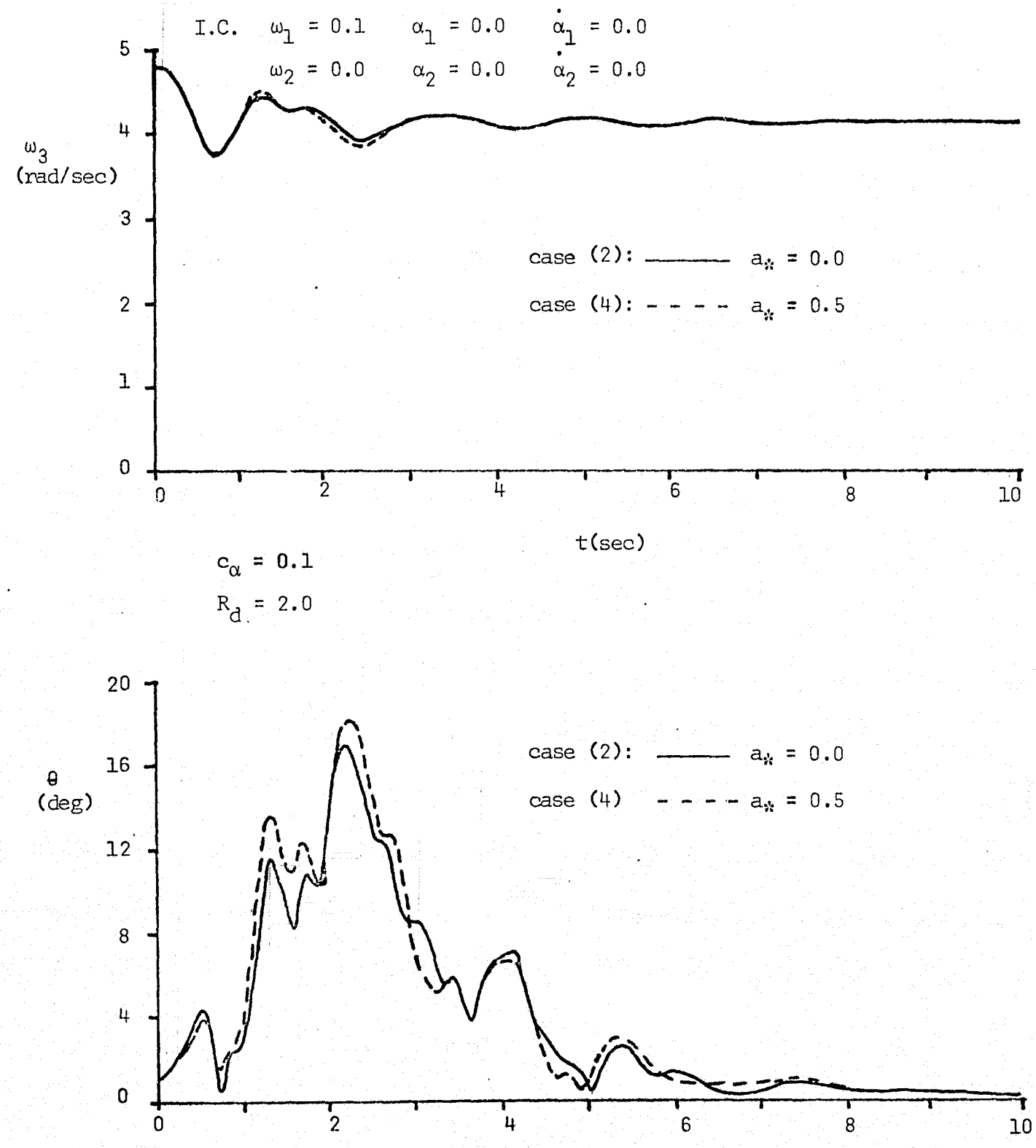

FIG. 2.9(c). DEPLOYMENT DYNAMICS OF THE MORE GENERAL CASE.

III. EQUATIONS OF MOTION WITH TELESCOPIC TYPE CONTROL BOOMS

The complete equations of motion of a rigid spacecraft with telescopic type control booms are developed. The system is assumed to consist of (Fig. 3.1) a central hub with center of mass at point Q and one or two extendible telescoping booms with end masses m_1 and m_2, respectively. The mass along the boom lengths is assumed negligible in comparison with the end masses. It is assumed that, in general, the two booms will be offset from the hub principal axes with the coordinates a,b,c,d indicating the amount of offset.

The generalized vector equation of motion for such a system containing a central hub and moving connected masses can be written [12]:

$$\bar{M}_Q = \dot{\bar{L}}_Q + \sum_{k=1}^{N} m_k \, (\bar{r}_{k/Q}) \times \ddot{\bar{r}}_Q \qquad (3.1)$$

where $\bar{M}_Q$ refers to the external moments, Q refers to the reference point which is assumed to be at the center of mass of the hub, $\ddot{\bar{r}}_Q$ is the inertial acceleration of the reference point and $\bar{r}_{k/Q}$ is the position vector of mass, m_k, with respect to point Q (Fig. 3.2). It should also be noted that $\bar{R}_c$ is the position vector of the composite system center of mass whose position will change with the movement of m_1 and m_2. The composite c.m. is assumed to move in a circular orbit, and it is assumed that coupling between orbital (translational) motion and the attitude dynamics is a higher order effect.

The angular momentum of the system measured with respect to point, Q, has three components,

$$\bar{L}_Q = \bar{L}_{b/Q} + \bar{L}_{m_1/Q} + \bar{L}_{m_2/Q} \tag{3.2}$$

where $\bar{L}_{b/Q}$ describes the momentum of the hub, and $\bar{L}_{m_i/Q}$ describes the momentum of mass m_i. The hub momentum may be expressed in terms of the hub principal moments of inertia and angular velocity components as:

$$\bar{L}_{b/Q} = I_1\omega_1\bar{i} + I_2\omega_2\bar{j} + I_3\omega_3\bar{k} \tag{3.3}$$

where $\bar{i},\bar{j},\bar{k}$ are unit vectors along the hub principal axes, and

$$\bar{L}_{m_i/Q} = m_i\ (\bar{r}_i \times \dot{\bar{r}}_i)\ ;\quad i = 1,2 \tag{3.4}$$

where $\bar{r}_i$ describes the position of m_i relative to $Q(\bar{r}_{i/Q})$.

We will now consider the inertial acceleration of the reference point (Fig. 3.2)

$$\ddot{\bar{r}}_Q = \ddot{\bar{R}}_c - \ddot{\bar{r}}_c \tag{3.5}$$

In the absence of external perturbation forces and within the previous assumptions $\ddot{\bar{R}}_c = 0$, and,

$$\ddot{\bar{r}}_Q = -\ddot{\bar{r}}_c \tag{3.6}$$

From the definition of the system center of mass we can relate

$$\ddot{\bar{r}}_Q = -\frac{m_1\ddot{\bar{r}}_1 + m_2\ddot{\bar{r}}_2}{M + \Sigma m} \tag{3.7}$$

where M represents the hub mass and

$$\Sigma m = m_1 + m_2$$

After substituting Eqs. (3.3), (3.4) and (3.7) into Eq. (3.1) and assuming the external torques vanish, the following vector rotational equation results:

$$\dot{\bar{L}}_{b/Q} + \bar{\mu}_1 (\bar{r}_1 \times \ddot{\bar{r}}_1) + \ddot{\mu}_2 (\bar{r}_2 \times \ddot{\bar{r}}_2) + \mu_3 (\bar{r}_1 \times \ddot{\bar{r}}_2 + \bar{r}_2 \times \ddot{\bar{r}}_1) = 0 \tag{3.8}$$

where

$$\mu_1 = m_1 (M + m_2)/(M + \Sigma m)$$

$$\ddot{\mu}_2 = m_2 (M + m_1)/(M + \Sigma m)$$

$$\mu_3 = - m_1 m_2/(M + \Sigma m)$$

Eq. (3.8) is then expanded using the familiar relationship,

$$\dot{\bar{L}}_{b/Q} = \left.\frac{dL_b}{dt}\right|_{body} + \bar{\omega} \times \bar{L}_{b/Q} \tag{3.9}$$

and for the specific geometry of Fig. 3.1,

$$r_1 = a\bar{i} + b\bar{j} + z\bar{k} \tag{3.10}$$

$$r_2 = x\bar{i} + c\bar{j} + d\bar{k} \tag{3.11}$$

The acceleration terms $\ddot{\bar{r}}_i$ $(i = 1,2)$ may be calculated by using[12],

$$\ddot{\bar{r}}_i = \bar{\omega} \times (\bar{\omega} \times \bar{r}_i) + \dot{\bar{\omega}} \times \bar{r}_i + 2\bar{\omega} \times [\dot{\bar{r}}_i]_{body} + [\ddot{\bar{r}}_i]_{body}$$

together with Eqs. (3.10) and (3.11).

The complete nonlinear equations of motion are obtained by expansion of Eq. (3.8) and are expressed as

$$I_1\dot{\omega}_1 + (I_3 - I_2)\,\omega_2\omega_3 + \mu_1 [(b^2+z^2)\,\dot{\omega}_1 - ab\dot{\omega}_2 - az\dot{\omega}_3 - az\omega_1\omega_2 + (b^2-z^2)\,\omega_2\omega_3 + ab\omega_1\omega_3 + 2z\dot{z}\,\omega_1 + bz\,(\omega_3^2 - \omega_2^2) + b\ddot{z}] + \mu_2 [(c^2+d^2)\,\dot{\omega}_1$$

$$-cx\dot{\omega}_2 - dx\dot{\omega}_3 - dx\omega_1\omega_2 + (c^2-d^2)\,\omega_2\omega_3$$
$$+cx\omega_1\omega_3 - 2c\dot{x}\omega_2 - 2d\dot{x}\omega_3 + cd\,(\omega_3^2-\omega_2^2)]$$
$$+\mu_3[2(bc+dz)\,\dot{\omega}_1 - (ac+bx)\,\dot{\omega}_2 - (ad+xz)\,\dot{\omega}_3$$
$$-(ad+zx)\omega_1\omega_2 + 2(bc-dz)\,\omega_2\omega_3 + (ac+bx)\,\omega_1\omega_3$$
$$+2d\dot{z}\omega_1 - 2b\dot{x}\omega_2 - 2\dot{x}z\omega_3 + (bd+cz)\,(\omega_3^2-\omega_2^2) + c\ddot{z}] = 0 \qquad (3.13)$$

$$I_2\dot{\omega}_2 + (I_1-I_3)\,\omega_3\omega_1 - \mu_1\,[ab\dot{\omega}_1 - (a^2+z^2)\,\dot{\omega}_2$$
$$+bz\dot{\omega}_3 - bz\omega_1\omega_2 + ab\omega_2\omega_3 + (a^2-z^2)\,\omega_3\omega_1$$
$$-2z\dot{z}\omega_2 + az(\omega_3^2-\omega_1^2) + a\ddot{z}] - \mu_2[cx\dot{\omega}_1$$
$$-(d^2+x^2)\dot{\omega}_2 + cd\dot{\omega}_3 - cd\omega_1\omega_2 + cx\omega_2\omega_3$$
$$+(x^2-d^2)\omega_3\omega_1 - 2x\dot{x}\omega_2 + dx(\omega_3^2-\omega_1^2) - d\ddot{x}]$$
$$-\mu_3[(ac+bx)\dot{\omega}_1 - 2(ax+dz)\dot{\omega}_2 + (bd+cz)\dot{\omega}_3$$
$$-(bd+cz)\omega_1\omega_2 + (ac+bx)\omega_2\omega_3 + 2(ax-dz)\omega_3\omega_1$$
$$-2(a\dot{x}+d\dot{z})\omega_2 + (ad+xz)\,(\omega_3^2-\omega_1^2)$$
$$+x\ddot{z} - z\ddot{x}] = 0 \qquad (3.14)$$

$$I_3\dot{\omega}_3 + (I_2-I_1)\,\omega_1\omega_2 - \mu_1[az\dot{\omega}_1 + bz\dot{\omega}_2$$
$$-(a^2+b^2)\,\dot{\omega}_3 + (b^2-a^2)\,\omega_1\omega_2 - az\omega_2\omega_3 + bz\omega_3\omega_1$$
$$+2az\dot{\omega}_1 + 2bz\dot{\omega}_2 + ab(\omega_1^2-\omega_2^2)] - \mu_2[dx\dot{\omega}_1$$
$$+cd\dot{\omega}_2 - (c^2+x^2)\,\dot{\omega}_3 + (c^2-x^2)\,\omega_1\omega_2$$
$$-dx\omega_2\omega_3 + cd\omega_3\omega_1 - 2x\dot{x}\omega_3 + cx(\omega_1^2$$
$$-\omega_2^2) + c\ddot{x}] - \mu_3\,[(ad+xz)\,\dot{\omega}_1 + (bd+cz)\,\dot{\omega}_2$$
$$-2(bc+ax)\,\dot{\omega}_3 + 2\,(bc-ax)\,\omega_1\omega_2 - (ad+xz)\,\omega_2\omega_3$$
$$+(bd+cz)\,\omega_3\omega_1 + 2x\dot{z}\omega_1 + 2c\dot{z}\omega_2 - 2a\dot{x}\omega_3$$
$$+(ac+bx)\,(\omega_1^2 - \omega_2^2) + b\ddot{x}] = 0 \qquad (3.15)$$

Eqs. (3.13) - (3.15) are three coupled, non-linear differential equations for the spacecraft dynamics in terms of the angular rates $(\omega_1,\omega_2,\omega_3)$, the positions of the control boom end - masses (a,b,z) and (x,c,d), and the corresponding velocities $(\dot{z},\dot{x})$, and accelerations $(\ddot{z},\ddot{x})$. These equations are valid irrespective of the physical mechanism which causes the control booms to excute their motions. For the special case where $m_2 = 0$, these equations correspond identically with Eqs. (2) - (4) of Ref. [4], when $\bar{r}_1$ has been defined according to Eq. (3.10).

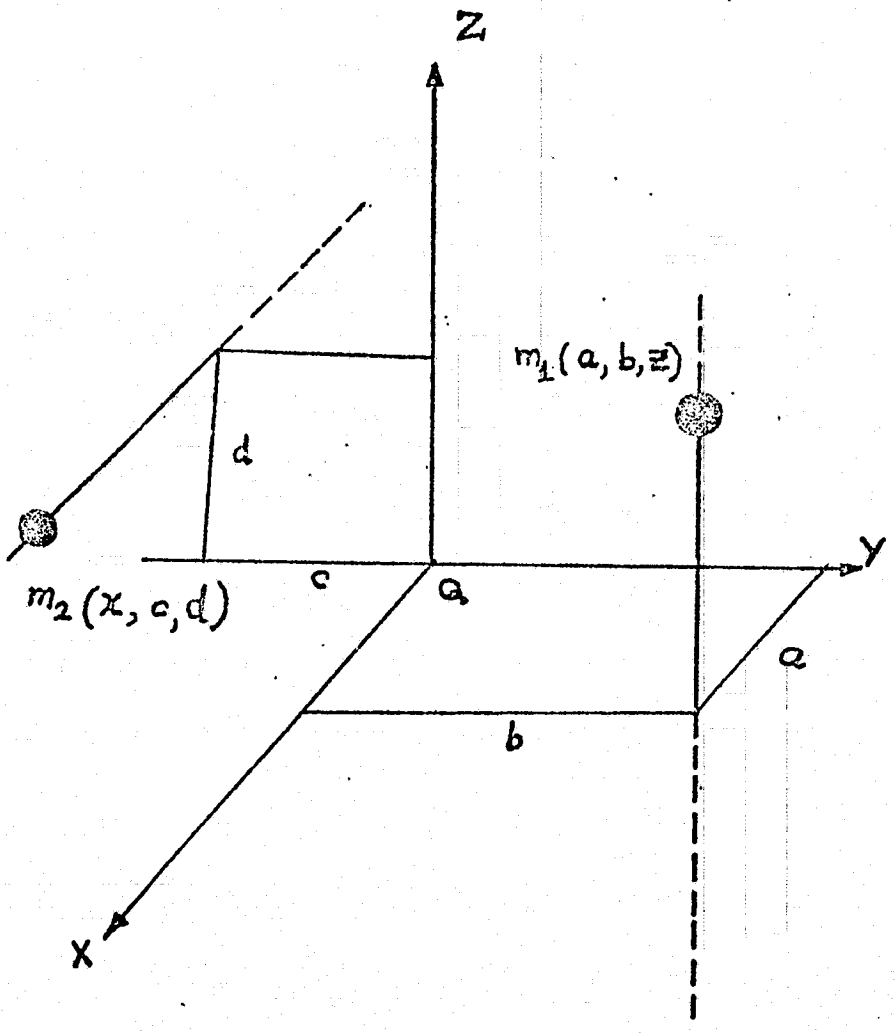

FIG. 3.1. TWO BOOM OFFSET ORIENTATION SYSTEM.

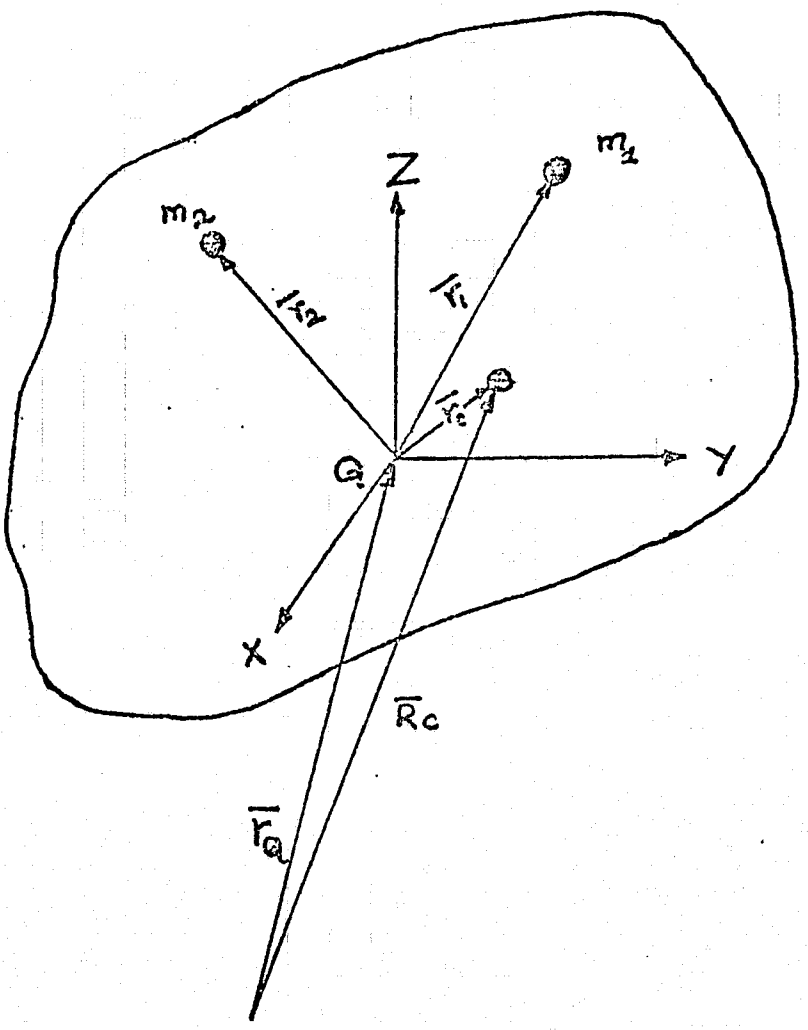

FIG. 3.2. GENERAL CASE OF TWO MASS OFFSET SYSTEM.

IV. OPTIMAL CONTROL WITH QUADRATIC PERFORMANCE CRITERIA

1. Linearization of Equations of Motion

The equations of motion developed in Chapter III represented by Eqs. (3.13)-(3.15) are linearized about the following desired final state: $\omega_1 = \omega_2 = 0$, $\omega_3 = \Omega$. It is assumed that $\omega_i/\Omega << 1$ $(i = 1,2)$, $|\omega_3 - \Omega|/\Omega << 1$, and that x/ℓ_m, and z/ℓ_m are both $<<1$, where ℓ_m is the maximum boom length. In order to develop the linear system equations in non-dimensional form we further let: $\alpha = \omega_1/\Omega$; $\beta = \omega_2/\Omega$; $1 + \gamma = \omega_3/\Omega$; $\tau = \Omega t$; $\bar{I}_i = I_i/\mu\ell_m^2$ $(i = 1,2,3)$ where μ=reference mass; $\xi = x/\ell_m$; $\zeta = z/\ell_m$; $c_1 = a/\ell_m$; $c_2 = b/\ell_m$; $c_3 = c/\ell_m$; $c_4 = d/\ell_m$; and denote derivatives with respect to the nondimensional time, τ, by primes ('). The variational coordinates are α, β, γ whereas ξ and ζ represent the control variables and describe the end mass positions.

For the case of a single-boom system (Fig. 4.1), $m_2 = \mu_3 = 0$, and letting $\mu = \mu_1$ the linear system can be expressed by:

$$\begin{bmatrix} \bar{I}_1 + c_2^2 & -c_1c_2 & 0 \\ -c_1c_2 & \bar{I}_2+c_1^2 & 0 \\ 0 & 0 & \bar{I}_3+c_1^2+c_2^2 \end{bmatrix} \begin{bmatrix} \alpha' \\ \beta' \\ \gamma' \end{bmatrix} =$$

$$\begin{bmatrix} -c_1c_2 & -(\bar{I}_3-\bar{I}_2+c_2^2) & 0 \\ (\bar{I}_3-\bar{I}_1+c_1^2) & c_1c_2 & 0 \\ 0 & 0 & 0 \end{bmatrix} \begin{bmatrix} \alpha \\ \beta \\ \gamma \end{bmatrix} + \begin{bmatrix} -c_2 \\ c_1 \\ 0 \end{bmatrix} [U] \qquad (4.1)$$

where

$$[U]=[\zeta'' + \zeta] \qquad (4.2)$$

It should be noted that for such a system three-axis control with a single boom can not be achieved since $\gamma' = 0$. Eq. (4.1) can be reduced to the standard from: $X' = AX + BU$, where $X^T = (\alpha\ \beta)$ and the elements of A are:

$$A_{11} = c_1c_2(\bar{I}_3-\bar{I}_1-\bar{I}_2)\ /\Delta$$

$$A_{12} = -\{(\bar{I}_3-\bar{I}_2)(\bar{I}_2+c_1^2) + \bar{I}_2c_2^2\}/\Delta$$

$$A_{21} = \{(\bar{I}_3-\bar{I}_1)(\bar{I}_1+c_2^2) + \bar{I}_1c_1^2\}/\Delta$$

$$A_{22} = -c_1c_2(\bar{I}_3-\bar{I}_1-\bar{I}_2)/\Delta \qquad (4.3)$$

$$B = \begin{bmatrix} -\bar{I}_2c_2/\Delta \\ \bar{I}_1c_1/\Delta \end{bmatrix} \qquad (4.4)$$

and $\Delta = \bar{I}_1\bar{I}_2 + c_1^2\bar{I}_1 + c_2^2\ \bar{I}_2$

It is further noted that offset of the single m_1 boom from at least one of the hub principal axes is required for control, since if $c_1 = c_2 = 0$ the system is uncontrolled.

A final state of zero inertial angular velocity can also be considered by nondimensionalizing using an arbitrary reference value of ω_R such that $\omega_i/\omega_R \ll 1$ for $i = 1,2,3$ in place of Ω. Here the non-dimensional variational coordinates are: $\alpha = \omega_1/\omega_R$; $\beta = \omega_2/\omega_R$; $\delta = \omega_3/\omega_R$; and other parameters are defined as earlier. The resulting linear system reduces to

$$X' = A\ \delta(0)\ X + BU \qquad (4.5)$$

where

$$\delta(0) = \omega_3(0) / \omega_R$$

$$U = \zeta'' + \delta(0)\zeta$$

Eq. (4.5) is similar to the standard form $X' = AX + BU$.

For the two-boom case when $d = c_4 = 0$ and the equilibrium state is: $\omega_1 = \omega_2 = 0$, $\omega_3 = \Omega$, it is also possible to reduce the linear system to the standard form:

$$DX' = EX + FU \tag{4.6}$$

where the non-zero elements of the D and E matrices are:

$$D_{11} = \bar{I}_1 + (\mu_1/\mu)\, c_2^2 + (\mu_2/\mu)\, c_3^2 + 2\,(\mu_3/\mu)\, c_2 c_3$$

$$D_{12} = -(\mu_1 c_1 c_2 + \mu_3 c_1 c_3) / \mu = D_{21}$$

$$D_{22} = \bar{I}_2 + (\mu_1/\mu)\, c_1^2$$

$$D_{33} = \bar{I}_3 + (\mu_1/\mu)\,(c_1^2 + c_2^2) + (\mu_2/\mu)\, c_3^2 + 2\,(\mu_3/\mu)\, c_2 c_3$$

$$E_{11} = -(\mu_1 c_1 c_2 + \mu_3 c_1 c_3) / \mu$$

$$E_{12} = -(\bar{I}_3 - \bar{I}_2 + (\mu_1/\mu)\, c_2^2 + (\mu_2/\mu)\, c_3^2 + 2\,(\mu_3/\mu)\, c_2 c_3)$$

$$E_{21} = \bar{I}_3 - \bar{I}_1 + (\mu_1/\mu)\, c_1^2$$

$$E_{22} = (\mu_1/\mu)\, c_1 c_2 + (\mu_3/\mu)\, c_1 c_2$$

and:

$$F = \begin{bmatrix} -(\mu_1 c_2 - \mu_3 c_3) / \mu & 0 \\ (\mu_1 c_1) / \mu & 0 \\ 0 & (\mu_2 c_3 + \mu_3 c_2) / \mu \end{bmatrix} \tag{4.7}$$

$$U = \begin{bmatrix} \zeta'' + \zeta \\ \xi'' + f_1\, \xi' \end{bmatrix} \tag{4.8}$$

where

$$f_1 = -2c_1\mu_3/(\mu_2 c_3 + \mu_3 c_2)$$

Eq. (4.6) can be written as $X' = AX + BU$, where

$$A = D^{-1}E \tag{4.9}$$

$$B = D^{-1}F \tag{4.10}$$

The two-boom offset system will now provide three-axis control. The systems, Eqs. (4.1) and (4.6), have been linearized about a desired final state of spin about the '3' axis; while Eq. (4.5) has been linearized about a final state of zero inertial angular velocity.

2. Application of the Linear Regulator Problem

It is desired to design a constant gain regulator for the time invariant system

$$X' = AX + BU \tag{4.11}$$

which minimizes the quadratic performance index

$$J = \int_0^\infty (X^T QX + U^T RU)dt \tag{4.12}$$

where Q and R are constant positive definite symmetric weighting matrices. From the theory of optimal control[13] it is known that the control law is of the form:

$$U = -R^{-1}B^T KX \tag{4.13}$$

where K is the symmetric positive definite solution of the algebraic matrix Riccati equation:

$$KA + A^T K - KBR^{-1}B^T K + Q = 0 \tag{4.14}$$

In general the solution of Eq. (4.14) must be done using numerical algorithms because of the algebraic complexity of the problem.

For the applications considered here the control will be of the form:

$$U = g_1 \alpha + g_2 \beta = \zeta'' + \zeta \tag{4.15}$$

for the two-axis system;

and $$U_1 = h_{11} \alpha + h_{12} \beta + h_{13} \gamma = \zeta'' + \zeta \tag{4.16}$$

$$U_2 = h_{21} \alpha + h_{22} \beta + h_{23} \gamma = \xi'' + f_1 \xi' \tag{4.17}$$

for the three-axis system, where the g's and h's represent the calculated gain constants. For actual implementation of the control it will be necessary to measure the components of the main hub angular velocity vector (which are proportional to α,β,γ), perhaps with rate gyroscopes, and also to determine the length of z boom extension and time rate of x-boom extension, perhaps optically or with a counter attached to the motor which drives the booms. The necessary acceleration terms ζ'' and ξ'' can then be provided by adjusting the motor torque to a sufficient level. In this report it will be assumed that all measurements occur instantaneously and that there are no errors in measurements. It is hoped to treat these important effects in a later study with an application of the estimator problem.

3. Numerical Results

a. Two-axis control using a single boom to reduce nutation angle

When a single boom is offset from the z axis and the hub is symmetrical ($I = I_1 = I_2$) it is possible to solve the matrix Riccati equation analytically.

It is assumed that the boom is offset only along the '1' axis (b = 0) without any further loss of generality. The standard form of the equations of motion can be written, from Eqs. (4.1) - (4.4), as

$$\begin{bmatrix} \alpha' \\ \beta' \end{bmatrix} = \begin{bmatrix} 0 & -e \\ d & 0 \end{bmatrix} \begin{bmatrix} \alpha \\ \beta \end{bmatrix} + \begin{bmatrix} 0 \\ n \end{bmatrix} \quad [\zeta'' + \zeta] \qquad (4.18)$$

where

$$d = (\bar{I}_3 - \bar{I} + c_1^2) \; / \; (\bar{I} + c_1^2)$$

$$e = (\bar{I}_3 - \bar{I}) \; / \bar{I}$$

$$n = c_1 / \; (\bar{I} + c_1^2)$$

For this application of two-axis control it is logical to select the weighting matrix, Q, in the performance index, J, Eq. (4.12), to have diagonal elements inversely proportional to the maximum expected value of transverse rate[6]

$$Q = \begin{bmatrix} f & 0 \\ 0 & f \end{bmatrix} \text{ where } f = \Omega^2 / \omega_{T_{max}}^2 \qquad (4.19)$$

and we will select R as a unit weighting matrix (following Ref. 6).

The expansion of the matrix Riccati equation Eq. (4.14), with the use of Eqs. (4.18) and 4.19), yields

$$2K_{12}d - n^2K_{12}^2 + f = 0 \qquad (4.20)$$

$$-K_{11}e + K_{22}d - n^2K_{12}K_{22} = 0 \qquad (4.21)$$

$$-2K_{12}e - n^2K_{22}^2 + f = 0 \qquad (4.22)$$

Eqs. (4.20) - (4.22) can then be solved for the elements of the two dimensional symmetric K matrix as:

$$K_{12} = [d \pm \sqrt{d^2 + n^2 f}\,]/n^2 \qquad (4.23)$$

$$K_{22} = \pm \sqrt{f - 2e K_{12}}\ /n \qquad (4.24)$$

$$K_{11} = K_{22}\,(d - n^2 K_{12})\ /e \qquad (4.25)$$

where the choices of signs in front of the radicals are selected such that K is positive definite. From Eq. (4.13) it is seen that the control has the form

$$U = -[nK_{12}\ nK_{22}]\ (X) \qquad (4.26)$$

As an illustrative example the system parameters and initial conditions are selected from Ref. 5, pp. 72-79, where the movable mass system is considered as a two-axis nutation damper for the NASA 21 Man Space Station (Fig. 4.2),

$I = 1.42 \times 10^7$ kg -m^2 (10.5×10^6 slug-ft^2)

$I_3 = 2.03 \times 10^7$ kg -m^2 (15.0×10^6 slug-ft^2)

$M = 6.21 \times 10^4$ kg (1.37×10^5 lbm)

$\Omega = 0.314$ rad/sec (3 rpm)

$m = 816$ kg (1800 lbm)

$a = 19.8$ m (65 ft), $b = 0$, $\ell_m = z_{max} = 5.4$m (17.72 ft)

$\omega_1(0) = 0.0391$ rad/sec, $\omega_2(0) = 0$, $\omega_{T_{max}} = 0.04$ rad/sec.

This results in the following values for the parameters:

$$d = 0.666,\ e = 0.428,\ n = 0.113,\ f = 61.63$$

and it is seen that K is positive definite if $K_{11} = 219.13$, $K_{12} = -34.69$, $K_{22} = 84.57$. For $\omega_2(0) = \beta(0) = 0$, the response of the state vector components is then calculated as

$$\alpha(\tau) = e^{-0.54\tau}(\cos 0.428\tau + 1.262 \sin 0.428\tau)\alpha(0) \qquad (4.27)$$

$$\beta(\tau) = e^{-0.54\tau}\ 2.591 \sin (0.428\tau)\ \alpha(0) \qquad (4.28)$$

under the optimal control:

$$U(\tau) = 3.92\alpha - 9.57\beta = \zeta'' + \zeta \qquad (4.29)$$

The solution for $\zeta(\tau)$, assuming $\zeta(0) = \zeta'(0) = 0$, is:

$$\zeta(\tau) = 0.655 \sin \tau + 0.417 \cos \tau - e^{-0.54\tau}(0.417 \cos 0.428\tau + 2.056 \sin 0.428\tau) \qquad (4.30)$$

indicating that the boom will experience a steady state oscillation after the initial transient. The initial nutation angle is calculated to be 5.0 degrees and for small angles may be approximated by:

$$\theta \simeq I\sqrt{\alpha^2 + \beta^2}\,/I_3 \qquad (4.31)$$

The decay of nutation angle for this case is shown in Fig. 4.3 (the curve labeled Q_1 for $\ell_m = 17.72$ ft.) and compared with two of the results from Ref. 5. When the maximum amplitude of boom length is 5.4m (17.72 ft.) it is seen that the time constant associated with the nutation decay is approximately one order of magnitude better when the linear quadratic performance criterion is used instead of the non-optimal methods of Refs. 4 and 5. In Fig. 4.4(a) for the same case the motion of the boom end mass during nutation decay is illustrated.

It is seen that within 30-35 secs. the transient part of this motion is removed leaving a remaining steady state oscillation with an a amplitude of 13.04 ft as predicted by Eq. (4.30). Also, the initial disturbances in both the transverse angular velocity components are removed by the motion of the control boom. At this point the nutation angle reaches a (small) value within mission tolerances and the z boom could be withdrawn to the zero-length position and ready for re-use. This operation would require a temporary boom-motor command or the activation of internal damping in the boom extension mechanism so that the steady state amplitude would eventually approach zero.

Also shown in Fig. 4.3 are the affects of varying the Q weighting matrix. For the case already discussed the Q matrix has the two dimensional form:

$$Q_1 = \begin{bmatrix} 61.63 & 0 \\ 0 & 61.63 \end{bmatrix}$$

which yields the optimal control law given in Eq. (4.29) and repeated here:

$$U(\tau) = 3.92\alpha - 9.57\beta \qquad (4.32)$$

If for the same boom offset and z_{max} we let the maximum expected value of transverse angular velocity be, $\omega_{T_{max}} = 0.1$ rad/sec, then

$$Q_2 = \begin{bmatrix} 9.86 & 0 \\ 0 & 9.86 \end{bmatrix}$$

with the result that

$$U(\tau) = 0.787\alpha - 3.974\beta \qquad (4.33)$$

The nutation angle decay for this case has a slightly longer time constant which can possibly be explained by the smaller negative coefficient of β in Eq. (4.33). The dynamic response of this case is illustrated in Fig. 4.4(b). The amplitude of the steady state boom motion is 7.45 ft which is smaller than the amplitude of 13.04 ft. for the case considered in Fig. 4.4(a).

For the same offset and a reduced z_{max} = 3m (9.84ft) it is seen that with the control law resulting from Q_1 the boom end mass will actually exceed a displacement amplitude of 3m and the dynamics of such a discontinuous system can not be approached analytically. For $\omega_{T_{max}}$ = 0.1 rad/sec. Q_2 yields a control law of the form:

$$U(\tau) = 0.4566\alpha - 4.0077\beta \qquad (4.34)$$

and the corresponding decay of nutation angle is shown in Fig. 4.3. The time response of the case considered here is shown in Fig. 4.4(c). The steady state oscillation of the control boom end mass has an amplitude of 4.40 ft. and the nutation angle becomes zero after 130 secs.

In all the cases considered to this point the spin rate is assumed to be constant ($\omega_3(0) = \Omega$). Next, we consider the case where the initial angular velocity about the '3' axis is not the same as the final desired spin rate. The control gains are calculated from the linearized equations and the dynamic response of the system is obtained from numerical integration of the nonlinear equations of motion of the system Eqs. (3.13) - (3.15).

The details of the numerical integration[9] computer program listings are given in the section COMPUTER PROGRAMS.

The results of this numerical integration are shown in Figs. 4.5(a) and (b) with weighting matrices selected as Q_2 and Q_3, respectively. The maximum amplitude of the boom end mass is assumed to be 100 ft. The numerical results indicate that more than 200 secs. would be required to achieve a zero nutation angle. The transverse angular velocity responses are more oscillatory than those shown earlier (e.g. Fig. 4.4); and the angular velocity about the '3' axis reaches a steady state value equal to the desired final spin rate within 150 secs. For this application, the three-axis control is achieved using only a single boom due to the nonlinear coupling.

As Edwards and Kaplan[4,5] have previously noted, performance is improved by increased boom lengths but in all cases considered here where the boom motion remains continuous there is a marked improvement in system performance by using the quadratic performance criterion from linear optimal control theory.

b. Three-axis control using two offset booms

For more complicated applications of two-axis control ($a \neq 0$, $b \neq 0$) with asymmetrical hubs and for the general case of three-axis control numerical methods were used to solve the matrix Riccati equation[14]. Ref. 14 contains both a sample problem and computer listings which were adopted for use with the NOVA 840 computer system. For the general case, the dynamics of the controlled system were simulated by numerical integration of the general (nonlinear) form of Eqs. (3.13) - (3.15), as developed in cartesian components.

The computer listings and the program details are given in the section COMPUTER PROGRAMS.

An example of the application of a two-boom system for three-axis control is shown in Fig. 4.6(a) where initial perturbations are assumed in both the transverse angular velocity magnitude as well as the component along the spin ('3') axis. Furthermore the initial disturbance amplitude is assumed to be less than 0.04 rad/sec. in both transverse and spin axis components. The non-zero elements of the Q matrix are calculated to be

$$f = \Omega^2/(\alpha,\beta,\gamma)^2_{max} = (0.314)^2/(0.1)^2 = 9.86$$

The hub moments of inertia, boom end masses and hub mass are the same as in Sect. a. Based on this information the matrix Riccati equation was solved numerically yielding the following control law:

$$U_1 = 2.2242\alpha - 3.8489\beta = \zeta'' + \zeta \qquad (4.35)$$

$$U_2 = -3.1401\gamma = \xi'' + f_1\,\xi' \qquad (4.36)$$

The steady state values of the feedback gains were obtained by numerically integrating the matrix Riccati differential equation until steady state conditions were obtained. This information was then incorporated into the simulation of the general nonlinear equations of motion, Eqs. (3.13) - (3.15). It is seen from Fig. 4.6(a) that within 50 seconds the initial disturbance in both the transverse angular velocity component as well as ω_3 (about the spin axis) are removed by the motions of the two control booms. After this time the z boom continues to exhibit a steady state oscillation according to the U_1 control law whereas the x boom

reaches a constant steady state amplitude of -47.5 ft (14.48m). The offset of the z and x booms are assumed to be equal (65 ft.)

Fig. 4.6(b) illustrates the dynamics of the system for a change in the offset value of the x boom from 65 ft. to 45 ft. The responses in Fig. 4.6(b) are similar to those shown in Fig. 4.6(a) except that the constant steady state amplitude of x is reduced to a value of -43.4 ft.

In an actual mission after the disturbances have been removed these steady state motions could be stopped by physically retracting the booms to the zero position. During all boom maneuvers simulated here the extension (or retraction rates) fall within 0-10ft/sec which is thought to be within that currently obtainable with such mechanisms.

Another example of three-axis control using two offset booms is depicted in Fig. 4.7. The initial conditions are identical to those of Fig. 4.6(a) as are all parameters relating to maximum boom lengths, masses, and offsets. In Fig. 4.7 it is assumed that the main part of the spacecraft is no longer symmetric with

$$I_1 = 1.42 \times 10^7 \text{kg-m}^2 \ (10.5 \times 10^6 \ \text{slug-ft}^2)$$

and

$$I_2 = 1.69 \times 10^7 \text{kg-m}^2 \ (12.5 \times 10^6 \ \text{slug-ft}^2).$$

It is seen that for the same weighting of the state variables and control, the system in Fig. 4.7 requires a longer settling time to reach steady state and that the steady-state amplitude of the x-boom is slightly reduced to about -45ft.

c. Application of offset system during the terminal phase of detumbling maneuver.

A recent study[3] has shown that a tumbling spacecraft may be recovered by extending three sets of telescoping booms along the hub principal axes. With an application of Lyapunov's second method[3] sequences of boom extension maneuvers can be determined so that the spacecraft will approach either of two desired final states: close to a zero inertial angular velocity state or a final spin about only one of the principal axes. The numerical results of Ref. 3 show that there is always a small residual remaining in the components of the state vector and that extremely long times (and boom lengths along the principal axes) are required for a significant reduction in the residual nutation angle when a final spin is the desired final state. It is suggested that the offset telescoping boom system can be used as a means of rapidly reducing the residual components of the state vector after an initial detumbling maneuver using the strategy of Ref. 3.

As an example of the application of such a system, we consider the NASA 21 Man Space Station under the following nonlinear initial conditions: $\omega_1(0) = 0.1$ rad/sec; $\omega_2(0) = 0.2$ rad/sec.; $\omega_3(0) = 0.5$ rad/sec.; where the desired final state is: $\omega_{1_f} = \omega_{2_f} = 0$; $\omega_{3_f} = 0.314$ rad/sec. $= \Omega$. It is assumed that three sets of booms with a uniformly distributed mass of 1.5 slug/ft can be extended along the hub (main part) principal axes from the center of the hub. Following the strategy of Ref. 3, and noting that the hub '3' axis remains an axis of symmetry during deployment, all booms can be extended until $T_{3_f} = 41.0$ secs. at which time the transverse booms are stopped and only the extension of the '3' axis booms is continued.

It is assumed that the principal axis booms have a constant extension rate of 4ft/sec. The dynamics of this recovery operation is illustrated in Figs. 4.8(a) and (b).

Suppose that at 50 secs. all operations with the uniformly distributed mass booms are halted. At this time the transverse booms each have a length of 164ft (49.99m) while ℓ_3 = 200 ft (60.96m). At t = 50 secs., it should be noted that although ω_1/Ω, $\omega_2/\Omega<1$ and $\omega_3=\Omega$, the nutation angle remains at 17.4^o. The composite moments of inertia at this time (including space station plus three sets of uniformly distributed mass booms) are:

$I_1 = I_2 = I = 22.91 \times 10^6$ slug-ft^2 (30.98×10^6kg-m^2)

$I_3 = 23.82 \times 10^6$ slug-ft^2 (32.204kg-m^2) and I_3 is still greater than I.

At 50 secs. control is initiated using two pairs of offset telescoping booms each with end mass of 816kg and an assumed maximum length of 100 ft. (30.48m). For this application both the Q and R weighting matrices are selected to be the unit matrix, yielding a control law of the form:

$U_1(\tau) = 0.4996\alpha - 1.3249\beta$

$U_2(\tau) = -0.9998\gamma$

It can be seen from Figs. 4.8 that within 150 secs. of the beginning of the recovery operation the nutation angle has been virtually reduced to zero and that the x offset boom end mass has a steady state position of -22.05 ft (-6.72m) while the z offset boom exhibits a steady state oscillation with an amplitude of 42.7 ft (13.015m).

If, on the other hand, we had continued to extend the uniformly distributed mass booms along the '3' axis during the same time period instead of activating the offset system, even though the transverse angular velocity components would have been reduced, the nutation angle would have remained essentially constant. The effectiveness of the offset system in rapidly reducing both transverse rates as well as nutation angle should be noted here.

Instead of stopping all operations with the uniformly distributed mass booms at 50 secs., we now consider the case where the operations are continued past t = 50 secs. and halted at 75 secs. The control is initiated using the z and x offset telescoping booms. The time responses of the system as seen from Figs. 4.9 are similar in nature to those of Figs. 4.8 except that the time of stopping the principal axes booms is changed. At t = 75 secs., it is to be noted that I_3 is smaller than I and also the transverse angular velocities are smaller in magnitude compared to their values at t = 50 secs. From the simulation results (Figs. 4.9), it is observed that within 200 secs. of the beginning of the recovery operation the nutation angle has been reduced to essentially zero. Also, the x offset boom end mass has a steady state position of -22.77 ft. which is nearly the same value as in Figs. 4.8; but, the z offset boom exhibits a steady state oscillation with an amplitude of 16.72 ft. which is smaller than the amplitude of 42.7 ft. shown in Figs. 4.8.

This is an advantage, since the magnitude of the control effort with the z offset boom is reduced when the time of stopping the operations of the principal axes booms is increased from 50 secs. to 75 secs. It is also to be noted that the control action of the offset booms takes place in the linear region of the system dynamics (Figs. 4.9), whereas in Figs. 4.8, the control action of the offset booms initially occurs in the quasi-linear region of the system dynamics.

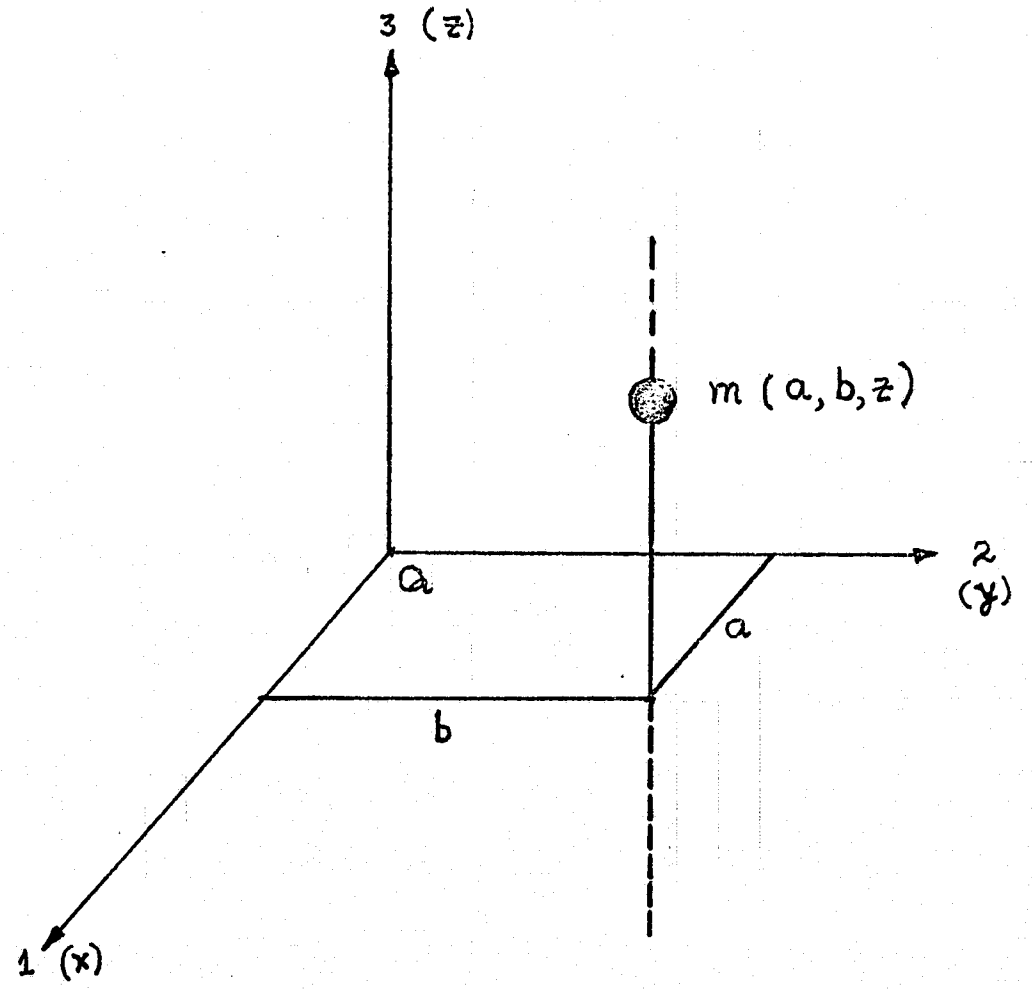

FIG. 4.1. SINGLE BOOM OFFSET SYSTEM

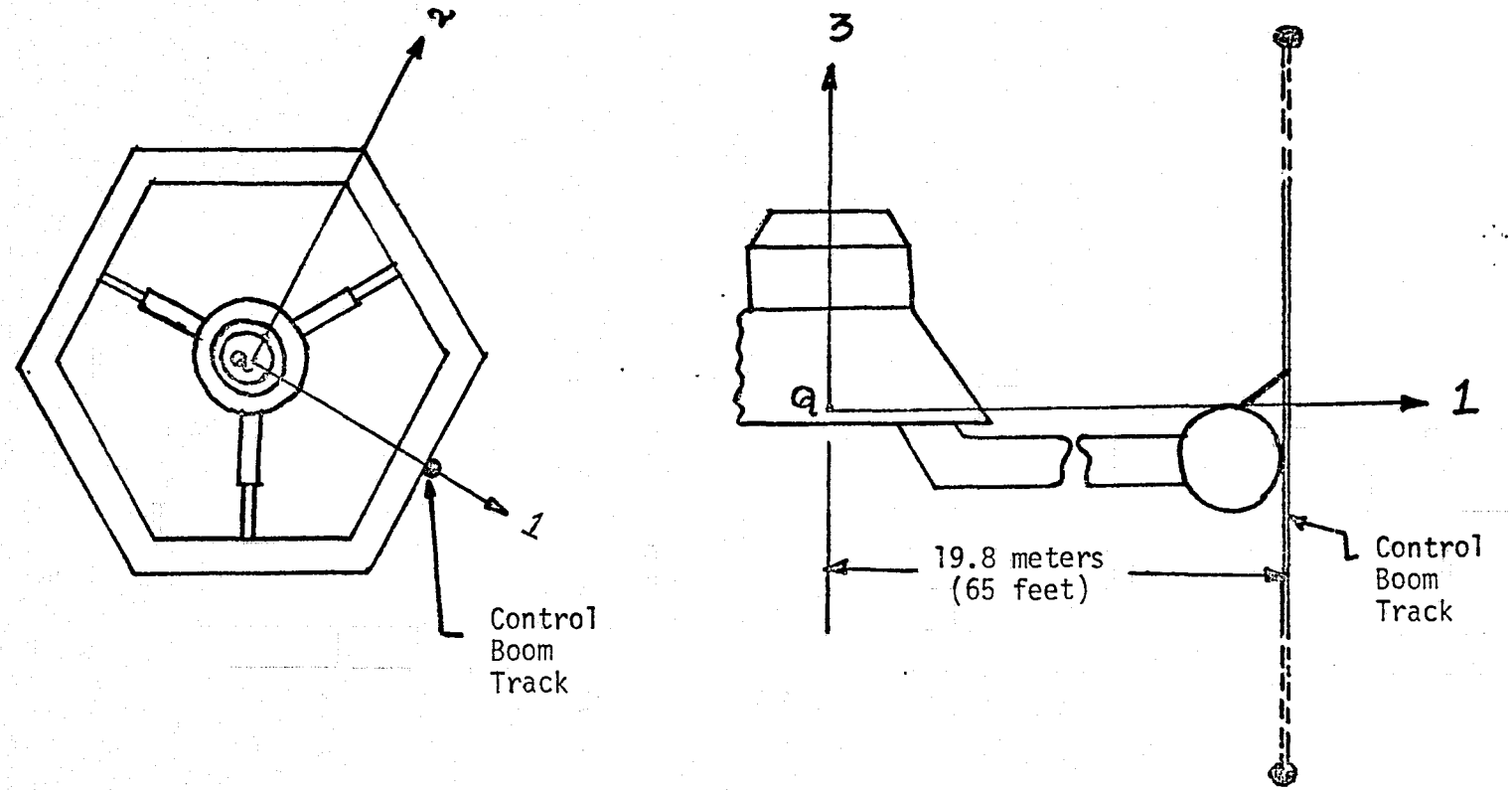

Plan View

Elevation

Fig. 4.2. NASA 21 MAN SPACE STATION CONFIGURATION

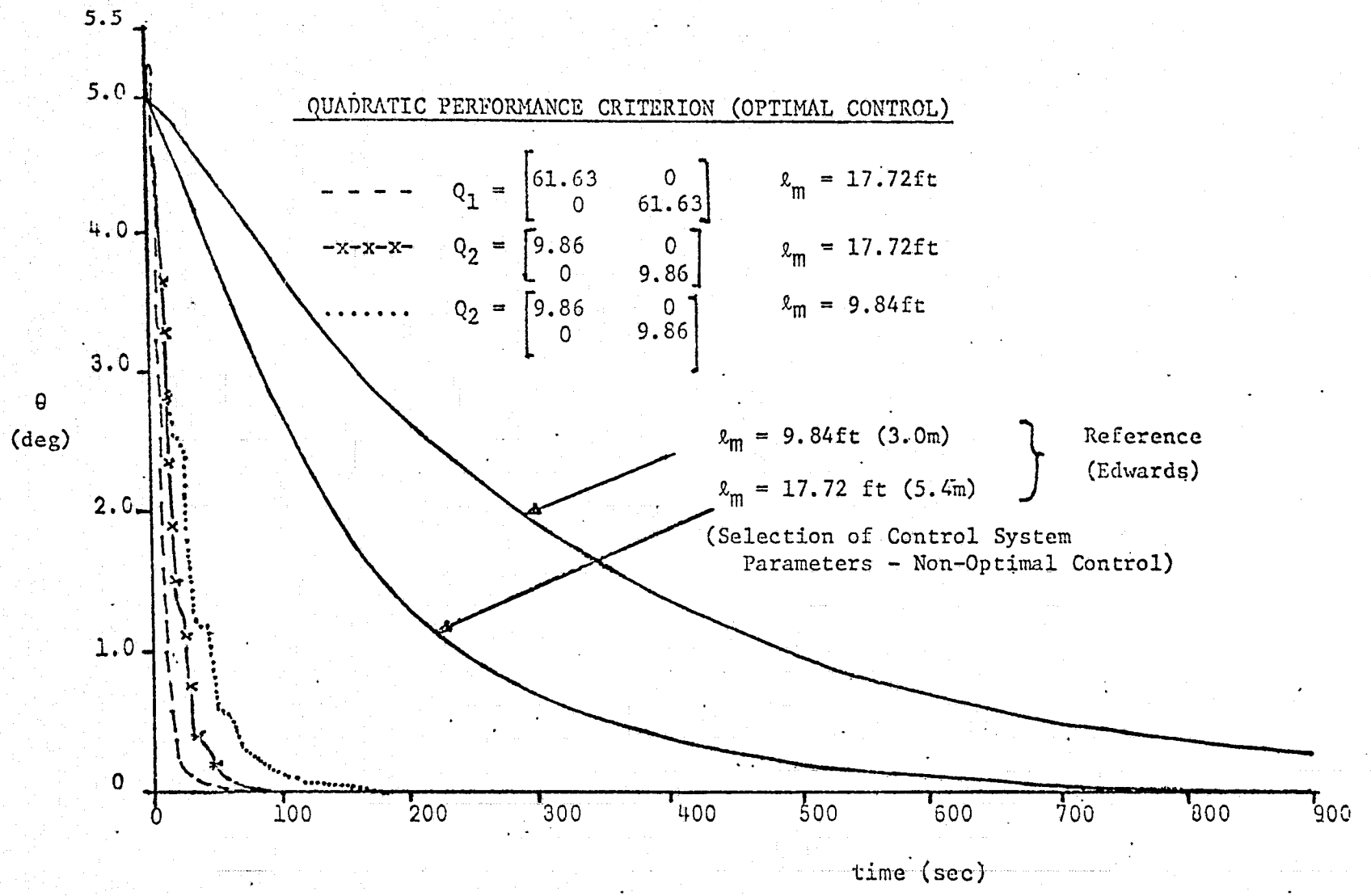

FIG. 4.3 DECAY OF NUTATION ANGLE WITH DIFFERENT CONTROL LAWS (SINGLE BOOM SYSTEM)

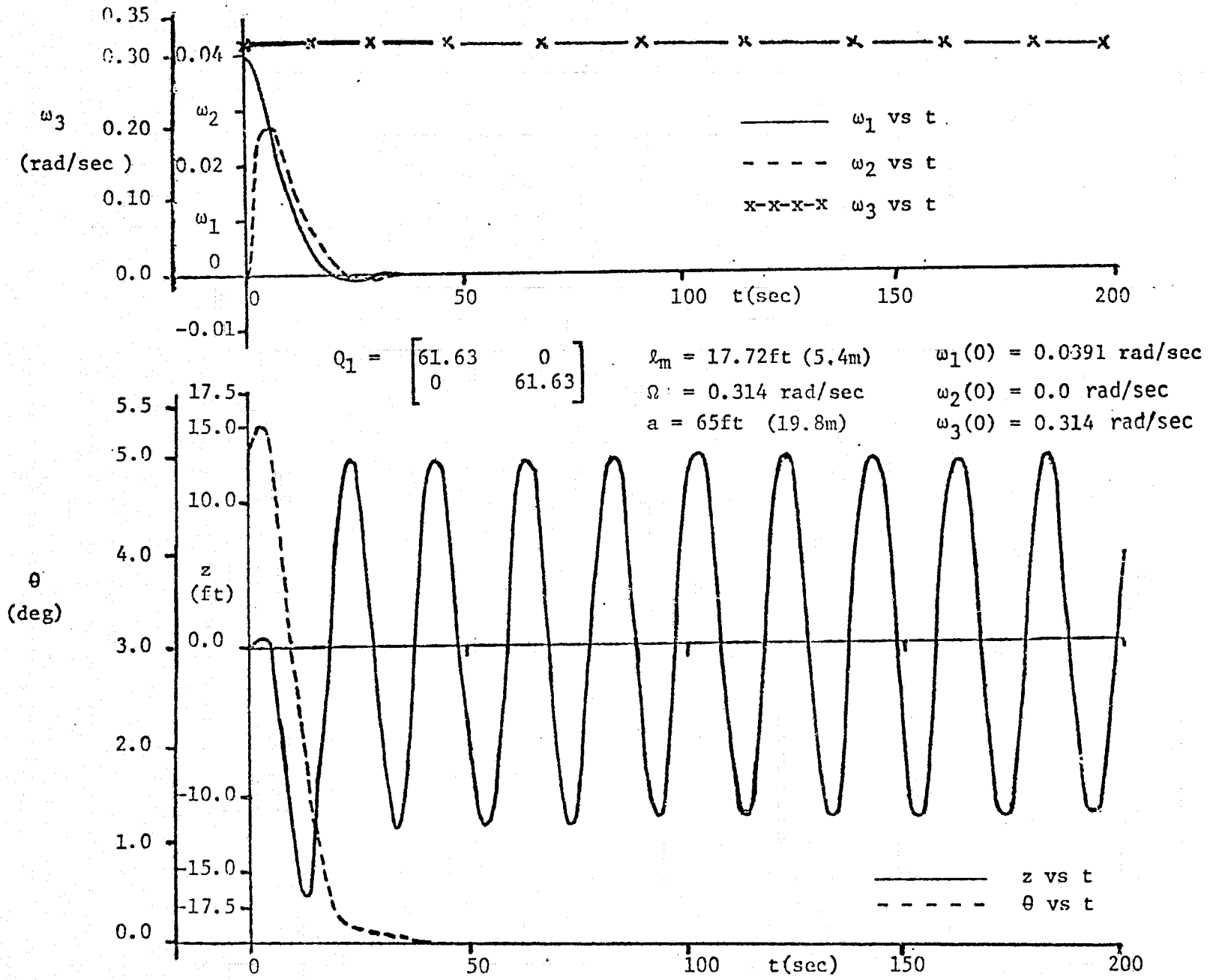

FIG. 4.4(a). DYNAMIC RESPONSE OF THE SYSTEM USING SINGLE BOOM FOR TWO-AXIS CONTROL

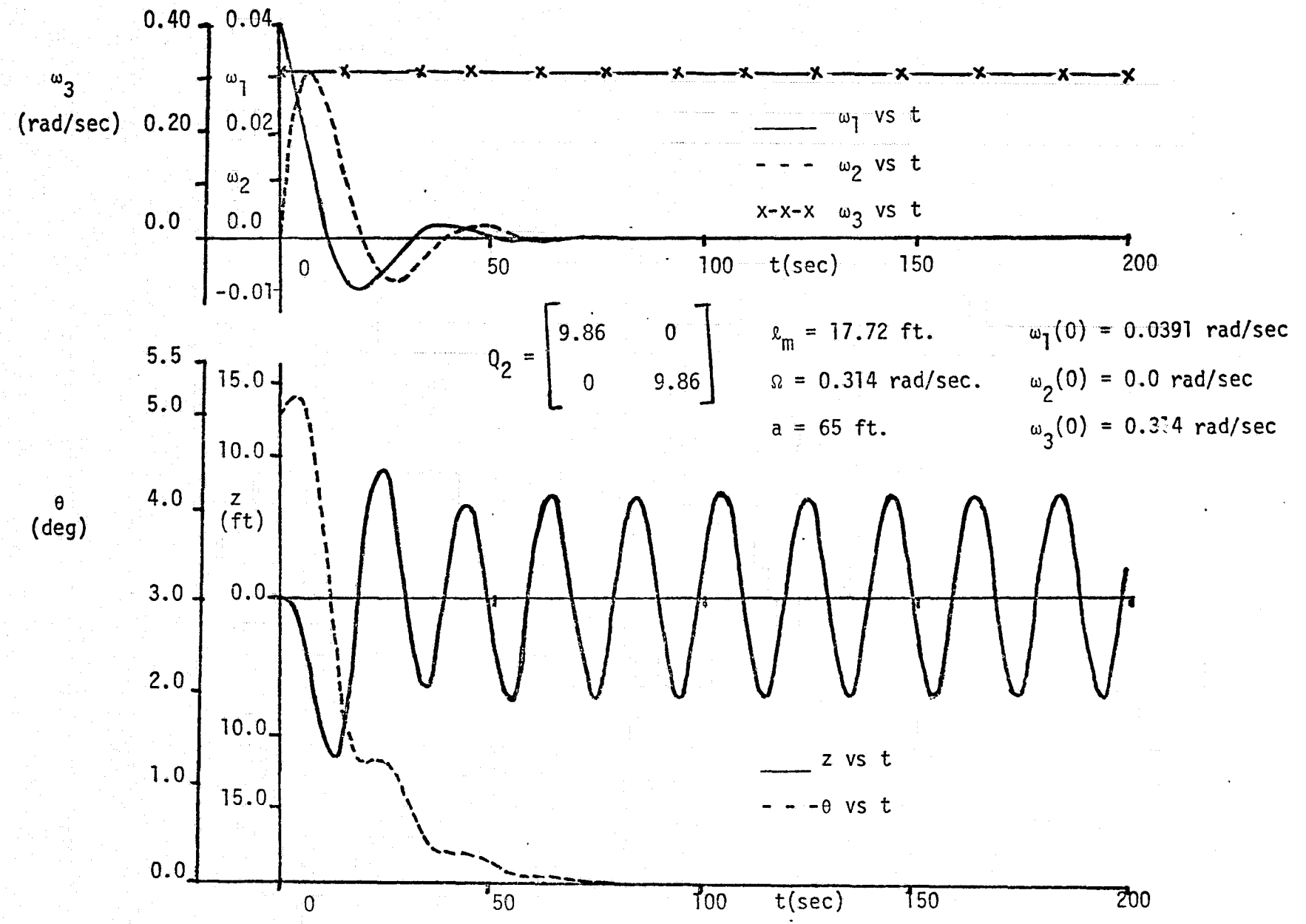

FIG. 4.4(b). DYNAMIC RESPONSE OF THE SYSTEM USING SINGLE BOOM FOR TWO-AXIS CONTROL

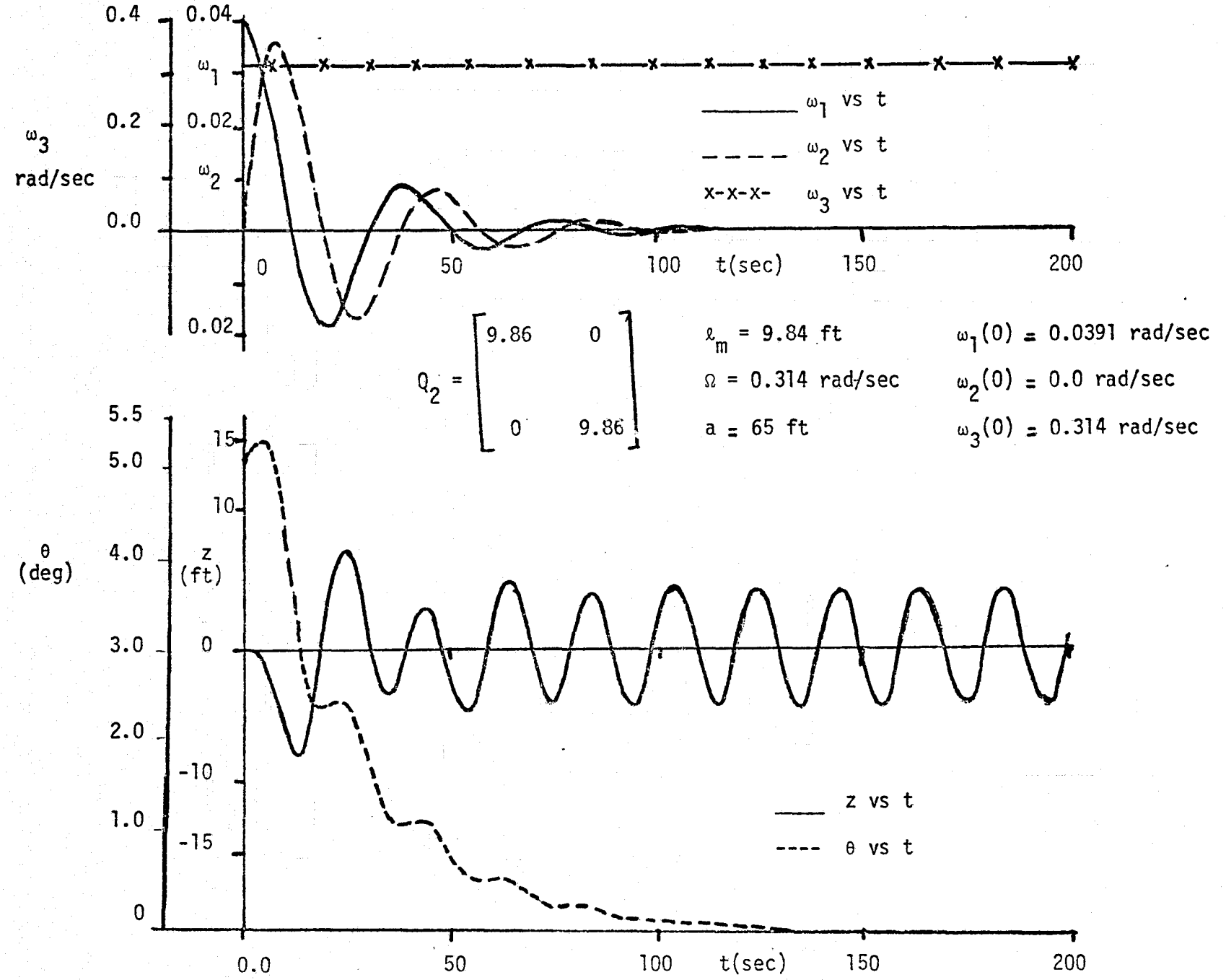

FIG. 4.4(c). DYNAMIC RESPONSE OF THE SYSTEM USING SINGLE BOOM FOR TWO-AXIS CONTROL

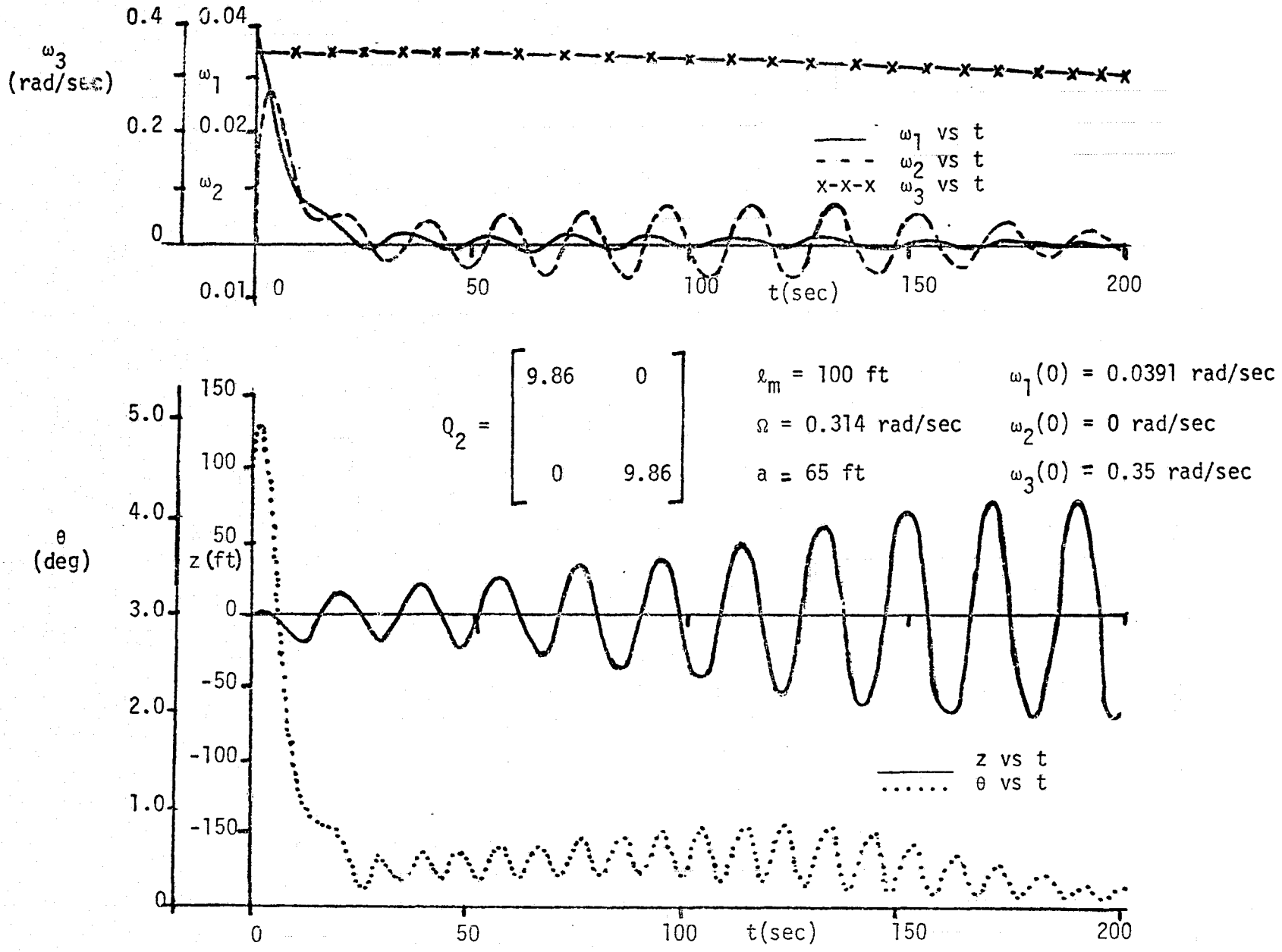

FIG. 4.5(a). DYNAMIC RESPONSE OF THE SYSTEM USING SINGLE BOOM

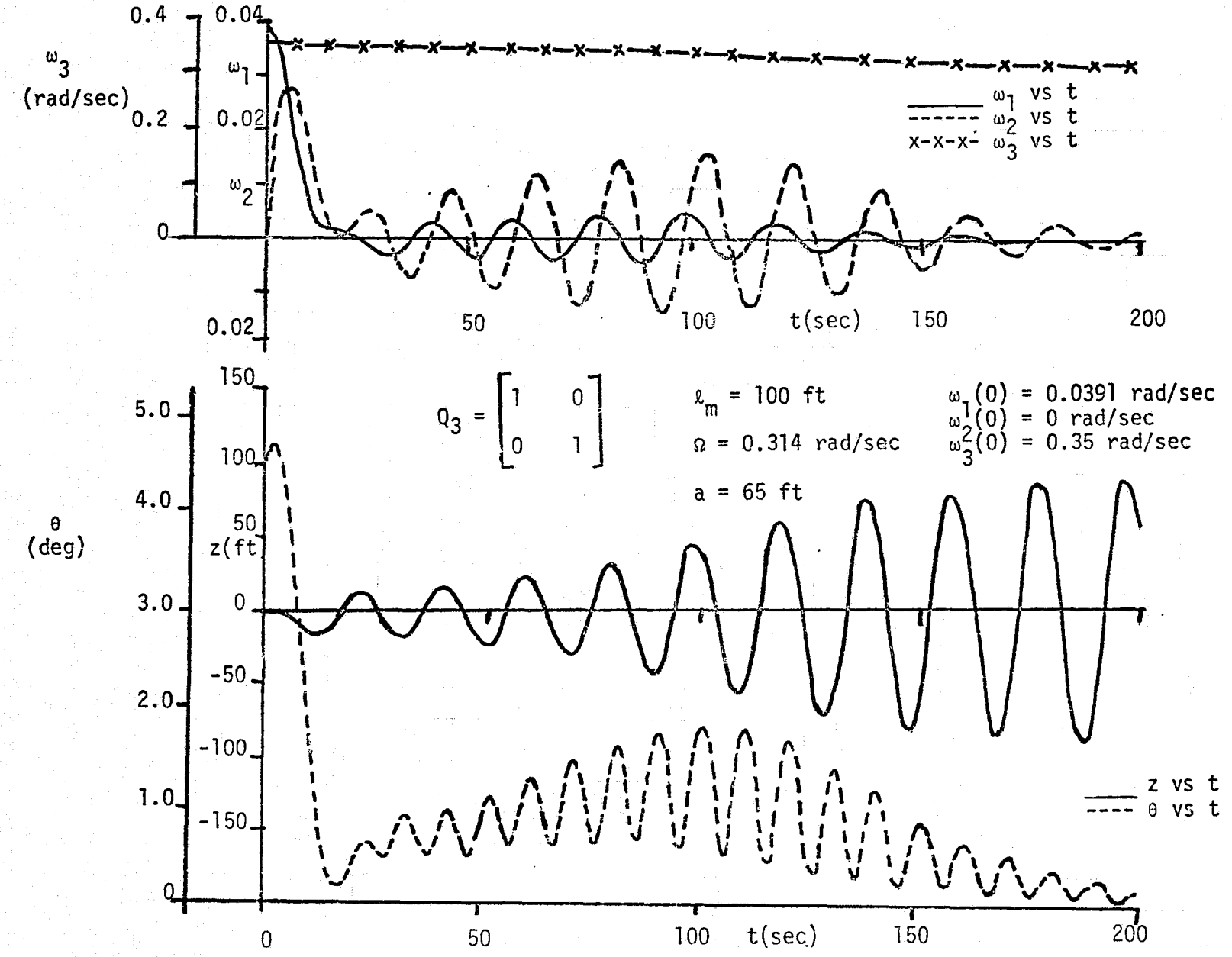

FIG. 4.5(b). DYNAMIC RESPONSE OF THE SYSTEM USING SINGLE BOOM

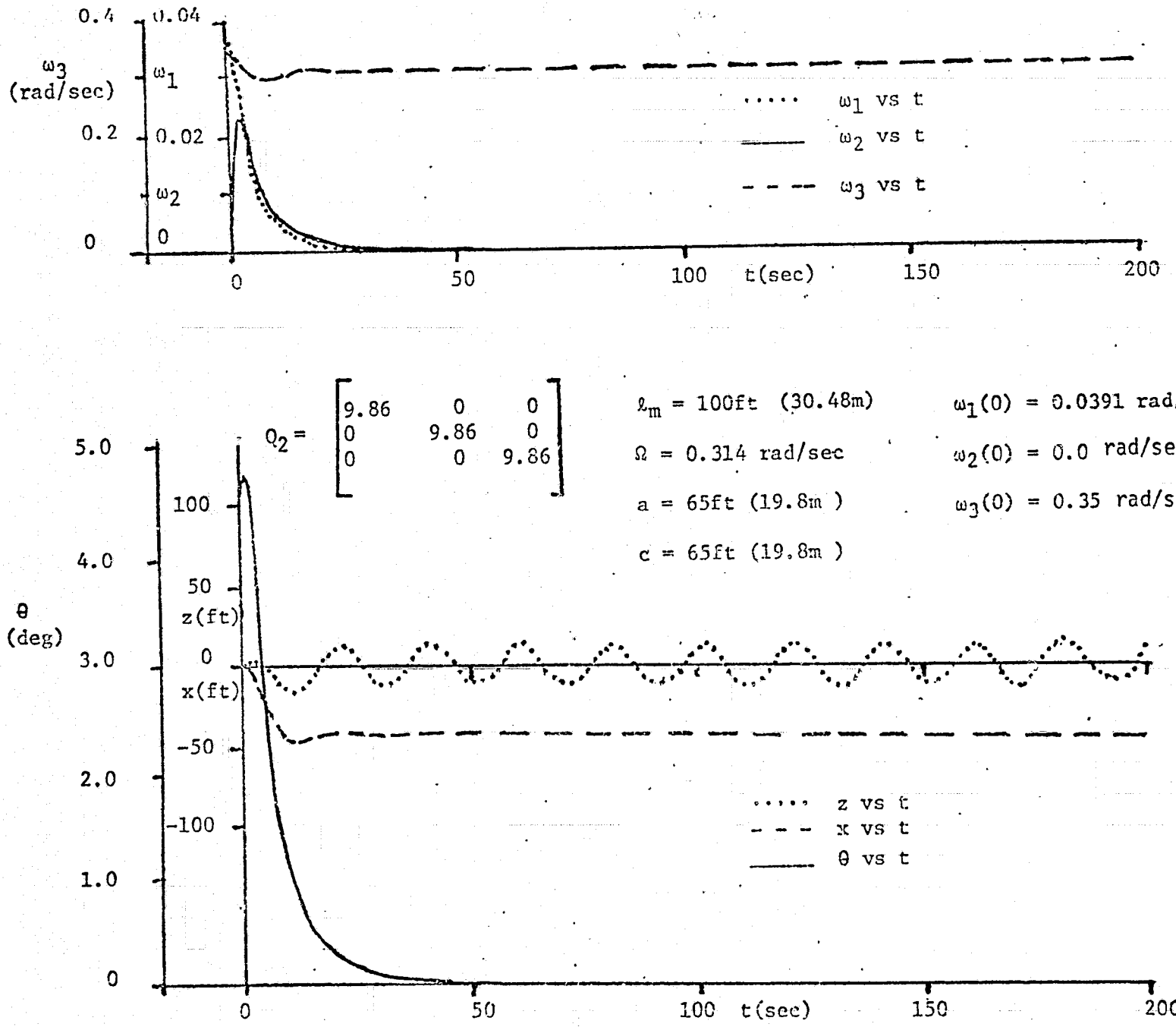

FIG. 4.6(a). DYNAMIC RESPONSE OF SYSTEM USING TWO-BOOMS FOR THREE-AXIS CONTROL (I_1=I_2)

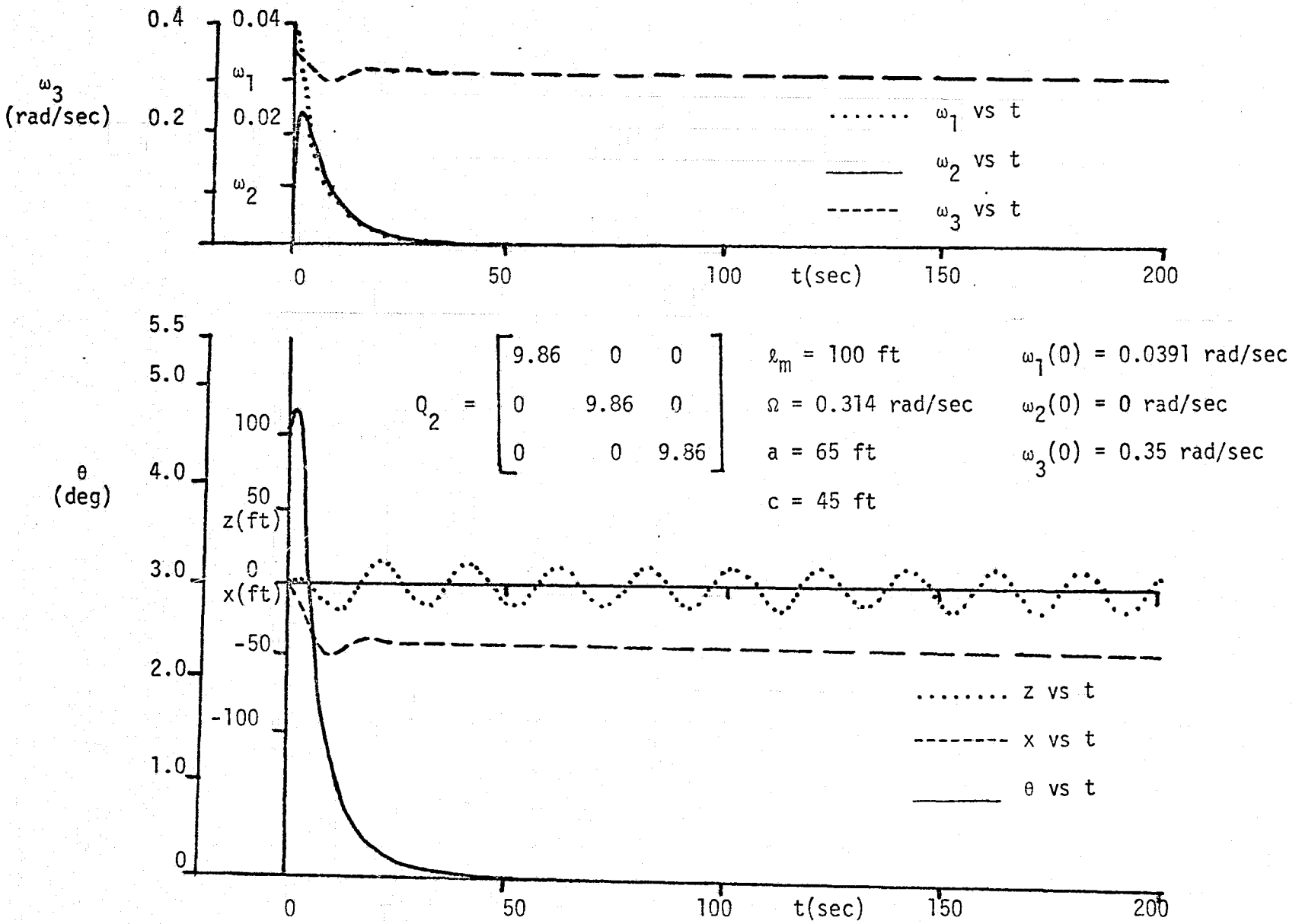

FIG. 4.6(b). DYNAMIC RESPONSE USING TWO BOOMS FOR THREE-AXIS CONTROL (I_1=I_2)

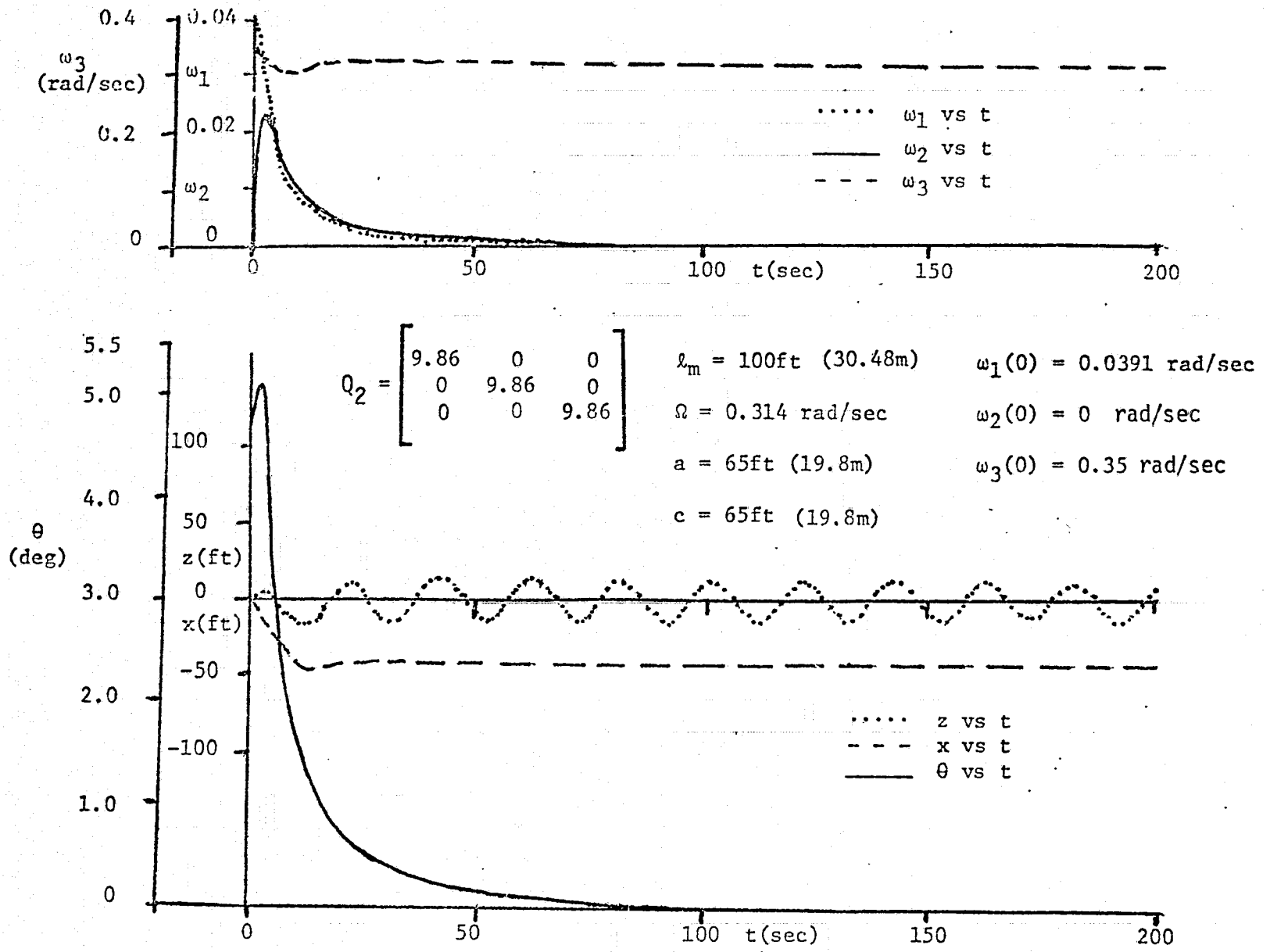

FIG. 4.7. DYNAMIC RESPONSE OF SYSTEM USING TWO BOOMS FOR THREE - AXIS CONTROL ($I_1 \neq I_2$)

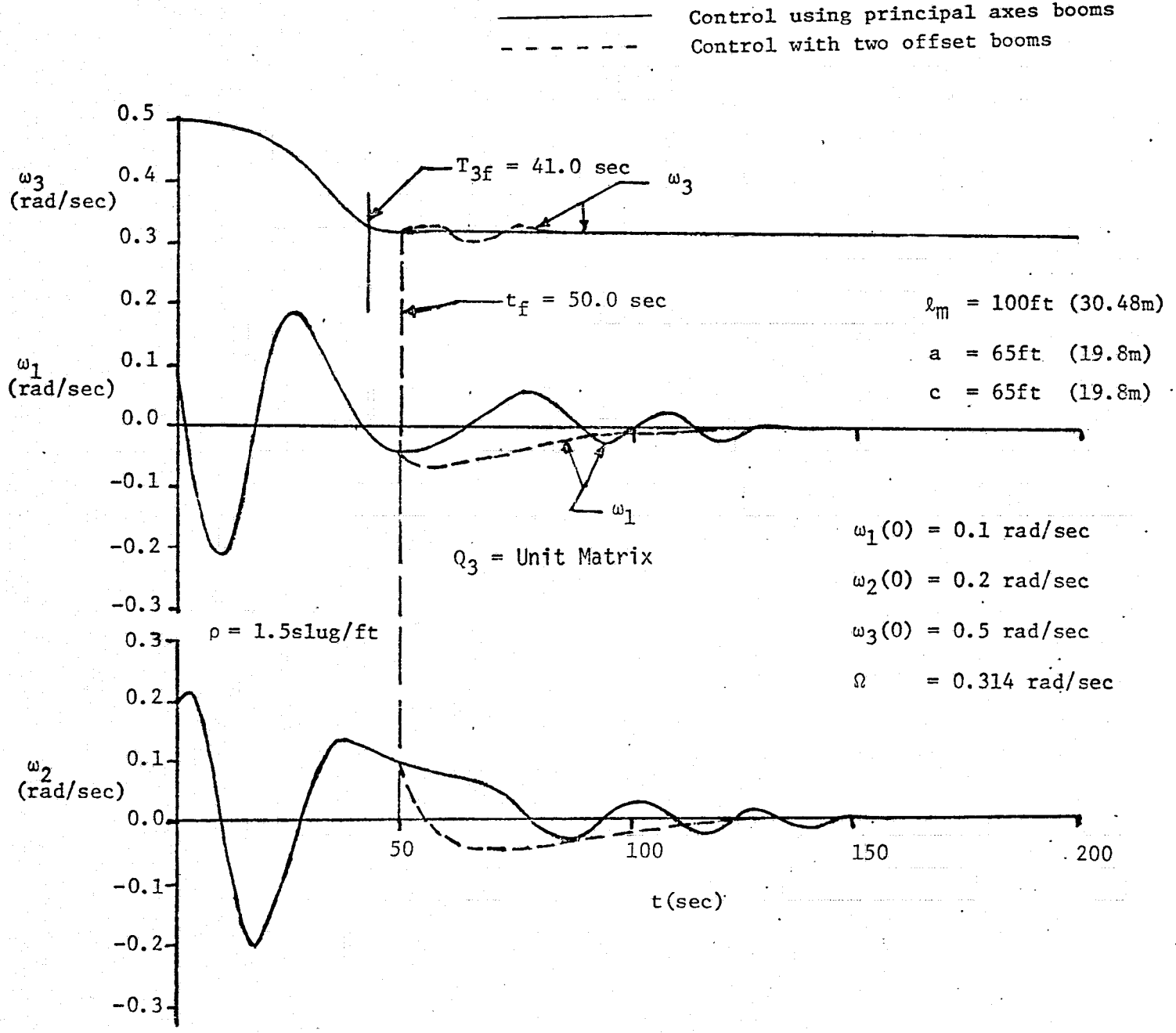

FIG. 4.8(a). APPLICATION OF OFFSET BOOM SYSTEM DURING DETUMBLING(t_f = 50.0 sec)

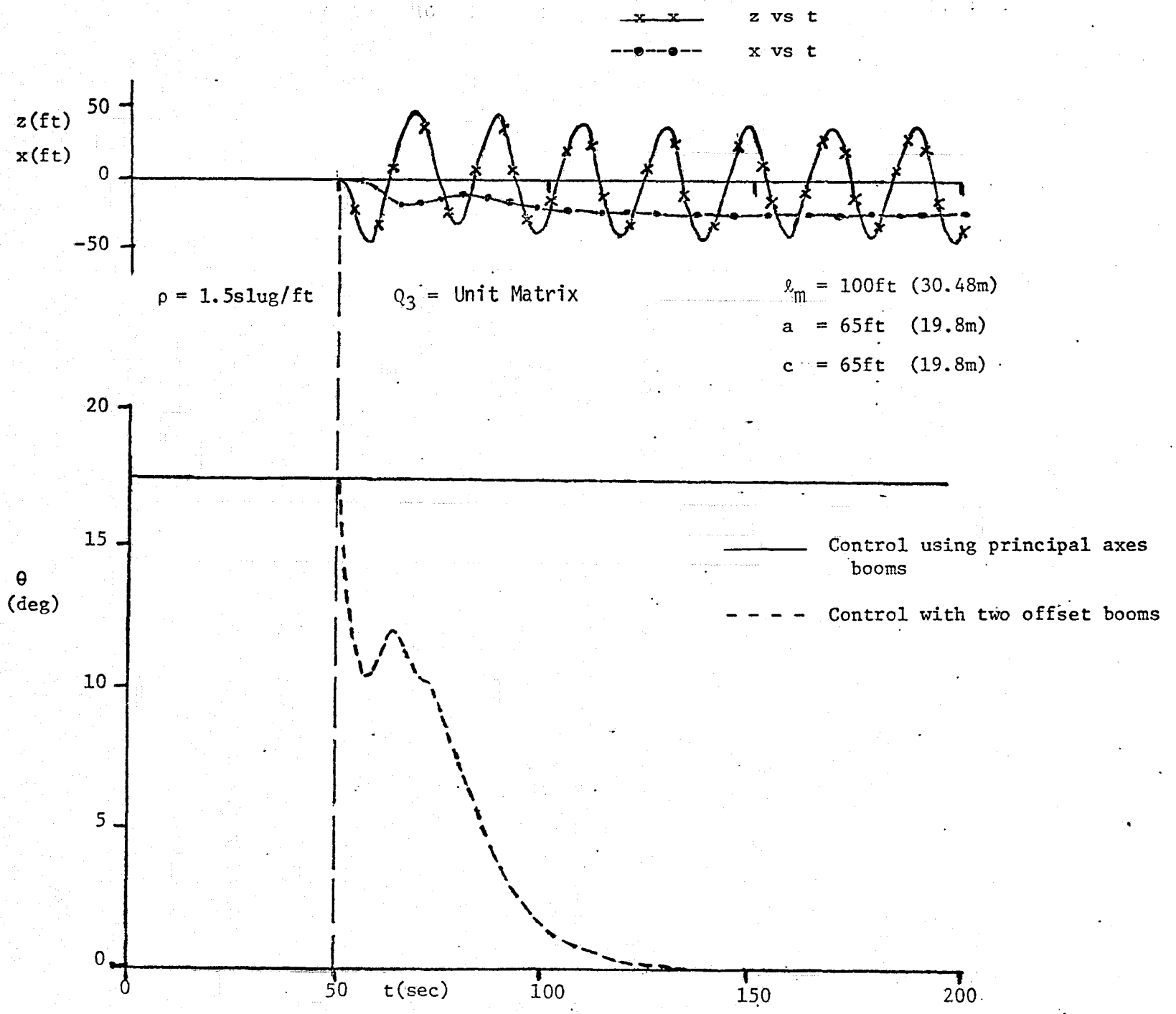

FIG. 4.8(b). APPLICATION OF OFFSET BOOM SYSTEM DURING DETUMBLING (t_f=50.0 sec)

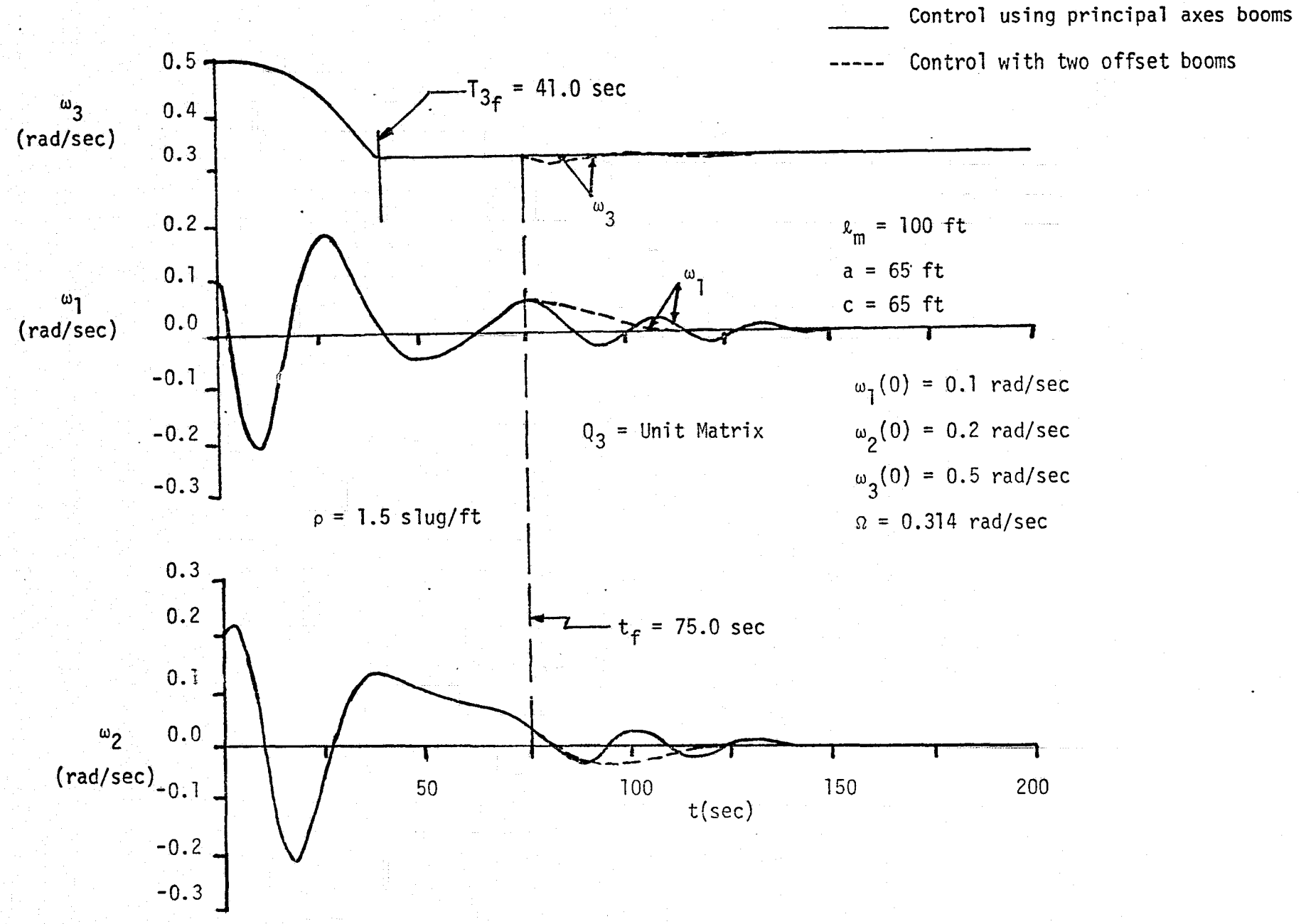

FIG. 4.9(a). APPLICATION OF OFFSET BOOM SYSTEM DURING DETUMBLING (t_f-75.0 sec)

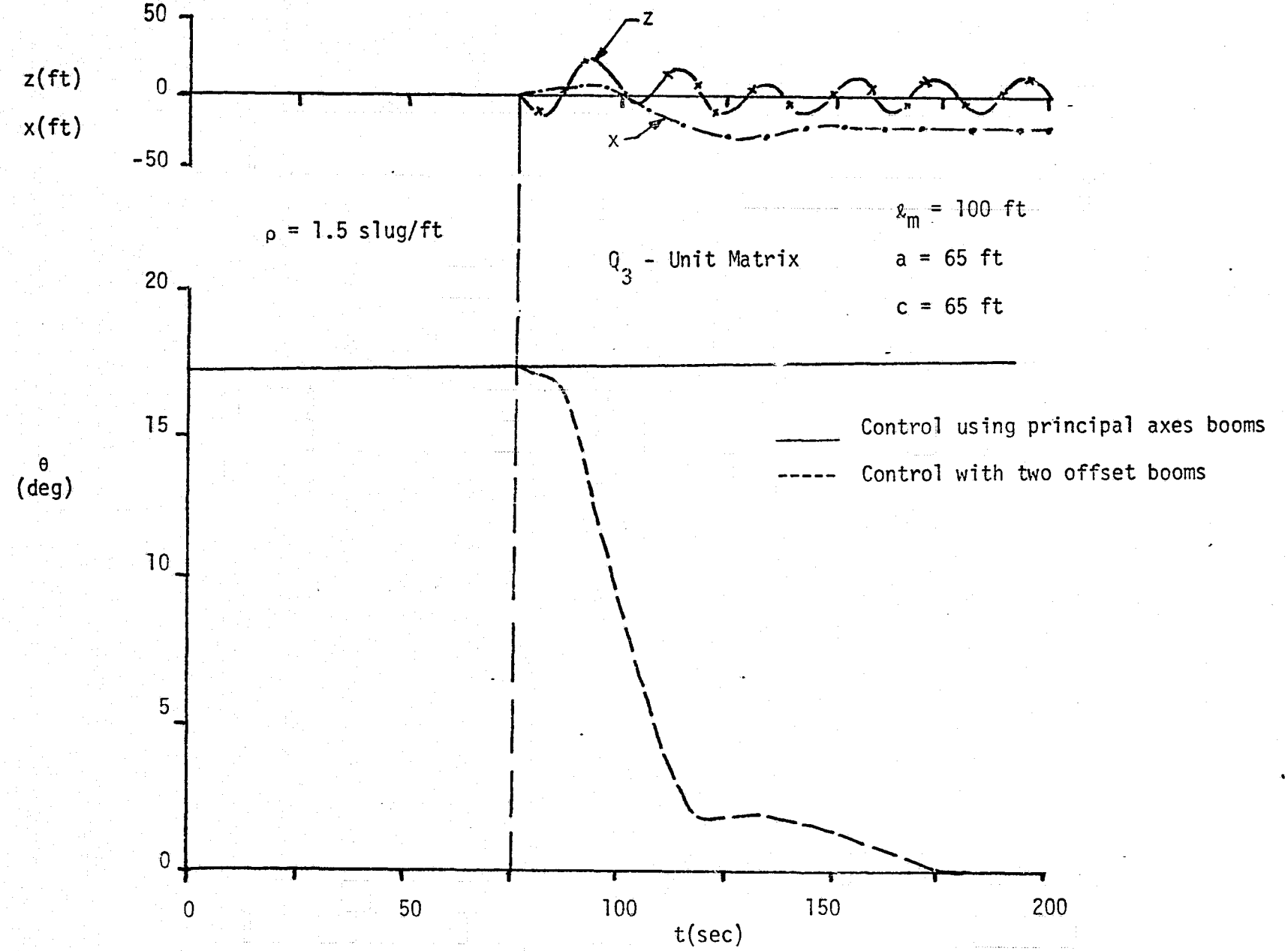

FIG. 4.9(b). APPLICATION OF OFFSET BOOM SYSTEM DURING DETUMBLING (t_f = 75.0 sec)

V. TIME OPTIMAL CONTROL WITH SINGLE OFFSET BOOM

The investigations presented in Chapter IV considered the design of a constant gain regulator for the time invariant system

$$X' = AX + BU \tag{5.1}$$

which minimizes the quadratic performance index. In this chapter, the problem of determining the control U ($|U| \leq C^*$) which forces the system (5.1) from the initial state X(0) to zero state in minimum time is treated.

An admissible control $U(\tau)$, transferring the system state from X(0) to $X(\tau_f) = 0$, is found from the solution of Eq. (5.1) given by

$$X(\tau) = e^{A\tau} X(0) + \int_0^\tau e^{A(\tau-\phi)} BU(\phi)\, d\phi \tag{5.2}$$

For $X(\tau_f) = 0$, Eq. (5.2) reduces to

$$\int_0^{\tau f} e^{-A\phi} BU(\phi)\, d\phi = -X(0) \tag{5.3}$$

As an application of the time optimal theory developed, the movable mass system is considered as a two-axis nutation damper for the NASA 21 Man Space Station (Fig. 4.2). The standard form of the equations of motion, given in Eq. (4.18), is repeated here

$$X' = AX + BU$$

where

$$X = \begin{bmatrix} \alpha \\ \beta \end{bmatrix}, A = \begin{bmatrix} 0 & -e \\ d & 0 \end{bmatrix}, B = \begin{bmatrix} 0 \\ 1 \end{bmatrix} \tag{5.4}$$

$$U = n(\zeta'' + \zeta) \tag{5.5}$$

The quantities d,e,n and the primes have been defined already with reference to Eq. (4.18). The solution for $U(\tau)$, bringing the system state to rest in minimum τ_f, is known to be $U(\tau) = \pm C^*$, with the number of switches depending upon the initial state of the system[15].

Considering the initial states that can be driven to rest in a single switch (Fig. 5.1(a)), the control takes the form[16]

$$U(\tau) = K_1 \text{ for } 0 \leq \tau \leq \tau_s;\ U(\tau) = K_2 \text{ for } \tau_s \leq \tau \leq \tau_f \qquad (5.6)$$

where

$$|K_1| = |K_2| = C^*$$

Substitution of Eqs. (5.4) and (5.6) into Eq. (5.3) leads to

$$(1 - \cos\omega_o\tau_s)\, K_1 - (\cos\omega_o\tau_f - \cos\omega_o\tau_s)\, K_2 = \alpha(0)\omega_o^2/e \qquad (5.7)$$

$$\sin\omega_o\tau_s K_1 + (\sin\omega_o\tau_f - \sin\omega_o\tau_s)\, K_2 = -\beta(0)\omega_o \qquad (5.8)$$

where

$$\omega_o = \sqrt{de}$$

The expressions for the switching time, τ_s, and the final time, τ_f, are obtained from the solutions of Eqs. (5.7) and (5.8) as:

$$\tau_s = \frac{1}{\omega_o}\left\{\cos^{-1}\left[\frac{(2K_2-K_1)K_1-(A^2+B^2)}{2(K_2-K_1)\sqrt{A^2+B^2}}\right] - \tan^{-1}\frac{B}{A}\right\} \qquad (5.9)$$

$$\tau_f = \frac{1}{\omega_o}\left\{\cos^{-1}\left[\frac{(2K_2-K_1)K_1+(A^2+B^2)}{2K_2\sqrt{A^2+B^2}}\right] - \tan^{-1}\frac{B}{A}\right\} \qquad (5.10)$$

where

$$A = K_1 + \alpha(0)\,\omega_o^2/e$$

$$B = \beta(0)\,\omega_o$$

The control scheme for a single switching for $\alpha(0) > 0$ and $\beta(0) > 0$ is shown in Fig. 5.1(b) where

$$U(\tau) = -C^* \text{ for } 0 \leq \tau \leq \tau_s$$

$$= +C^* \text{ for } \tau_s \leq \tau \leq \tau_f \,. \qquad (5.11)$$

The system response for an initial condition $(\alpha(0), \beta(0))$ is shown in Fig. 5.1(c) where the initial state $X(0)$ is driven to rest in a single switching at $\tau = \tau_s$. The equation of motion of the boom end mass is obtained from Eqs. (5.5) and (5.11) as

$$n(\zeta''(\tau) + \zeta(\tau)) = -C^* \text{ for } 0 \leq \tau \leq \tau_s$$

$$= + C^* \text{ for } \tau_s \leq \tau \leq \tau_f$$

and hence the time response of the control mass is given by the following equation $(\tau \leq \tau_f)$:

$$\zeta(\tau) = -\frac{C^*}{n} \{u(\tau) - \cos\tau u(\tau) - 2u(\tau-\tau_s) + 2\cos(\tau-\tau_s)u(\tau-\tau_s)\} \qquad (5.12)$$

where $u(\tau)$ is a step input $(\tau>0)$.

For the general case, where the initial conditions do not lie in the single switching region, piecewise solutions can be used to obtain the system response analytically. Also, a time optimal control solution can be obtained numerically using the techniques of dynamic programming. This approach was employed by Kunciw[17] in analyzing the optimal detumbling of the system treated in Refs. 4 and 5.

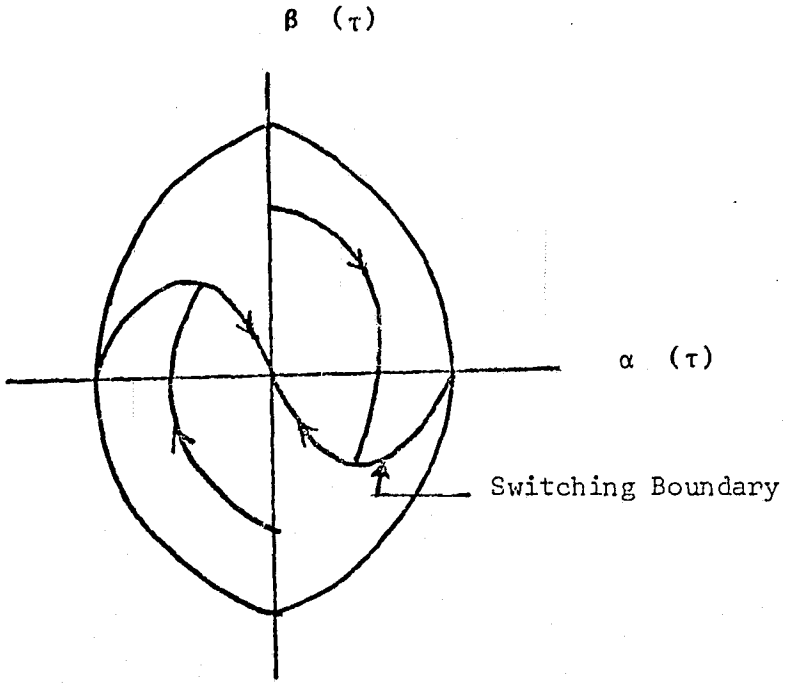

FIG. 5.1(a) PHASE PLANE PORTRAIT OF THE SYSTEM

(FOR SINGLE SWITCHING)

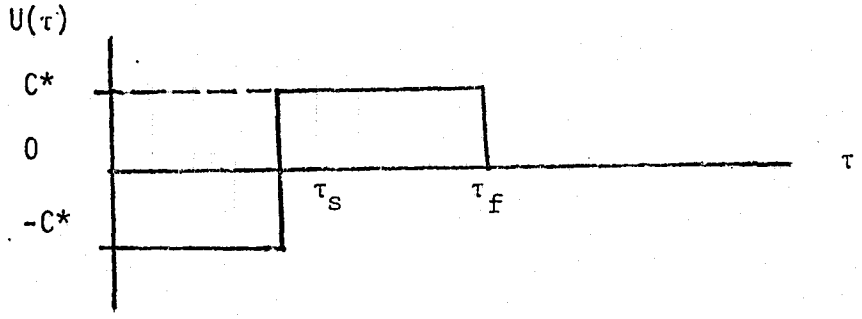

FIG. 5.1(b). CONTROL SCHEME FOR SINGLE SWITCHING

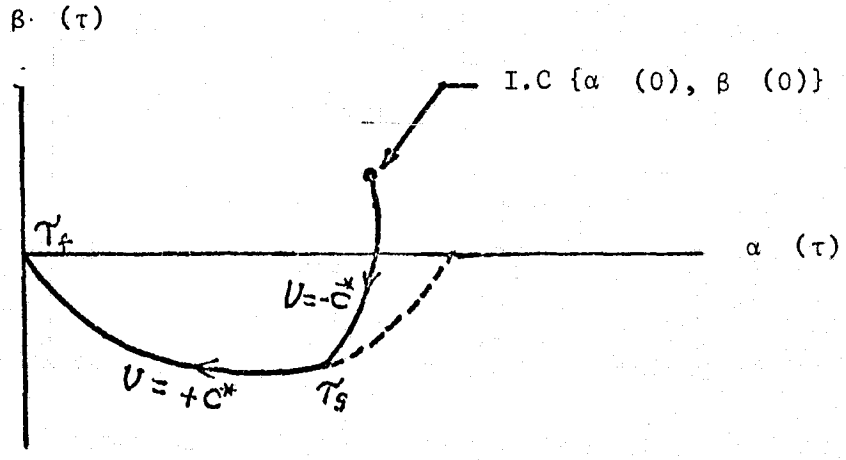

FIG. 5.1 (c). PHASE PLANE OF THE SYSTEM FOR GIVEN INITIAL CONDITIONS.

VI. CONCLUDING COMMENTS

As a result of the analysis and numerical results the following conclusions regarding the hinged system and the optimal control with the telescoping booms can be made:

1. Hinged System (Chapter II)

   (a) For the case of a symmetrical spacecraft closed form analytical solutions are obtained for two dimensional motion.

   (b) For stability (necessary conditions) certain inequalities relating the hinge point offset coordinates to the moment of inertia ratio and end masses must be satisfied for the three dimensional motion (small amplitude case).

   (c) Hinge damping is always required for the nominal deployment of the hinge members.

   (d) Other types of (nutation) damping are required to remove transverse angular rates effectively since the hinge dampers alone do not provide satisfactory nutation decay time constants with the system parameters selected here.

   (e) The vertical offset of the hinge points increases the time period of the damped transverse rates which may be due to the redistribution of moments of inertia for the three dimensional motion (small amplitude case).

   (f) The selection of the vertical offset of the hinge points for the general case of three dimensional motion for large amplitudes can not be done easily as there is no criteria which assures the stability of the system as in the case of small amplitude motion.

For the system parameters considered here it is recommended that the vertical offset be as small as possible.

2. Optimal Control (Chapters III,IV and V)

(a) Three axis linear optimal control of a spinning spacecraft system may be achieved by using more than one set of movable telescoping booms (with end masses) which are each offset from different hub principal axes.

(b) When only two-axis optimal control is desired only a single offset boom is required. The time constants achieved by such a system when used for the reduction of nutation (wobble) angle are one order of magnitude smaller than those previously achieved using non-optimal control logic.

(c) It is assumed that for the implementation of such a control system instantaneous measurements of angular velocity components, boom end mass positions, and extension rates would be available as well as an on-board computational capability. It is hoped to consider the effect of errors and delays in measurements on such a system in a subsequent study.

(d) A further application of the offset telescoping boom system could be during the terminal phase of a detumbling maneuver to quickly remove the residual components of angular velocity.

(e) The time optimal control problem is solved analytically for a single offset boom where the initial conditions are such that the system can be driven to the equilibrium state with a single switching in the bang-bang optimal sequence.

VII. RECOMMENDED FUTURE STUDIES

1. Further Studies in Optimal Control

A logical extension of our current application of the linear regulator problem for the optimal control of the telescoping system would be the examination of the effects of both uncertainties in measurements as well as errors in the modeling of the system by the linearization technique. The actual implementation of the optimal control law, once the gains have been set from a solution of the matrix Riccati equation, would involve the sensing of angular velocity components by rate gyroscopes and the determination of the instantaneous boom lengths, either by a mechanical counter or by relating end mass position relative to an optical sensor. In other words, physical sensors would actually be involved in the real-time determination of state variable components. These uncertainties could be included with an application of the estimator problem where the differences between the desired state vector components and the actual components due to measurement uncertainties would be incorporated within the control logic. The effect of errors in the modeling (due to linearization) could be examined by simulating the performance of the system using the nonlinear rotational equations in both linear and nonlinear regions. Finally the effect of time delays in the actual measurements (assuming such measurements could be performed with zero uncertainties) could be analyzed by considering the state estimator-filter problem.

C.2

The general problem of finding a control law that will result in a minimum time recovery could be studied with an application of a first-order gradient optimization technique using a digital computer. The control variable will involve the boom end mass acceleration with respect to body coordinates. Boom position can be limited to defined quantities and a penalty function can be used to insure a given range of positions. The problem of optimal control with a minimum time criterion has been examined analytically for the special case of a single offset boom where it is assumed that the initial conditions are such that the system can be driven to the equilibrium (rest) state with only a single switching maneuver in the bang-bang optimal sequence. For this system it is possible to obtain an analytical solution for the switching and final times in terms of the initial conditions and magnitude of the maximum value of the control force,[16,18] The general time optimal control solution for this problem can only be obtained numerically using the techniques of dynamic programming. This approach has been employed by Kunciw[17] in analyzing the optimal detumbling of the system treated in Refs. 4 and 5.

2. Effect of Gravity-Gradient and Solar Pressure External Perturbations

To date all of the results have been obtained by neglecting any and all external perturbations (i.e. in torque - free space). As a tumbling spacecraft is recovered by appropriate maneuvers of the appendages such effects as those due to gravity-gradient torques and solar pressure must be considered.

Previous studies have been completed showing the effect of gravity-gradient torques on the deployment of a gravity-gradient stabilized spacecraft which is librating only in the orbit plane and where the total libration amplitude is small.[19] Under these assumptions a series solution can be used to give an approximation of the actual dynamics.[19] Although the present problem can not be restricted to small amplitude motions because of the initial tumbling or spin, for special cases such as a symmetrical boom deployment and motion primarily within the orbit plane it is thought that an analytical approach using the techniques of Ref. 19 may be feasible. For the general case the effects of gravity-gradient torques could be evaluated numerically with particular attention to any readily identifiable gravity-gradient induced reasonances.[20] Solar pressure torques can be approximated by assuming that for homogeneous boom material the booms will bend away from the sun following a circular radius of curvature and these torques can be compared with those due to the gravity-gradient.

3. Effect of Flexibility During Boom Deployment

The problem of including flexibility effects during deployment of telescoping appendages has never been fully treated in the open literature. A recent examination of a related problem considers stability boundaries on the extension of a pair of axial antennas whose undeformed state lies along the nominal spin axis.[21] It was assumed that the rate of extension was sufficiently small so that Coriolis effects due to the rate of change of length could be neglected.[21]

Ref. 21 determines how far the antennas can be extended before a stability boundary is approached but does not simulate the actual dynamics during deployment. It is recommended that this problem could be considered using two alternative approaches: a) by assuming the deployable members to be compound spherical pendulums of variable length (according to the control law) where the degree of flexibility can be treated by varying effective spring constants associated with each of the two Euler angles. If deflections are assumed to occur primarily in one plane, the spring constant associated with the "out-of-plane" Euler angle can be selected several orders of magnitude greater than the "in-plane" spring constant and b) the booms can be considered as a varying number of finite elements depending on how much boom is actually deployed. At any given time the combination of rigid body and structural dynamics can be examined in a quasi-static manner. The limitations of the second method, especially if external continuously acting perturbations would be considered later should be noted. However, in the absence of external effects it is thought that the two approaches could be considered as alternate methods of treating the deployment dynamics with first order flexibility effects included, and these results then compared with the previous results which assume that the booms are competely rigid.

REFERENCES

1. Bainum, P.M. and Sellappan, R., "The Dynamics of Spin Stabilized Spacecraft with Movable Appendages," Part I, Final Report, NASA Grant NGR-09-011-053 (Suppl. No. 1), Howard University, Dept. of Mechanical Engineering, May 1975.

2. Lang, W. and Honeycutt, G.H., "Simulation of Deployment Dynamics of Spinning Spacecraft," NASA TN D4074, August 1967.

3. Bainum, P.M. and Sellappan, R., "Spacecraft Detumbling Using Movable Telescoping Appendages," XXVIth International Astronautical Congress, Lisbon, Sept. 21-27, 1975, Paper No. 75-113.

4. Edwards, T.L. and Kaplan, M.H., "Automatic Spacecraft Detumbling by Internal Mass Motion," AIAA Journal, Vol. 12, No. 4, 1974, pp. 496-502.

5. Edwards, T.L., "A Movable Mass Control System to Detumble a Disabled Space Vehicle," Astronautics Research Report No. 73-5, Department of Aerospace Engineering, The Pennsylvania State University, University Park, Pennsylvania, June 1973.

6. Amieux, J.C. and Liegeois, A., "Design and Ground Test of a Pendulum-Type Active Nutation Damper," Journal of Spacecraft and Rockets, Vol. 11, No. 11, 1974, pp. 790-792.

7. Bainum, P.M. and Sellappan, R., "Semi-Annual Status Report - NASA Grant: NGR 09-011-053 (Suppl. No. 1), "The Dynamics of Spin Stabilized Spacecraft with Movable Appendages - Part I," Howard University, Nov. 15, 1974.

8. Meirovitch, L., Methods of Analytical Dynamics, McGraw-Hill Book Co., 1970, pp. 157-160.

9. IBM 1130 Scientific Subroutine Package Programmer's Manual, IBM Technical Publications Department, White Plains, N.Y.; pp. 61-62, pp. 92-95, p. 115.

10. Bainum, P.M., Fueschsel, P.G., and Mackison, D.L., "Motion and Stability of a Dual-Spin Satellite with Nutation Damping," Journal of Spacecraft and Rockets, Vol. 7, No. 6, June 1970, pp. 690-696.

11. Auelmann, R.R. and Lane, P.T., "Design and Analysis of Ball-in-Tube Nutation Dampers," Proceedings of the Symposium on Attitude Stabilization and Control of Dual-Spin Spacecraft, August 1967, pp. 81-90, Aerospace Corporation Report No. TR-0158, (3-307-01)-16, November 1967.

12. Halfman, R.L., Dynamics Vol. I - Particles, Rigid Bodies and Systems, Addison-Wesley Publishing Co., 1962, Chapter 4, pp. 130-134, p. 159.

13. Athans, M. and Falb, P.L., Optimal Control - An Introduction to the Theory and its Applications, McGraw-Hill, 1966, pp. 750-851.

14. Melsa, J.L. and Jones, S.K., Computer Programs for Computational Assistance in the Study of Linear Control Theory, Second Ed., McGraw-Hill Book Co., 1973, pp. 78-87.

15. Pontryagin, L.S., Boltyanskii, V.G., Gamkrelidze, R.V. and Mischenko, E.F., The Mathematical Theory of Optimal Processes, Pergamon, New York, 1964, pp. 26-34.

16. Pande, K.C., Davies, M.S. and Modi, V.J., "Time-Optimal Pitch Control of Satellites Using Solar Radiation Pressure," Journal of Spacecraft and Rockets, Vol. 11, No. 8, 1974, pp. 601-603.

17. Kunciw, B.G., "Optimal Detumbling of Large Manned Spacecraft Using an Internal Moving Mass," Ph.D. Thesis, Dept. of Aerospace Engineering, The Pennsylvania State University, June 1973.

18. Bainum, Peter M. and Sellappan, R., "Semi-Annual Status-Report NASA Grant: NSG-1181 - The Dynamics of Spin Stabilized Spacecraft with Movable Appendages - Part II," Howard Univ., Nov. 15, 1975.

19. Puri, V. and Bainum, P.M., "Planar Librational Motion of a Gravity-Gradient Satellite During Deployment," Astronautical Research 1971, D. Reidel Publishing Co., Dordrecht, Holland, 1973, pp. 63-80.

20. Bainum, P.M. and Evans, K.S., "The Effect of Gravity-Gradient Torques on the Three Dimensional Motion of a Rotating Space Station - Cable - Counterweight System" AIAA - 13th Aerospace Sciences Meeting, Pasadena, Calif., Jan. 20-22, 1975, Paper No. 75-157; also in AIAA Journal, Vol. 14, No. 1, Jan. 1976, pp. 26-32.

21. Meirovitch, L., "Bounds on the Extension of Antennas for Stable Spinning Satellites," Journal of Spacecraft and Rockets, Vol. 11, No. 3, March 1974, pp. 202-204.

COMPUTER PROGRAMS

1. Hinged System (Chapter II)

   a. Subroutines used: RKSCL, RKGS, SIMQ, RKNXT

   b. Program listing

```
!JOB
!FORT/A/B/E/P/S FORT.LS/L
!LISTING
; C       DYNAMICS OF HINGED DEPLOYMENT SYSTEM
;         EXTERNAL HSR01 , HSR02
;         DIMENSION PARM(5), Y(7), DY(7), WORK(8,7), SIZE(7)
;         REAL I1,I2,I3,L
;         COMMON Y
;         COMMON I1,I2,I3,AM,N,M,A,R0,L,CD,RD1,RD2
;         COMMON C(5,5)
;         EQUIVALENCE(Y(1),W1),(Y(2),W2),(Y(3),W3),(Y(4),A1)
;         EQUIVALENCE(Y(5),A2),(Y(6),ALPHA1),(Y(7),ALPHA2)
;         CALL INOUT(2,5)
;         CALL OPEN (1, 'SELLAPPAN' ,3,IER)
;         IF(IER.NE.1) STOP UNABLE TO OPEN FILE
;         READ(2,91) TMAX,STEP,TOL
;         READ(2,91) SIZE
;      91 FORMAT(8F10.0)
;         PARM(1)=0.0
;         PARM(2)=TMAX
;         PARM(3)=STEP
; C       INITIAL VALUES
;         W1=0.1
;         W2=0.0
;         W3=4.82
;         A1=0.0
;         A2=0.0
;         ALPHA1=1.67
;         ALPHA2=1.67
;         I1=8.5
;         I2=8.5
;         I3=10.5
;         AM=0.125
;         R0=1.0
;         L=4.0
;         A=0.0
;         CD=0.1
```

```
;       RD1=2.0
;       RD2=2.0
;       N=7
;       M=5
;       WRITE(5,92) TMAX, STEP, TOL
;       WRITE(5,93) W1,W2,W3
;       WRITE(5,941) A1,A2
;       WRITE(5,942) ALPHA1,ALPHA2
;       WRITE(5,95) I1,I2,I3
;       WRITE(5,96) AM,RO,L,A
;       WRITE(5,97) SIZE
;       WRITE(5,98)
;    92 FORMAT('1TMAX=',F8.2,10X,'STEP=',F8.4,10X,'TOL=',F8.6)
;    93 FORMAT('0W1=',F10.6,10X,'W2=',F10.6,10X,'W3=',F10.6)
;   941 FORMAT('0A1=',F8.4,5X,'A2=',F8.4)
;   942 FORMAT('0ALPHA1=',F8.4,5X,'ALPHA2=',F8.4)
;    95 FORMAT('0I1=',F8.4,5X,'I2=',F8.4,5X,'I3=',F8.4)
;    96 FORMAT('0AM=',F8.4,5X,'RO=',F8.4,5X,'L=',F8.4,5X,'A=',F8.4)
;    97 FORMAT('0SIZE',7F8.4)
;    98 FORMAT('1',T6,'T',T17,'W1',T30,'W2',T43,'W3',T55,'A1',
;      2T69,'A2',T81,'ALPHA1',T94,'ALPHA2',T108,'IHLF',T115,'THETA',/)
;       CALL RKSCL(N,SIZE,DY,TOL,PARM)
;       CALL RKGS(PARM,Y,DY,N,IHLF,HSR01,HSP02,WORK)
;       WRITE(5,99)IHLF
;    99 FORMAT('0IHLF=',I3)
;       CALL EXIT
;       END


PROGRAM IS RELOCATABLE
                          .TITL   .MAIN
!FORT/A/B/E/P/S FORT.LS/L
!LISTING
;       SUBROUTINE HSR01(T,Y,DY)
;       DIMENSION Y(7), DY(7), C(5,5), CX(5,5)
;       REAL I1,I2,I3,L
;       COMMON W1,W2,W3,A1,A2,ALPHA1,ALPHA2
;       COMMON I1,I2,I3,AM,N,M,A,RO,L,CO,RD1,RD2
;       COMMON C
; C     A1=DER. OF ALPHA1; A2=DER. OF ALPHA2
; C     CAL. OF COEFF. FOR LHS OF MATRIX EQN
;       S1=SIN(ALPHA1)
;       S2=SIN(ALPHA2)
;       C1=COS(ALPHA1)
;       C2=COS(ALPHA2)
;       A11=2.0*(RO*RO+A*A+L*L)
;       A12=RO*(S1+S2)
;       A13=A*(C1+C2)
;       C(1,1)=I1+AM*(A11+2.0*L*(A12-A13))
;       C(1,2)=0.0
;       C(1,3)=0.0
;       A14=AM*L*(L+RO*S1-A*C1)
;       C(1,4)=A14
```

```
;       A15=-AM*L*(L+R0*S2-A*C2)
;       C(1,5)=A15
;       C(2,1)=0.0
;       A16=2.0*A*A-2.0*A*L*(C1+C2)
;       A17=L*L*(C1*C1+C2*C2)
;       C(2,2)=I2+AM*(A16+A17)
;       A18=A*(S1-S2)-R0*(C1-C2)
;       A19=-0.5*L*(2.0*S1*C1-2.0*S2*C2)
;       C(2,3)=-AM*L*(A18+A19)
;       C(2,4)=0.0
;       C(2,5)=0.0
;       C(3,1)=0.0
;       C(3,2)=-AM*L*(A18+A19)
;       A20=2.0*R0*R0+2.0*R0*L*(S1+S2)+L*L*(S1*S1+S2*S2)
;       C(3,3)=I3+AM*A20
;       C(3,4)=0.0
;       C(3,5)=0.0
;       C(4,1)=A14
;       C(4,2)=0.0
;       C(4,3)=0.0
;       C(4,4)=AM*L*L
;       C(5,1)=A15
;       C(5,2)=0.0
;       C(5,3)=0.0
;       C(5,4)=0.0
;       C(5,5)=AM*L*L
;       DO 100 J=1,M
;       DO 100 I=1,M
;  100  CX(I,J)=C(I,J)

;C      CALCULATION OF RHS OF MATRIX EQN
;       B11=I2-I3
;       B12=2.0*A*A-2.0*A*L*(C1+C2)
;       B13=L*L*(COS(2.0*ALPHA1)+COS(2.0*ALPHA2))-2.0*R0*R0
;       B14=-2.0*R0*L*(S1+S2)
;       C11=(B11+AM*(B12+B13+B14))*W2*W3
;       B15=R0*(C1*A1+C2*A2)+A*(S1*A1+S2*A2)
;       C12=-2.0*AM*L*B15*W1
;       B16=A*(S1-S2)-R0*(C1-C2)-0.5*L*(2.0*S1*C1-2.0*S2*C2)
;       C13=-AM*L*B16*(W3*W3-W2*W2)
;       B17=A1*A1*(R0*C1+A*S1)-A2*A2*(R0*C2+A*S2)
;       C14=-AM*L*B17
;       DY(1)=C11+C12+C13+C14-RD1*W1
;       B18=I3-I1
;       B19=L*L*(S1*S1+S2*S2)-2.0*(A*A+L*L)+2.0*L*A*(C1+C2)
;       D11=(B18+AM*B19)*W3*W1
;       B20=A*(S1-S2)-R0*(C1-C2)-0.5*(2.0*S1*C1-2.0*S2*C2)*L
;       D12=-AM*L*B20*W1*W2
;       B21=2.0*A*L*(S1*A1+S2*A2)-L*L*(2.0*S1*C1*A1+2.0*A2*S2*C2)
;       D13=-AM*B21*W2
;       B22=L*(A1-A2)-2.0*A*(C1*A1-C2*A2)
;       B220=L*(COS(2.0*ALPHA1)*A1-COS(2.0*ALPHA2)*A2)
;       B221=B22+B220
;       D14=-AM*L*B221*W3
;       DY(2)=D11+D12+D13+D14-RD2*W2
```

```
;       B23=I1-I2
;       B24=2.0*(R0*R0+L*L)+2.0*L*R0*(S1+S2)
;       B25=-L*L*(C1*C1+C2*C2)
;       E11=(B23+AM*(B24+B25))*W1*W2
;       B26=A*(S1-S2)-R0*(C1-C2)-0.5*L*(2.0*S1*C1-2.0*S2*C2)
;       E12=AM*L*B26*W3*W1
;       B27=2.0*R0*(S1*A1-S2*A2)-L*(COS(2.0*ALPHA1)*A1)
;       B28=L*(A1-A2)+L*(COS(2.0*ALPHA2)*A2)
;       E13=AM*L*(B27+B28)*W2
;       B29=2.0*R0*L*(C1*A1+C2*A2)
;       B30=L*L*(2.0*S1*C1+2.0*S2*C2)
;       E14=-AM*(B29+B30)*W3
;       DY(3)=E11+E12+E13+E14
;       B31=R0*C1+0.5*L*2.0*S1*C1
;       B32=A*S1-0.5*L*2.0*S1*C1
;       B33=R0*C1+A*S1.
;       B34=-(A*C1+R0*S1-L*COS(2.0*ALPHA1))
;       B341=CD*L*L*A1
;       DY(4)=AM*L*(B31*W3*W3+B32*W2*W2+B33*W1*W1+B34*W3*W2)-B341
;       DY(6)=A1
;       B35=R0*C2+0.5*L*2.0*S2*C2
;       B36=A*S2-0.5*L*2.0*S2*C2
;       B37=R0*C2+A*S2
;       B38=A*C2+R0*S2-L*COS(2.0*ALPHA2)
;       B381=CD*L*L*A2
;       DY(5)=AM*L*(B35*W3*W3+B36*W2*W2+B37*W1*W1+B38*W3*W2)-B381
;       DY(7)=A2
;       CALL STMQ(CX,DY,M,KS)
;       IF(KS) 3,2,3
;     2 RETURN
;     3 WRITE(5,4)
;     4 FORMAT(///'SINGULAR EQUATIONS')
;       RETURN
;       END


PROGRAM IS RELOCATABLE
                        .TITL   HSR01

!FORT/A/B/E/P/S FORT.LS/L
!LISTING
;       SUBROUTINE HSR02(T,Y,DY,IHLF,NDUM,P)
;         LOGICAL RKNXT
;       DIMENSION Y(7),DY(7),DUMMY(7)
;       DIMENSION X(7)
;       REAL I1,I2,I3,L
;       COMMON W1,W2,W3,A1,ALPHA1,A2,ALPHA2
;       COMMON I1,I2,I3,AM,N,M,A,R0,L,CD,RD1,RD2
;       COMMON C(5,5)
;       DEG=57.2957795
;       CALL HSR01(T,Y,DUMMY)
;       H1=C(1,1)*Y(1)
;       H2=C(2,2)*Y(2)
;       H3=C(3,3)*Y(3)
;       THETA=ATAN2(SQRT(H1*H1+H2*H2),H3)*DEG
```

```
;       X(1)=Y(1)
;       X(2)=Y(2)
;       X(3)=Y(3)
;       X(4)=Y(4)
;       X(5)=Y(5)
;       X(6)=Y(6)*DEG
;       X(7)=Y(7)*DEG
;       TP=T+0.00005
;       IF(.NOT.RKNXT(IHLF)) GO TO 8
;       WRITE(5,1) TP,X,IHLF,THETA
;     1 FORMAT(1X,F9.4,7E13.7,I10,F9.4)
;       WRITE BINARY(1) T,X(3),X(2),X(1),X(7),X(6)
;     8 CONTINUE
;       RETURN
;       END
```

```
PROGRAM IS RELOCATABLE
                        .TITL   HSR02


TMAX=   10.00           STEP=  0.0500           TOL=0.001000

W1=  0.100000           W2=  0.000000           W3=  4.820000

A1=  0.0000     A2=  0.0000

ALPHA1=  1.6700     ALPHA2=  1.6700

I1=  8.5000     I2=  8.5000     I3= 10.5000

AM=  0.1250     RO=  1.0000     L=  4.0000     A=  0.0000

SIZE  0.1000  0.1000  5.0000  5.0000  5.0000  4.0000  4.0000
```

c. Computer time

For 10 secs. of dynamic response simulated, 490 secs. of NOVA 840 computer time were required for a step size of 0.05 secs.

d. Subroutine RKNXT

```
!JOB
!FORT/A/B/E/P/S FORT.LS/L
!LISTING
;       LOGICAL FUNCTION RKNXT(IHLF)
;           COMMON /RKNXT/ IHOLD, NEXT
;           DATA  IHOLD/0/, NEXT/1/
;       IDIFF = IHLF - IHOLD
;       IF (IDIFF .EQ. 0) GO TO 5
;           IF (IDIFF .LT. 0) GO TO 35
;               NEXT = NEXT*2**IDIFF
;               GO TO 39
;   35      CONTINUE
;               NEXT = NEXT/2**(-IDIFF)
;   39      CONTINUE
;           IHOLD = IHLF
;   5   CONTINUE
;       NEXT = NEXT - 1
;       IF (NEXT .GT. 0) GO TO 75
;           RKNXT = .TRUE.
;           NEXT = 2**IHLF
;           GO TO 79
;   75  CONTINUE
;           RKNXT = .FALSE.
;   79  CONTINUE
;       RETURN
;       END

PROGRAM IS RELOCATABLE.
                            .TITL   RKNXT
```

e. Plotting program

```
!JOB
!FORT/A/B/E/P/S FORT.LS/L
!LISTING
;       PARAMETER NPTS=201, NV=5
;       DIMENSION T(NPTS), V(NPTS,NV)
; C
;       CALL INOUT(2,5)
;       CALL SPERL("SPLT", IER)
;       IF (IER .NE. 1)  STOP -- ON SPOOLING
;       WRITE(5,90)
;       CALL OPEN(1, 'SELLAPPAN' ,1,IER)
;       IF(IER.NE.1) STOP UNABLE TO OPEN FILE
;       READ BINARY(1) (T(I),(V(I,J),J=1,NV),I=1,NPTS)
;       DO 8 N=1,NV
;       READ(2,9)  WIDTH,HEIGHT,TMAX,VMIN,VMAX
;       WRITE(5,92) WIDTH, HEIGHT, TMAX, VMIN, VMAX
;       CALL PSIZE(WIDTH,HEIGHT)
;       CALL PROX
;       CALL PAXES
;       CALL PLOB(0.0,T,TMAX,VMIN,V(1,N),VMAX,NPTS)
;       CALL PLOT(1.0+HEIGHT,0.0,-3)
;     8 CONTINUE
;       CALL EXIT
;     9 FORMAT(8F10.0)
;    90 FORMAT('1')
;    92 FORMAT(2X, /, 1X, 1P5E15.5)
;       END

PROGRAM IS RELOCATABLE
                          .TITL    .MAIN
!RLDR/M TMP/S 001 DP0:PLOT.LB FORT.LB
!EXEC
```

2. Optimal Control (Chapters III and IV)

a. Subroutine used: MINV, RKSCL, RKGS, SIMQ, RKNXT

b. Program listing

PROGRAM I

```
!JOB
!FORT/A/B/E/P/S FORT.LS/L
!LISTING
;C      PROGRAM I
;C      PROGRAM TO FIND A AND B FROM G-H-F MATRICES
;       DIMENSION A(3,3),B(3,2),G(3,3),F(3,3),H(3,3),F(3,2),
;      *LL(3),MM(3)
;       REAL I1,I2,I3,MB,M1,M2,LM
;       CALL INOUT(2,5)
;   106 FORMAT(5X,13H THE A MATRIX/)
;   107 FORMAT(5X,13H THE B MATRIX/)
;   108 FORMAT(6(1PE20.8))
;       N=3
;       L=2
;       READ(2,101) I1,I2,I3,MB
;       WRITE(5,101)I1,I2,I3,MB
;   101 FORMAT(4F20.2)
;       READ(2,102) M1,M2,LM
;       WRITE(5,102)M1,M2,LM
;   102 FORMAT(4F20.2)
;       READ(2,103) AA,BB,CC
;       WRITE(5,103)AA,BB,CC
;   103 FORMAT(4F20.2)
;       C1=AA/LM
;       C2=BB/LM
;       C3=CC/LM
;       U2=M2/(MB+M2)
;       U=M1*(MB+M2)/(MB+M1+M2)
;       ULM=U*LM*LM
;       AI1=I1/ULM
;       AI2=I2/ULM
;       AI3=I3/ULM
;C      CAL. OF G MATRIX
;       G(1,1)=AI1+C2*C2+C3*C3-2.0*U2*C2*C3
;       G(1,2)=-C1*C2+U2*C1*C3
;       G(1,3)=0.0
;       G(2,1)=-C1*C2+U2*C1*C3
```

```
;         G(2,2)=AI2+C1*C1
;         G(2,3)=0.0
;         G(3,1)=0.0
;         G(3,2)=0.0
;         G(3,3)=AI3+C1*C1+C2*C2+C3*C3-2.0*U2*C2*C3
;  C      CAL.OF H MATRIX
;         H(1,1)=-C1*C2+U2*C1*C3
;         H(1,2)=-(AI3-AI2+C2*C2+C3*C3)+2.0*U2*C2*C3
;         H(1,3)=0.0
;         H(2,1)=-(AI1-AI3-C1*C1)
;         H(2,2)=C1*C2-U2*C1*C3
;         H(2,3)=0.0
;         H(3,1)=0.0
;         H(3,2)=0.0
;         H(3,3)=0.0
;  C      CAL. OF F MATRIX
;         F(1,1)=-C2+U2*C3
;         F(1,2)=0.0
;         F(2,1)=C1
;         F(2,2)=0.0
;         F(3,1)=0.0
;         F(3,2)=C3-U2*C2
;  C      INVERSE OF G=E
;         DO 13 I=1,N
;         DO 13 J=1,N
;      13 E(I,J)=G(I,J)
;         CALL MINV(E,N,D,LL,MM)
;  C      CAL. OF A=E*H
;         WRITE(5,106)
;         DO 15 I=1,N
;         DO 15 J=1,N
;         A(I,J)=0.0
;         DO 15 K=1,N
;      15 A(I,J)=A(I,J)+E(I,K)*H(K,J)
;         DO 16 I=1,N
;      16 WRITE(5,108) (A(I,J),J=1,N)
;  C      CAL. OF B=E*F
;         WRITE(5,107)
;         DO 17 I=1,N
;         DO 17 J=1,L
;         B(I,J)=0.0
;         DO 17 K=1,N
;      17 B(I,J)=B(I,J)+E(I,K)*F(I,J)
;         DO 18 I=1,N
;      18 WRITE(5,108)(B(I,J),J=1,L)
;         CALL EXIT
;         END
```

```
PROGRAM IS RELOCATABLE
                              .TITL    .MAIN
!RLDR/M TMP/S 001 DP0:SSP.LB FORT.LB
!EXEC
```

```
  10500000.00          12500000.00          15000000.00  137000.00
      1800.00              1800.00               100.00
        65.00                 0.00                65.00
THE A MATRIX

2.16190000E -3      -5.55732400E -1       0.00000000E  0
6.00141900E -1      -2.16189600E -3       0.00000000E  0
0.00000000E  0       0.00000000E  0       0.00000000E  0
THE B MATRIX

8.27768800E -3       0.00000000E  0
5.74183700E -1       0.00000000E  0
0.00000000E  0       3.84811100E -1
```

PROGRAM II

```
!JOB
!FORT/A/B/E/P/S FORT.LS/L
!LISTING
;C      PROGRAM II
;C      RICCATI EQUATION PROGRAM (RICATI)
;       DIMENSION A(10,10),B(10,10),Q(10,10),R(10,10),
;      * K(10,10),D(10,10),X(10),F(10,10),E(10,10),
;      *  G(10,10),H(10,10),S(10,10)
;       REAL K
;       INTEGER OPTION,BLANK
;       COMMON/KALMAN/ICC,IFF,BLANK
;       DATA ICC,IFF,BLANK/'C ','F ',' '/
;       CALL INOUT(2,5)
; 1000 FORMAT(1H1,5X,37HOPTIMAL CONTROL/)
; 1001 FORMAT(2I2)
; 1003 FORMAT (1H0,5X,13H THE A MATRIX/)
; 1004 FORMAT (1H0,5X,13H THE B MATRIX/)
; 1006 FORMAT(8F10.3)
; 1007 FORMAT (A1,9X,2F10.3,I3)
; 1008 FORMAT(1H0,45(1H*))
; 1010 FORMAT (1H0,5X,22H*** CONTROL OPTION ***/)
; 1011 FORMAT(6(1PE20.8))
; 1012 FORMAT(1H0,5X,13H THE R MATRIX/)
; 1013 FORMAT(1H0,5X,13H THE Q MATRIX/)
; 1014 FORMAT (1H0,5X,19H INITIAL CONDITIONS/)
; 1015 FORMAT(1H0,5X,8H TIME = ,1PE20.8/6X,5HGAINS)
; 1016 FORMAT(1H0,5X,21HSTEADY STATE SOLUTION//
;      * 6X,6H GAINS/)
;  100 READ(2,1001) N,M
;       WRITE(5,1000)
;       WRITE(5,1001) N,M
;       WRITE(5,1008)
;       WRITE(5,1003)
;       DO 110 I=1,N
;       READ(2,1006) (A(I,J),J=1,N)
;  110 WRITE(5,1011) (A(I,J),J=1,N)
;       WRITE(5,1004)
;       DO 120 I=1,M
;       READ(2,1006) (B(J,I),J=1,N)
;  120 WRITE(5,1011) (B(J,I),J=1,N)
;  150 READ(2,1007,END=999) OPTION,T1,T2,NPT
;       WRITE(5,1008)
;       IF(OPTION.EQ.BLANK) GO TO 100
;       IF(OPTION.EQ.ICC) GO TO 300
;  300 WRITE(5,1010)
;       NR=M
;       NQ=N
;       DO 330 I=1,N
;       DO 310 J=1,M
;  310 E(I,J)=B(I,J)
;       DO 330 J=1,N
;  330 F(I,J)=A(J,I)
```

```
;       GO TO 400
;   400 WRITE(5,1012)
;       DO 410 I=1,NR
;       READ(2,1006) (R(I,J),J=1,NR)
;   410 WRITE(5,1011) (R(I,J),J=1,NR)
;       WRITE(5,1013)
;       DO 420 I=1,NQ
;       READ(2,1006) (Q(I,J),J=1,NQ)
;   420 WRITE(5,1011) (Q(I,J),J=1,NQ)
;       DO 430 I=1,NR
;       DO 430 J=1,NR
;   430 H(I,J)=R(I,J)
;       DO 440 I=1,NR
;       DO 440 J=1,N
;       R(I,J)=0.0
;       DO 440 II=1,NR
;   440 R(I,J)=R(I,J)+H(I,II)*E(J,II)
;       IF(OPTION.EQ.ICC) GO TO 500
;   500 IF(NPT.GT.0) GO TO 530
;       DO 520 I=1,N
;       DO 510 J=1,N
;   510 G(I,J)=0.0
;   520 G(I,I)=1.0
;       EPS=0.1
;       GO TO 570
;   530 WRITE(5,1014)
;       DO 540 I=1,N
;       READ(2,1006) (G(I,J),J=1,N)
;   540 WRITE(5,1011) (G(I,J),J=1,N)
;       WRITE(5,1008)
;       TIME=ABS(T2-T1)
;       PTS=200.0*TIME
;       XX=NPT
;       XX=PTS/XX
;       ID=XX
;       DI=ID
;       YY=ABS(XX-DI)
;       IF(YY.GT.0.05) ID=ID+1
;       IT=PTS
;       EPS=0.005
;       IF(OPTION.EQ.ICC) TIME=T2
;       WRITE(5,1015) TIME
;       DO 560 I=1,NR
;       DO 550 J=1,N
;       K(I,J)=0.0
;       DO 550 II=1,N
;   550 K(I,J)=K(I,J)+R(I,II)*G(II,J)
;   560 WRITE(5,1011) (K(I,J),J=1,N)
;   570 LC=0
;       ICH=ID
;   575 DO 580 I=1,NR
```

```
;       DO 580 J=1,N
;       K(I,J)=0.0
;       DO 580 II=1,N
;  580  K(I,J)=K(I,J)+R(I,II)*G(II,J)
;       DO 590 I=1,N
;       DO 590 J=1,N
;       H(I,J)=0.0
;       DO 590 II=1,NR
;  590  H(I,J)=H(I,J)+E(I,II)*K(II,J)
;       DO 610 I=1,N
;       DO 610 J=1,N
;       D(I,J)=0(I,J)
;       DO 600 II=1,N
;  600  D(I,J)=D(I,J)+F(I,II)*G(II,J)+G(I,II)*F(J,II)-G(I,II)*H(II,J)
;  610  S(I,J)=G(I,J)+D(I,J)*EPS
;       IF(NPT.LE.0) GO TO 640
;       LC=LC+1
;       IF(LC.LT.ICH) GO TO 625
;       ICH=ICH+ID
;       ALC=LC
;       T=ALC*EPS
;       IF(OPTION.EQ.ICC) TIME=T2-T
;       WRITE(5,1015) TIME
;       DO 620 I=1,NR
;  620  WRITE(5,1011) (K(I,J),J=1,N)
;       IF(LC.GE.IT) GO TO 150
;  625  DO 630 I=1,N
;       DO 630 J=1,N
;  630  G(I,J)=S(I,J)
;       GO TO 575
;  640  SUM=0.0
;       DO 650 I=1,N
;       DO 650 J=1,N
;       SUM=SUM+ABS(D(I,J))
;  650  G(I,J)=S(I,J)
;       IF(SUM.GT.0.01   ) GO TO 575
;       WRITE(5,1016)
;       DO 660 I=1,NR
;  660  WRITE(5,1011) (K(I,J),J=1,N)
;       GO TO 150
;  999  CONTINUE
;       CALL EXIT
;       END

PROGRAM IS RELOCATABLE
                              .TITL    .MAIN
!RLDR/M TMP/S 001 FORT.LB
!EXEC
```

ORIGINAL PAGE IS
OF POOR QUALITY

```
        OPTIMAL CONTROL

    3 2

    ************************************************

          THE A MATRIX

      2.16190000E -3      -5.55732400E -1       0.00000000E  0
      6.00141900E -1      -2.16190000E -3       0.00000000E  0
      0.00000000E  0       0.00000000E  0       0.00000000E  0

          THE B MATRIX

      8.27769200E -3       5.74183700E -1       0.00000000E  0
      0.00000000E  0       0.00000000E  0       3.84811100E -1

    ************************************************

          *** CONTROL OPTION ***

          THE R MATRIX

      1.00000000E  0       0.00000000E  0
      0.00000000E  0       1.00000000E  0

          THE Q MATRIX

      9.86000100E  0       0.00000000E  0       0.00000000E  0
      0.00000000E  0       9.86000100E  0       0.00000000E  0
      0.00000000E  0       0.00000000E  0       9.86000100E  0

          STEADY STATE SOLUTION

          GAINS

     -2.21919500E  0       3.80596200E  0       0.00000000E  0
      0.00000000E  0       0.00000000E  0       3.14006300E  0
    !EOF
```

PROGRAM III

```
!JOB
!FORT/A/B/E/P/S FORT.LS/L
!LISTING
; C      PROGRAM III
; C      OPTIMAL CONTROL - TIME RESPONSES
;        EXTERNAL BSOC1,BSOC2
;        DIMENSION PARM(5),Y(7),DY(7),WORK(8,7),SIZE(7)
;        REAL I1,I2,I3,MB,M1,M2,LM
;        REAL   KC11,KC12,KC13,KC21,KC22,KC23
;        COMMON Y
;        COMMON I1,I2,I3,MB,M1,M2,LM
;        COMMON N,M
;        COMMON AA,BB,CC,DD
;        COMMON KC11,KC12,KC13,KC21,KC22,KC23
;        COMMON C(3,3)
;        EQUIVALENCE (Y(1),W1N),(Y(2),W2N),(Y(3),W3N),(Y(4),DZN)
;        EQUIVALENCE (Y(5),DXN),(Y(6),ZN),(Y(7),XN)
;        CALL INOUT(2,5)
;        CALL OPEN (1, 'SELLAPPAN' ,3,IER)
;        IF(IER.NE.1) STOP UNABLE TO OPEN FILE
;        READ(2,91) TMAX,STEP,TOL
;        READ(2,91) SIZE
;     91 FORMAT(8F10.0)
;        PARM(1)=0.0
;        PARM(2)=TMAX
;        PARM(3)=STEP
; C      INITIAL VALUES
;        READ(2,911) I1,I2,I3,MB
;        READ(2,911) M1,M2,LM
;        READ(2,911) AA,BB,CC,DD
;    911 FORMAT(4F20.4)
;        W1N=0.0391/0.314
;        W2N=0.0
;        W3N=(0.35-0.314)/0.314
;        DZN=0.0
;        DXN=0.0
;        ZN=0.0
;        XN=0.0
;        READ(2,913) KC11,KC12,KC13
;        READ(2,913) KC21,KC22,KC23
;    913 FORMAT(8F10.0)
;        N=7
;        M=3
;        WRITE(5,92) TMAX,STEP,TOL
;        WRITE(5,95) I1,I2,I3
;        WRITE(5,96) M1,M2,LM
;        WRITE(5,97) AA,BB,CC,DD
;        WRITE(5,98) SIZE
;        WRITE(5,981) KC11,KC12,KC13
;        WRITE(5,981) KC21,KC22,KC23
```

```
;         WRITE(5,99)
;      92 FORMAT('1TMAX=',F8.4,10X,'STEP=',F8.4,10X,'TOL=',F8.6)
;      95 FORMAT('0I1=',F15.2,2X,'I2=',F15.2,2X,'I3=',F15.2)
;      96 FORMAT('0M1=',F15.2,2X,'M2=',F15.2,2X,'LM=',F15.2)
;      97 FORMAT('0AA=',F8.4,5X,'BB=',F8.4,5X,'CC=',F8.4,5X,'DD=',F8.4)
;      98 FORMAT('0SIZE',7F8.4)
;     981 FORMAT(8F10.4)
;      99 FORMAT('1',T6,'T',T17,'W1',T30,'W2',T43,'W3',T55,'DZ',
;        2T69,'DX',T81,'Z',T94,'X',T108,'THETA',T115,'IHLF',/)
;         CALL RKSCL(N,SIZE,DY,TOL,PARM)
;         CALL RKGS(PARM,Y,DY,N,IHLF,BSOC1,BSOC2,WORK)
;         WRITE(5,100) IHLF
;     100 FORMAT('0IHLF=',I3)
;         CALL EXIT
;         END


PROGRAM IS RELOCATABLE
                              .TITL    .MAIN
!FORT/A/B/E/P/S FORT.LS/L
!LISTING
;         SUBROUTINE BSOC1(T,Y,DY)
;         DIMENSION Y(7),DY(7),C(3,3)
;         REAL I1,I2,I3,MB,M1,M2,LM
;         REAL    KC11,KC12,KC13,KC21,KC22,KC23
;         COMMON W1N,W2N,W3N,DZN,DXN,ZN,XN
;         COMMON I1,I2,I3,MB,M1,M2,LM
;         COMMON N,M
;         COMMON AA,BB,CC,DD
;         COMMON KC11,KC12,KC13,KC21,KC22,KC23
;         COMMON C
;  C      CAL.OF.COEFF.FOR LHS OF MATRIX EQN
;         U=M1*(MB+M2)/(MB+M1+M2)
;         ULM=U*LM*LM
;  C      NONDIMENSIONALIZATION
;         AI1=I1/ULM
;         AI2=I2/ULM
;         AI3=I3/ULM
;         C1=AA/LM
;         C2=BB/LM
;         C3=CC/LM
;         C4=DD/LM
;         U1=M1*(MB+M2)/((MB+M1+M2)*U)
;         U2=M2*(MB+M1)/((MB+M1+M2)*U)
;         U3=M1*M2/((MB+M1+M2)*U)
;         C(1,1)=AI1+U1*(C2*C2+ZN*ZN)+U2*(C3*C3+C4*C4)
;        *-2.0*U3*(C2*C3+C4*ZN)
;         C(1,2)=-U1*(C1*C2)-U2*C3*XN+U3*(C1*C3+C2*XN)
;         C(1,3)=-U1*(C1*ZN)-U2*C4*XN+U3*(C1*C4+ZN*XN)
;         C(2,1)=-U1*(C1*C2)-U2*C3*XN+U3*(C1*C3+C2*XN)
;         C(2,2)=AI2+U1*(C1*C1+ZN*ZN)+U2*(C4*C4+XN*XN)
;        *-2.0*U3*(C1*XN+C4*ZN)
```

```
      C(2,3)=-U1*(C2*ZN)-U2*C3*C4+U3*(C2*C4+C3*ZN)
      C(3,1)=-U1*(C1*ZN)-U2*C4*XN+U3*(C1*C4+ZN*XN)
      C(3,2)=-U1*(C2*ZN)-U2*C3*C4+U3*(C2*C4+C3*ZN)
      C(3,3)=AI3+U1*(C1*C1+C2*C2)+U2*(C3*C3+XN*XN)
     *-2.0*U3*(C2*C3+C1*XN)
C     CAL. OF RHS OF MATRIX EQN
      AZN=-(KC11*W1N+KC12*W2N+KC13*W3N)-ZN
      IF(M2.EQ.0.0) GO TO 75
      F1=2.0*U3*C1/(U2*C3-U3*C2)
      GO TO 76
   75 F1=0.0
   76 AXN=-(KC21*W1N+KC22*W2N+KC23*W3N)-F1*DXN
      SN=1.0+W3N
      A11=(AI3-AI2)*W2N*SN
      A121=-C1*ZN*W1N*W2N+(C2*C2-ZN*ZN)*W2N*SN+C1*C2*W1N*SN
      A122=2.0*ZN*DZN*W1N+C2*ZN*(SN*SN-W2N*W2N)+C2*AZN
      A123=-C4*XN*W1N*W2N+(C3*C3-C4*C4)*W2N*SN+C3*XN*W1N*SN
      A124=-2.0*C3*DXN*W2N-2.0*C4*DXN*SN+C3*C4*(SN*SN-W2N*W2N)
      A12=U1*(A121+A122)+U2*(A123+A124)
      A15=-(C1*C4+ZN*XN)*W1N*W2N+2.0*(C2*C3-C4*ZN)*W2N*SN
      A16=(C1*C3+C2*XN)*W1N*SN+2.0*C4*DZN*W1N-2.0*C2*DXN*W2N
      A17=-2.0*DXN*ZN*SN+(C2*C4+C3*ZN)*(SN*SN-W2N*W2N)+C3*AZN
      A13=U3*(A15+A16+A17)
      DY(1)=-(A11+A12-A13)
      B11=(AI1-AI3)*SN*W1N
      B121=-C2*ZN*W1N*W2N+C1*C2*W2N*SN+(C1*C1-ZN*ZN)*SN*W1N
      B122=-2.0*ZN*DZN*W2N+C1*ZN*(SN*SN-W1N*W1N)+C1*AZN
      B123=-C3*C4*W1N*W2N+C3*XN*W2N*SN+(-C4*C4+XN*XN)*SN*W1N
      B124=-2.0*XN*DXN*W2N+C4*XN*(SN*SN-W1N*W1N)-C4*AXN
      B12=U1*(B121+B122)+U2*(B123+B124)
      B15=-(C2*C4+C3*ZN)*W1N*W2N+(C1*C3+C2*XN)*W2N*SN
      B16=2.0*(C1*XN-C4*ZN)*SN*W1N-2.0*(C1*DXN+C4*DZN)*W2N
      B17=(C1*C4+XN*ZN)*(SN*SN-W1N*W1N)+XN*AZN-ZN*AXN
      B13=U3*(B15+B16+B17)
      DY(2)=-(B11-B12+B13)
      C11=(AI2-AI1)*W1N*W2N
      C121=(C2*C2-C1*C1)*W1N*W2N-C1*ZN*W2N*SN+C2*ZN*SN*W1N
      C122=2.0*C1*DZN*W1N+2.0*C2*DZN*W2N+C1*C2*(W1N*W1N-W2N*W2N)
      C123=(C3*C3-XN*XN)*W1N*W2N-C4*XN*W2N*SN+C3*C4*SN*W1N
      C124=-2.0*XN*DXN*SN+C3*XN*(W1N*W1N-W2N*W2N)+C3*AXN
      C12=U1*(C121+C122)+U2*(C123+C124)
      C15=2.0*(C2*C3-C1*XN)*W1N*W2N-(C1*C4+XN*ZN)*W2N*SN
      C16=(C2*C4+C3*ZN)*SN*W1N+2.0*XN*DZN*W1N+2.0*C3*DXN*W2N
      C17=-2.0*C1*DXN*SN+(C1*C3+C2*XN)*(W1N*W1N-W2N*W2N)+C2*AXN
      C13=U3*(C15+C16+C17)
      DY(3)=-(C11-C12+C13)
      DY(4)=AZN
      DY(5)=AXN
      DY(6)=DZN
      DY(7)=DXN
      CALL SIMQ(C,DY,M,KS)
      IF(KS) 3,2,3
```

```
;       2 RETURN
;       3 WRITE(5,4)
;       4 FORMAT(// ' SINGULAR EQUATIONS')
;         RETURN
;         END


PROGRAM IS RELOCATABLE
                              .TITL   BSOC1
!FORT/A/B/E/P/S FORT.LS/L
!LISTING
;         SUBROUTINE BSOC2(T,Y,DY,IHLF,NDUM,P)
;           LOGICAL RKNXT
;         DIMENSION Y(7),DY(7),DUMMY(7)
;         DIMENSION X(7)
;         REAL I1,I2,I3,MB,M1,M2,LM
;         REAL   KC11,KC12,KC13,KC21,KC22,KC23
;         COMMON W1N,W2N,W3N,DZN,DXN,ZN,XN
;         COMMON I1,I2,I3,MB,M1,M2,LM
;         COMMON N,M
;         COMMON AA,BB,CC,DD
;         COMMON KC11,KC12,KC13,KC21,KC22,KC23
;         DEG=57.2957795
;         CALL BSOC1(T,Y,DUMMY)
;         WS=0.314
;         X(1)=Y(1)*WS
;         X(2)=Y(2)*WS
;         X(3)=(1.0+Y(3))*WS
;         X(4)=Y(4)*LM*WS
;         X(5)=Y(5)*LM*WS
;         X(6)=Y(6)*LM
;         X(7)=Y(7)*LM
;         H1=I1*X(1)
;         H2=I2*X(2)
;         H3=I3*X(3)
;         THETA=ATAN2(SQRT(H1*H1+H2*H2),H3)*DEG
;         TA=T/WS
;         TP=TA+0.00005
;         IF(.NOT.RKNXT(IHLF)) GO TO 8
;         WRITE(5,1) TP,X,THETA,IHLF
;       1 FORMAT(1X,F9.4,7F13.7,F9.4,I10)
;         WRITE BINARY(1) TA,THETA,X(7),X(6),X(3),X(2),X(1)
;       8 CONTINUE
;         RETURN
;         END


PROGRAM IS RELOCATABLE
                              .TITL   BSOC2
```

```
TMAX= 62.8000          STEP=  0.3140          TOL=0.001000

I1=    10500000.00  I2=    12500000.00  I3=    15000000.00

M1=        1800.00  M2=        1800.00  LM=         100.00

AA= 65.0000     BB=  0.0000     CC= 65.0000     DD=  0.0000

SIZE  0.1000  0.1000  0.1000  4.0000  4.0000  2.0000  2.0000
  -2.2192     3.8060     0.0000
   0.0000     0.0000     3.1401
```

c. Computer time (Optimal Control)

PROGRAM I: 109 secs. (matrix inversion)

PROGRAM II: 120 secs. (to reach steady state)

PROGRAM III: 382 secs. (to simulate 200 secs. real time response with stpe size= 1 sec.)